

**Mechanisms of quantitative disease  
resistance in the maize-*Ustilago maydis*  
interaction**



**Inaugural-Dissertation**

**zur**

**Erlangung des Doktorgrades der Naturwissenschaften  
(Dr. rer. nat.)**

der Mathematisch-Naturwissenschaftlichen Fakultät  
der Universität zu Köln

vorgelegt von

**Selma Schurack**

aus Berlin-Charlottenburg

Köln, 2021

Die Untersuchungen zur vorliegenden Arbeit wurden von Oktober 2016 bis September 2020 am Lehrstuhl für Terrestrische Mikrobiologie an der Universität zu Köln unter der Betreuung von Herrn Prof. Dr. Gunther Döhlemann durchgeführt.

**Erstgutachter:** Prof. Dr. Gunther Döhlemann  
**Zweitgutachterin:** Prof. Dr. Alga Zuccaro

**Tag der mündlichen Prüfung:** 16.02.2021

*'Taken steps like little mice – with the heart of a lion'*

HONIG – Golden Circle





## Summary

The biotrophic pathogen *Ustilago maydis* causes smut disease on maize (*Zea mays*) and induces the formation of tumours on all aerial parts of the plant. Unlike in other biotrophic interactions, no gene-for-gene interactions have been identified in the maize-*U. maydis* pathosystem. Thus, maize resistance to *U. maydis* is considered a polygenic, quantitative trait. In this study, the molecular mechanisms that underlie the interaction of *U. maydis* with maize lines of quantitatively different resistance levels were investigated. This aimed at elucidating whether the fungus' virulence strategy is adapted to different host genotypes and at identifying host processes involved in quantitative disease resistance (QDR) to *U. maydis*.

Based on quantitative scoring of disease symptoms in 26 maize lines, an RNA-Seq analysis of six *U. maydis*-infected maize lines of highly distinct resistance levels was performed. In accordance with the complex nature of QDR, the different maize lines showed specific responses of diverse cellular processes to *U. maydis* infection. On the fungal side, 406 genes were differentially expressed between maize lines, of which 102 encode predicted effector proteins.

Furthermore, correlation analysis of co-expressed *U. maydis* genes to the susceptibility levels of the different maize lines suggested differences in host nutrient availability as well as cell wall composition to be involved in QDR to *U. maydis*. On the host side, expression of genes related to cell division or photosynthesis was correlated with low or high resistance levels, respectively.

Based on the enrichment of predicted effector genes in differentially expressed *U. maydis* genes, *U. maydis* CRISPR/Cas9 knock-out mutants for selected maize line-specific effector sets were generated to investigate, if and how *U. maydis* effectors are adapted to the host genotype. Infections of different maize lines with the fungal mutants identified effectors with quantitative, maize-line-specific virulence functions. RNA-Seq revealed auxin-related processes as a possible target for one of those effectors, UMAG\_02297.

To identify genetic loci contributing to QDR to *U. maydis* in maize seedlings, a QTL mapping experiment using a population derived from a cross of two maize lines with highly distinct *U. maydis* resistance was performed in the field. Preliminary data identified one QTL on chromosome 9 that contributes to heavy tumour formation.

Taken together, this study showed that both transcriptional activity and virulence function of fungal effectors are modified according to the infected maize line, which provides new insights into the molecular mechanisms underlying the quantitative interaction of *U. maydis* and maize.

## Abbreviations

$\times g$	Gravitational acceleration on earth (9.81m/s <sup>2</sup> )
°C	Degree Celsius
µg	Microgram
µl	Microlitre
µm	Micrometre
µM	Micromolar
A	Ampere
aa	Amino acid
ABA	Abscisic acid
AC	Axenic culture
aem	Adjusted entry mean
ATP	Adenosine triphosphate
AUX	Auxin
Avr	Avirulence effector
bp	Base pairs
cAMP	Cyclic adenosine monophosphate
Carb	Carbenicillin
Cbx	Carboxin
cDNA	Complementary DNA
CDS	Coding sequence
CERK1	Chitin receptor kinase 1
cM	Centimorgan
Cmu1	Chorismate mutase 1
CRISPR	Clustered regularly interspaced short palindromic repeats
CSEP	Candidate secreted effector protein
DAMP	Damage-associated molecular pattern

## Abbreviations

---

DNA	Deoxyribonucleic acid
dpi	Days post infection
EFR	EF-Tu receptor
EGB	Early golden bantam
ER	Endoplasmic reticulum
ET	Ethylene
ETI	Effector-triggered immunity
EtOH	Ethanol
ETS	Effector-triggered susceptibility
f.c.	Final concentration
F <sub>3</sub>	Third filial generation
FC	Fold change
FDR	False discovery rate
FLS2	Flagellin-sensing 2
Fly1	Fungalysin 1
g	Gram
GO	Gene Ontology
h	Hour
H <sub>2</sub> O <sub>bid.</sub>	Double distilled water
hpi	Hours post inoculation
HR	Hypersensitive response
IAA	Indole acetic acid
ID	Identifier
<i>ip</i>	Iron–sulphur protein subunit of succinate dehydrogenase
JA	Jasmonic acid
Kan	Kanamycin
KASP	Competitive allele-specific PCR
kb	Kilobases

KO	Knock-out
LRR	Leucine rich repeat
LysM	Lysin motif
M	Molar
MAMP	Microbe-associated molecular pattern
MAPK	Mitogen-activated protein kinase
MgCl <sub>2</sub>	Magnesium chloride
min	Minute(s)
ml	Millilitre
MIs	Maize line-specific
mm	Millimetre
mRNA	Messenger RNA
NAM	Nested Association Mapping
ng	Nanogram
NLR	Nucleotide binding leucine rich repeat protein
nm	Nanometre(s)
No.	Number
nt	Nucleotide
O/N	Over night
OD	Optical density
p	Statistical probability value
PAMP	Pathogen-associated molecular pattern
PCR	Polymerase chain reaction
Pep1	Protein essential during penetration 1
PI	Propidium iodide
Pit2	Protein involved in tumours 2
POX12	Plant peroxidase 12
PRR	Pattern recognition receptor

## Abbreviations

---

PTI	Pattern-triggered immunity
QDR	Quantitative disease resistance
qPCR	Quantitative polymerase chain reaction
qRT-PCR	Quantitative real-time polymerase chain reaction
QTL	Quantitative trait locus
R protein	Resistance protein
RIL	Recombinant inbred line
RLK	Receptor-like kinase
RLP	Receptor-like protein
RNA	Ribonucleic acid
RNA-Seq	Ribonucleic acid sequencing
ROS	Reactive oxygen species
rpm	Rounds per minute
RT	Room temperature
s	Second(s)
SA	Salicylic acid
SAR	Systemic acquired resistance
See1	Seedling efficient effector 1
sgRNA	Single guide ribonucleic acid
SGT1	Suppressor of G2 allele of skp 1
SNP	Single nucleotide polymorphism
SP	Signal peptide
TE-buffer	Tris-EDTA buffer solution
TFR	Transferrin receptor-like dimerization domain
Tin2	Tumour inducing 2
TIR domain	Toll-interleukin 1 receptor domain
TM domain	Transmembrane domain
TNL	TIR-NB-LRR protein

TOR	Target of Rapamycin
tpm	Transcripts per million
U	Unit (Enzyme activity)
V	Volt
v/v	Volume/volume
w/v	Weight/volume
WAK1	Wall-associated kinase 1
WGA	Wheat germ agglutinin
WGCNA	Weighted gene co-expression network analysis

## Table of contents

<b>Summary</b> .....	<b>I</b>
<b>Abbreviations</b> .....	<b>II</b>
<b>1 Introduction</b> .....	<b>1</b>
1.1 Plant defence and microbe counteractions .....	2
1.1.1 Plant innate immunity .....	2
1.1.2 Effectors in plant-pathogen interactions .....	6
1.1.3 Quantitative disease resistance .....	9
1.2 <i>Ustilago maydis</i> : the causative agent of corn smut disease .....	12
1.2.1 Pathogenic development of <i>U. maydis</i> .....	12
1.2.2 Maize responses to <i>U. maydis</i> infection .....	14
1.2.3 Effectors in the <i>U. maydis</i> -maize interaction .....	16
1.2.4 Quantitative disease resistance in the <i>U. maydis</i> -maize interaction .....	18
1.3 Aims and objectives of the study .....	19
<b>2 Results</b> .....	<b>20</b>
2.1 <i>U. maydis</i> disease development in different maize lines .....	20
2.2 Transcriptome analysis of <i>U. maydis</i> infecting maize lines of distinct disease resistance levels .....	24
2.2.1 Weighted gene co-expression analysis of <i>U. maydis</i> genes during infection of maize lines of distinct disease resistance levels .....	27
2.3 Transcriptome analysis of <i>U. maydis</i> -infected maize lines of distinct disease resistance levels .....	31
2.3.1 Correlation analysis of maize gene expression to disease resistance levels ..	35
.....	35
2.4 Identification of <i>U. maydis</i> CSEPs targeting components of quantitative disease resistance .....	39
2.4.1 Intraspecific variation of UMAG_02297 .....	45
2.5 Host transcriptional changes induced by UMAG_02297 .....	49
2.6 QTL mapping for <i>U. maydis</i> disease resistance .....	52
2.6.1 Identification of local compatible <i>U. maydis</i> field isolates .....	52
2.6.2 Genetic map construction .....	54
2.6.3 QTL analysis .....	55
<b>3 Discussion</b> .....	<b>57</b>
3.1 <i>U. maydis</i> resistance levels of diverse maize lines .....	57
3.2 Maize processes involved in QDR against <i>U. maydis</i> .....	58

---

3.3	Maize line-specific gene expression in <i>U. maydis</i> .....	60
3.4	Maize line-specific activity of <i>U. maydis</i> CSEPs .....	62
3.5	The maize line-specific effector UMAG_02297.....	63
3.5.1	Sequence variation in UMAG_02297 orthologues .....	64
3.5.2	Manipulation of host gene expression by UMAG_02297 .....	66
3.5.3	Model for the maize line-specific function of UMAG_02297 .....	67
3.6	QTL mapping for <i>U. maydis</i> resistance in maize seedlings.....	69
3.7	Concluding remarks and perspectives.....	71
<b>4</b>	<b>Materials and Methods.....</b>	<b>73</b>
4.1	Materials and source of supply .....	73
4.1.1	Chemicals .....	73
4.1.2	Buffers and solutions.....	73
4.1.3	Enzymes, antibodies, and additional materials .....	73
4.1.4	Commercial kits.....	74
4.2	Media and cultivation methods for microorganisms .....	75
4.2.1	Media .....	75
4.2.2	Cultivation of <i>E. coli</i> .....	75
4.2.3	Cultivation of <i>U. maydis</i> .....	76
4.2.4	Determination of cell density .....	76
4.3	Microbial strains, plasmids, and oligonucleotides .....	76
4.3.1	<i>E. coli</i> strains.....	76
4.3.2	<i>U. maydis</i> strains.....	77
4.3.3	Oligonucleotides.....	78
4.3.4	Plasmids for transformation of <i>U. maydis</i> .....	84
4.4	Plant material and plant methods .....	86
4.4.1	Maize varieties .....	86
4.4.2	Cultivation of maize .....	87
4.4.3	Virulence assay of <i>U. maydis</i> on maize .....	87
4.5	Microbiology standard methods.....	88
4.5.1	Production of competent <i>E. coli</i> cells.....	88
4.5.2	Heat-shock transformation of <i>E. coli</i> .....	89
4.5.3	Preparation of <i>U. maydis</i> protoplasts.....	89
4.5.4	Transformation of <i>U. maydis</i> .....	90
4.5.5	Test for filamentous growth of <i>U. maydis</i> .....	90
4.6	Molecular biology standard methods .....	90
4.6.1	Plasmid isolation from <i>E. coli</i> .....	90



## Table of contents

---

4.6.2	Genomic DNA isolation from <i>U. maydis</i> .....	91
4.6.3	Genomic DNA isolation from colonised maize tissue .....	91
4.6.4	Total RNA isolation from colonised maize tissue .....	91
4.6.5	DNase digest after RNA isolation.....	92
4.6.6	Synthesis of cDNA.....	92
4.6.7	Quantification of nucleic acids .....	93
4.6.8	Polymerase chain reaction (PCR).....	93
4.6.9	Quantitative real-time PCR (qRT-PCR).....	93
4.6.10	Restriction enzyme digestion of DNA.....	93
4.6.11	Ligation of DNA fragments.....	94
4.6.12	Gibson assembly cloning.....	94
4.6.13	Agarose gel electrophoresis .....	94
4.6.14	Southern Blot analysis .....	95
4.6.15	Purification of DNA .....	97
4.6.16	Sequencing of DNA .....	97
4.6.17	Sequencing of RNA .....	97
4.6.18	KASP sequencing.....	97
4.7	Tissue fixation, staining and microscopy.....	98
4.7.1	WGA-AF488/Propidium iodide co-staining of colonised maize tissue .....	98
4.7.2	Fluorescence microscopy .....	98
4.7.3	Confocal laser-scanning microscopy .....	98
4.8	Bioinformatics .....	98
4.8.1	RNA-Seq analysis .....	98
4.8.2	WGCNA.....	99
4.8.3	GO enrichment analysis .....	100
4.8.4	Mapping of maize genes to Arabidopsis .....	100
4.8.5	Intraspecific sequence variation analysis .....	100
4.8.6	QTL Mapping.....	101
4.8.7	Further bioinformatics tools.....	101
4.8.8	Data availability .....	101
<b>5</b>	<b>Bibliography.....</b>	<b>102</b>
<b>6</b>	<b>Appendix .....</b>	<b>124</b>
	Eidesstattliche Erklärung.....	130
	Delimitation of own contribution.....	131
	Acknowledgements .....	132
	CV .....	133



## 1 Introduction

One of the major challenges for humankind is to supply sufficient food for a growing world population, intensified by harshening conditions due to climate change (Alexandratos and Bruinsma 2012). Grain crops are the main food supply and provide more than half of the world population's food energy intake. Cultivation success of such crop plants highly depends on the prevalent abiotic and biotic environmental conditions, which include light, temperature, soil properties, nutrient availability, and interactions with microbiota. Outbreaks of plant diseases have struck humans throughout history, such as the infamous Irish potato famine caused by the oomycete *Phytophthora infestans* (Turner 2005). Nowadays, diseases caused by parasitic microbes are still a persistent problem that seriously limits agricultural productivity (Figure 1.1). Pathogens including bacteria, fungi and viruses are estimated to account for 16% of crop losses (Oerke and Dehne 2004; Oerke 2006). Especially fungi and oomycetes are the causal agents of some of the most notorious plant diseases posing a true threat to global food security, and cause severe economic damage with annual losses of more than 200 billion USD (Birren et al. 2002; Fisher et al. 2012).

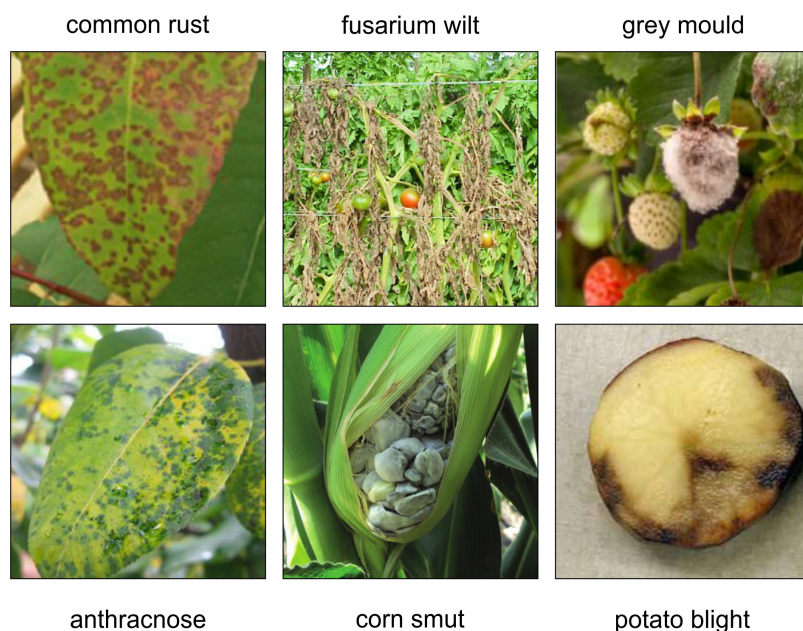


**Figure 1.1. Plant diseases.** Plant pathogenic microbes cause severe losses in agricultural production and are a true threat to global food security. Pictures from: Lim et al. 2006; Alves et al. 2011; Galicia-García et al. 2016; Fu et al. 2019; Petrasch et al. 2019; Giménez-Ibáñez 2020.

To develop new strategies for high yields in a sustainable agriculture, a deep understanding of the fundamental molecular processes that underlie the interactions of plants and pathogens is required.

## **1.1 Plant defence and microbe counteractions**

In natural environments, plants are constantly exposed to a myriad of microbes that they associate with in various ways. The establishment of symbiotic plant-microbe interactions is a highly complex and sophisticated process, which can have beneficial (mutualism), neutral (commensalism) or detrimental (parasitism) outcomes for the plant. Plant pathogens aim to colonise their host plants to gain nutrients and fulfil their life cycle, which often has substantial negative effects for the host. To this end, pathogens have evolved different lifestyles and strategies of infection: some actively kill host cells to live on the decomposing organic compounds (necrotrophy; Horbach et al. 2011), others, in contrast, feed on nutrients provided by the living host cells (biotrophy). Therefore, biotrophs establish an intimate and highly adapted interaction with the colonised tissue and manipulate diverse host processes to avoid recognition, and redirect nutrient supply towards their needs (Lo Presti et al. 2015). Combinations of these nutritional strategies exist, in which pathogens first go through an initial biotrophic phase, followed by a necrotrophic lifestyle (hemibiotrophy; Horbach et al. 2011). In all cases, pathogens must cope with various plant defence mechanisms to successfully colonise the host tissue.

### **1.1.1 Plant innate immunity**

To ward off herbivores or (unwanted) microbes, plants hold a first line of constitutive defence components, which include preformed physical barriers such as rigid cell walls, thorns or hairs and wax layers as well as chemical barriers including saponins, glucosinolates or antimicrobial enzymes (Heath 2000; Muthamilarasan and Prasad 2013). In addition to these constitutive barriers, effective defence responses are crucial for plant survival following pathogen attack. Plants have therefore evolved a sophisticated signalling network to mediate adequate responses depending on the invading pathogen's infection strategy. This signalling network is partly linked to the defence hormones salicylic acid (SA) and jasmonic acid (JA)/ethylene (ET; Bari and Jones 2009). The SA and JA/ET pathways act antagonistically: SA signalling is generally involved in activation of defence responses to biotrophic and hemibiotrophic pathogens, whereas JA/ET induce defence responses to necrotrophic pathogens and herbivorous insects (Glazebrook 2005;

Gamalero and Glick 2012; Wasternack and Hause 2013). SA signalling leads to the production of reactive oxygen species (ROS), which are highly toxic and can damage invading pathogens (Tamaoki 2008). ROS additionally serve as signaling molecules to control defence and induce programmed cell death at the site of pathogen attack, thereby hindering the spread of biotrophic pathogens (Apel and Hirt 2004). In contrast, JA acts as an antagonist to cell death, thereby counteracting necrosis induced by necrotrophic pathogens (Rao et al. 2000).

To respond appropriately, plants need to be able to perceive invading pathogens through the signals they produce (Müller et al. 2016). In contrast to mammals, which carry mobile defence cells and a somatic adaptive immune system, plants rely on the multi-layered innate immunity of each cell and on systemic signals emitted from sites of pathogen attack (Jones and Dangl 2006; Jones et al. 2016). The first layer is based on the recognition of broadly conserved pathogen- or microbe-associated molecular patterns (PAMPs/MAMPs), for example bacterial flagellin or fungal chitin, by cell surface-localised pathogen recognition receptors (PRRs), which include receptor-like kinases (RLKs) and receptor-like proteins (RLPs; Zipfel 2008; Yu et al. 2017, Figure 1.2). PRRs can form complexes with other RLKs or RLPs, leading to increased specificity and allowing cross-talk between multiple pathways, and thereby balancing PRR-signaling output (Couto and Zipfel 2016; Tang et al. 2017). Besides PAMP-recognition, PRR signaling can also be triggered by plant-derived damage-associated molecular patterns (DAMPs) that are released through e.g. cell wall degradation by an invading pathogen (Boller and Felix 2009; Brown and Tellier 2011; Albert 2013). PRR activation results in rapid responses leading to the induction of pattern-triggered immunity (PTI), which involves early and late defence responses (Boller and Felix 2009; Monaghan and Zipfel 2012, Figure 1.2, step 1). One of the first responses is the rapid influx of calcium ( $\text{Ca}^{2+}$ ) into the cell and the generation of extracellular ROS, resulting in the activation of defence-related mitogen-activated protein kinase (MAPK) cascades and ultimately expression changes of defence genes (Boller and Felix 2009; Seybold et al. 2014; Lee et al. 2015; Couto and Zipfel 2016). In later defence responses, signals released upon PTI can be amplified by phytohormones like SA or JA, which additionally induce the accumulation of antimicrobial compounds and reinforce cell wall components such as callose or lignin as well as the expression of pathogenesis-related (PR) genes like chitinases and glucanases (Lee et al. 2015; Couto and Zipfel 2016). In general, PTI is pathogen-unspecific and can elevate the responsiveness to other PAMPs and therefore might prime further defence responses (Zipfel et al. 2004).

To overcome PTI, successful pathogens secrete numerous molecules called effectors into the plant cell or the apoplast (Giraldo and Valent 2013, Figure 1.2, step 2). On the one hand, these effectors can contribute to virulence and cause effector-triggered

susceptibility (ETS); on the other hand, they can be targets of immune receptors, the resistance (R) proteins, which constitute the second branch of the innate immune system (Jones and Dangl 2006, Figure 1.2, step 3 and 4). Most R genes encode intracellular nucleotide-binding leucine-rich repeat proteins (NLRs), and hundreds of diverse NLR genes can be found in plant genomes (Dangl and Jones 2001; McHale et al. 2006; Cui et al. 2015). Depending on their specific N-terminal domain, NLRs can be grouped into two different classes: TIR-NLRs (TNLs) contain a Toll-interleukin 1 receptor (TIR) domain and are only present in dicots; CC-NLRs (CNLs) contain a coiled-coil (CC) domain and are present in both monocots and dicots (Jacob et al. 2013; Cui et al. 2015). R-gene recognition of effectors, which are then called avirulence factors, mounts effector-triggered immunity (ETI, Figure 1.2, step 5). The recognition of effectors by R proteins is highly specific and can either be direct by receptor binding of the effector, or indirect (Cesari 2018; Monteiro and Nishimura 2018). The process of indirect effector recognition is currently described by three different models: the guard model, the decoy model and the integrated decoy model (Cesari et al. 2014; Wu et al. 2015). In the guard and decoy model, NLRs monitor the integrity of host-effector targets or their structural mimics (decoys). In the integrated decoy model, the effector target decoy is directly integrated into the NLR (Cesari et al. 2014; Jones et al. 2016, Figure 1.2, step 4). Moreover, increasing evidence suggests that many NLRs function synergistically or antagonistically in pairs to trigger ETI responses by dimerization of their N-terminal regions (Wang et al. 2020; Feehan et al. 2020).

During ETI, PTI-triggered defence responses are amplified, and the accumulation of ROS and SA is induced. This leads to hypersensitive response (HR) and systemic acquired resistance (SAR), which result in programmed cell death of host cells and long-term priming for further pathogen attack (Dangl and Jones 2001; Dodds and Rathjen 2010; Fu and Dong 2013; Conrath et al. 2015). Again, successful pathogens need to secrete effectors to interfere with ETI, which yet again can be recognized by new plant R genes. In this arms race of pathogen and host, severe selective forces lead to the co-evolution of new pathogen effectors and plant R proteins, resulting in complex effector-R protein networks, as described in the 'zig-zag model' (Jones and Dangl, 2006).

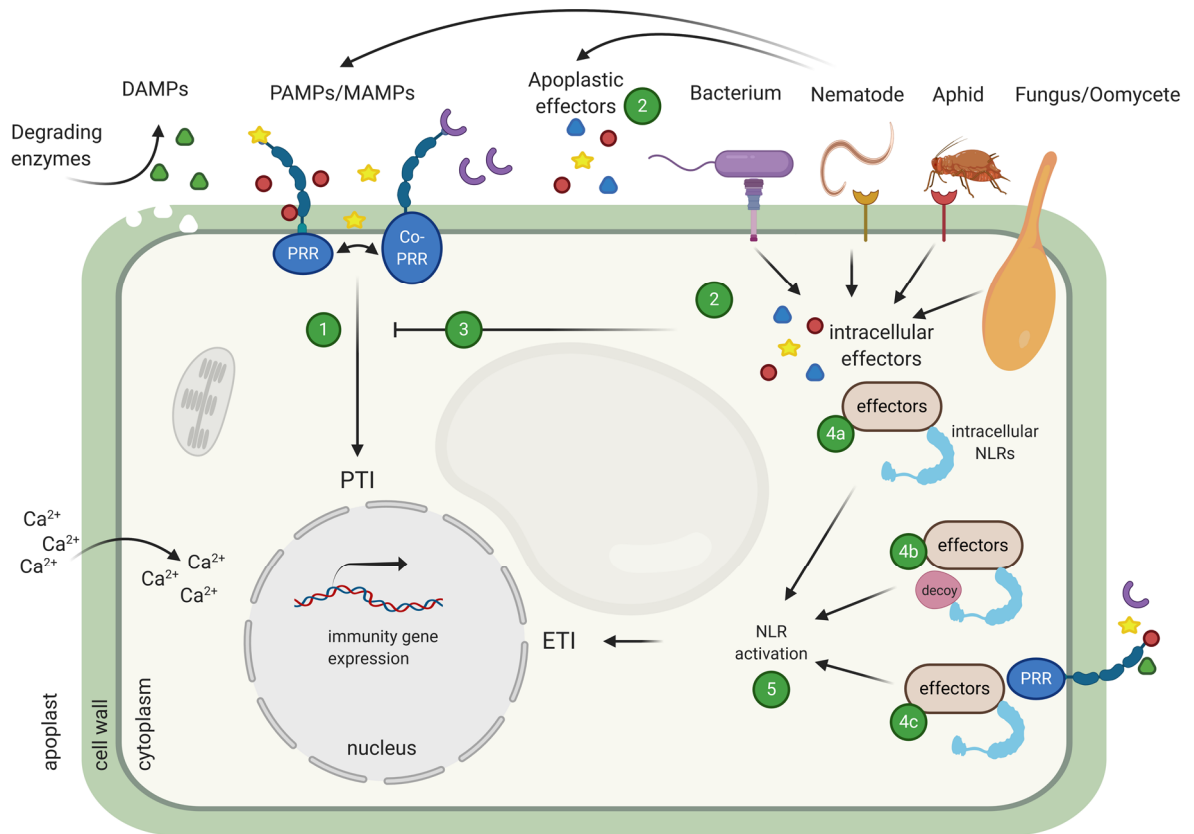


**Figure 1.2. Schematic of the plant immune system.** Damage-, pathogen- and microbe-associated molecular patterns (DAMPs, PAMPs and MAMPs, respectively) are perceived as danger signals through pattern recognition receptors (PRRs) and initiate PRR-mediated immunity (PTI, step 1). Pathogens deliver virulence effectors to both the apoplast and to the cytoplasm (step 2). These effectors can suppress PTI and facilitate virulence (step 3). Intracellular NLRs can perceive effectors in three ways: first, by direct receptor ligand interaction (step 4a); second, by sensing effector-induced changes in a decoy protein that structurally mimics an effector target, but has no other function in the plant cell (step 4b, integrated decoy model); and third, by sensing effector-induced changes of a host virulence target, like the cytosolic domain of a PRR (step 4c). Effector perception results in NLR-dependent effector-triggered immunity (ETI, step 5). Modified from Boller and Felix (2009); Dangl et al. (2013). Created with BioRender.com.

However, with new emerging knowledge, the two layers of plant immunity described by this model have been blurred. Since not all effectors are translocated into the host cell, they can also be recognised in the apoplast by extracellular receptors that are similar to PRRs, and can sometimes be widely conserved among pathogens, making them comparable to PAMPs. On the other side, similar to effectors, PAMPs can also exhibit some sequence diversity (Thomma et al. 2011; Kanyuka and Rudd 2019; van der Burgh and Joosten 2019). Furthermore, transcriptome analyses showed an important overlap of genes involved in PTI and ETI, suggesting that PTI and ETI activate interacting pathways leading to plant immunity (Navarro et al. 2004; Dong et al. 2015). Therefore, revised models of plant immunity that do not sharply discriminate between PTI and ETI have been proposed. The ‘spatial invasion model’, for example, is based on the spatial localisation of the receptors that recognise the immunogenic pattern and that induce immune responses

(Cook et al. 2015; Kanyuka and Rudd 2019). Therein, two spatially separated host receptor types detect microbe- or host-derived molecules that signal invasion ('invasion molecules', IMs) either in the apoplast ('cell surface immune receptors', CSIRs) or inside the host cell ('intracellular immune receptors', IIRs), triggering mechanistically distinct defence responses.

### **1.1.2 Effectors in plant-pathogen interactions**

Plants can be colonised by fungi that have developed highly diverse lifestyles such as necrotrophy, biotrophy or mutualism (Chapter 1.1). Irrespective of their lifestyle, all fungi that colonise plants are recognised by the plant immune system. Therefore, they must avoid eliciting host defence responses, cope with or suppress them in order to establish compatible interactions (Lo Presti et al. 2015). This is facilitated by secretion of effectors that e.g. mask the fungus, suppress PTI or ETI, or manipulate host cell physiology to provide nutrients (de Jonge et al. 2011; Giraldo and Valent 2013; Ökmen and Doehlemann 2014; Zuccaro et al. 2014). Most commonly, effectors are defined as small proteins that are secreted by a pathogen during host invasion and that promote colonisation (Dodds and Rathjen 2010; de Jonge et al. 2011). In addition to proteins, secreted small RNAs and secondary metabolites can act as effectors as well (Collemare et al. 2019). Pathogen effectors are employed in a spatio-temporal manner, acting either in the apoplast or within plant cells (Doehlemann and Hemetsberger 2013; Toruño et al. 2016). Apoplastic effectors often contain cysteine residues, that can form disulfide bridges and stabilise the protein in the harsh environment of the host apoplast, and many target host proteases (Doehlemann and Hemetsberger 2013; Wang and Wang 2018). Intracellular effectors are translocated to various cellular compartments where they interfere with plant physiology or target vulnerable immunity hubs (Lo Presti and Kahmann 2017). Effectors from gram-negative bacteria are delivered into the host cells through a type III secretion system (Navarro et al. 2008; Dangl et al. 2013). How effectors from filamentous pathogens are trafficked is in contrast poorly understood (Dodds et al. 2009; Giraldo and Valent 2013; Petre and Kamoun 2014). Often, effectors from filamentous pathogens bear a signal peptide for secretion via the endoplasmic reticulum, but delivery to the host also occurs via unconventional secretion (Lo Presti et al. 2015). In oomycetes, effector proteins lack a secretion signal but contain a conserved N-terminal RXLR motif which is required for their secretion (Whisson et al. 2007). Another frequent feature of effectors from filamentous pathogens is the lack of sequence identity with any known functional domain, which reflects the evolutionary pressure as a driver of effector



diversification (Stergiopoulos and de Wit 2009; Ökmen and Doehlemann 2014; Mukhi et al. 2020). As a result of the continuous selection pressure that is exerted from the host's immune system, effectors frequently represent the fastest evolving genes within a pathogen's genome and consequently are commonly species- or even race-specific (Sánchez-Vallet et al. 2018; Plissonneau et al. 2018; Depotter and Doehlemann 2020). However, also highly conserved effector proteins exist (Orbach et al. 2000; de Jonge et al. 2010; Djamei et al. 2011; Mentlak et al. 2012; Gan et al. 2013; Stergiopoulos et al. 2014; Hemetsberger et al. 2015).

### **Common effector targets in host plants**

Because plants depend on conserved defence strategies, invading pathogens must overcome similar defence responses. Hence, despite the high diversity of effectors, often a limited number of central defence processes are their targets (Ökmen and Doehlemann, 2014).

Plant proteases are involved in the perception and signaling upon pathogen attack and degrade effectors secreted by invading pathogens. This makes them one of the key targets of various effectors, such as EPIC1 and EPIC2B from the oomycete *P. infestans*, which inhibit host cysteine proteases (Tian et al. 2007; Song et al. 2009; Mueller et al. 2013). Plant immune receptors are crucial for pathogen perception and therefore represent another common target (Göhre and Robatzek 2008). For example AvrPto from *Pseudomonas syringae* impedes PTI signaling through kinase inhibition of FLS2 and EFR (Xiang et al. 2008). As chitin is an important structural component of the fungal cell wall and absent in plants, it represents an ideal PAMP recognised by plant immune receptors. Host chitinases degrade the fungal cell wall, resulting in loss of cell integrity and release of chitin fragments, which can trigger PTI. To counteract chitinases, fungal pathogens have developed different strategies: in the tomato pathogen *Cladosporium fulvum*, Avr4 protects the fungal cell wall against chitinase degradation (van den Burg et al. 2006; van Esse et al. 2007), while the LysM domain effector Ecp6 sequesters released chitin fragments to avoid PAMP recognition through CERK1 (de Jonge and Thomma 2009; de Jonge et al. 2010; Sánchez-Vallet et al. 2013). In addition to chitinases, also glucanases are secreted to attack the cell wall of invading pathogens, making them another important effector target (Rose et al. 2002; Sánchez-Rangel et al. 2012). Due to their fundamental role in plant defence and physiology, phytohormone pathways are manipulated by many effectors (reviewed by Kazan and Lyons 2014). The phytohormone SA is a key molecule in defence signaling against biotrophs and for induction of cell death. Therefore, biotrophic

pathogens have developed strategies to prevent SA accumulation. For example, the oomycete pathogen *Phytophthora sojae* secretes the isochorismatase Pslsc1 to inhibit SA synthesis (Liu et al. 2014). JA is mainly induced in resistance against necrotrophic pathogens and acts as an antagonist of SA signalling. Therefore, some biotrophic pathogens induce the JA pathway to suppress SA-mediated defences, as for example through the effector HopZ1a from *P. syringae* (Jiang et al. 2013; Plett et al. 2014). Because ROS serve as signalling molecules inducing defence responses like HR (Apel and Hirt 2004), biotrophic pathogens secrete effectors preventing their accumulation. The obligate biotrophic fungus *Blumeria graminis* f. sp. *hordei* for example secretes the catalase catB to scavenge H<sub>2</sub>O<sub>2</sub> at sites of fungal germ tube invasion during infection (Zhang et al. 2004).

Following the definition of effectors as proteins and small molecules that alter host-cell structure and function, all genomes of plant pathogenic fungi and oomycetes contain hundreds of putative effector genes (Hogenhout et al. 2009; Doehlemann and Hemetsberger 2013). As the effector repertoire is a major determinant of the success of plant-pathogen interactions, the discovery of effectors is of great interest. Proteomics, comparative genomics, as well as *in planta* expression studies have been employed as tools for effector discovery. Recently, association mapping approaches, the analysis of pan genomes, as well as machine learning bioinformatics pipelines such as EffectorP2.0 (effectorp.csiro.au; Sperschneider et al. 2018) have helped identifying effector candidates in pathogen genomes (reviewed in Kanja and Hammond-Kosack 2020). However, to date only few pathogen effectors have been characterised in depth. The further functional characterisation of the complex effector repertoires secreted by pathogens and their respective virulence targets will help to shed light into the mechanisms involved in plant defence and guide the development of effective disease control strategies.

### 1.1.3 Quantitative disease resistance

Large-effect R genes such as NLRs, which lead to either almost complete resistance or susceptibility, are crucial determinants of plant innate immunity (Chapter 1.1.1). Accordingly, R gene-mediated resistance is often also referred to as qualitative resistance (Figure 1.3A). However, both in natural populations as well as in crops, mostly incomplete resistance is observed, as shown by a continuous distribution of susceptible to resistant phenotypes (Bartoli and Roux 2017). This is usually referred to as quantitative disease resistance (QDR; Roux et al. 2014). Here, the disease resistance phenotype is determined by multiple quantitative trait loci (QTLs) that form an intricate network integrating multiple response pathways to several pathogen factors and environmental signals (Poland et al. 2009; St.Clair 2010; Roux et al. 2014; Niks et al. 2015; Corwin and Kliebenstein 2017, Figure 1.3B). Hence, genetic variation at hundreds of causal genes can determine QDR outcomes.

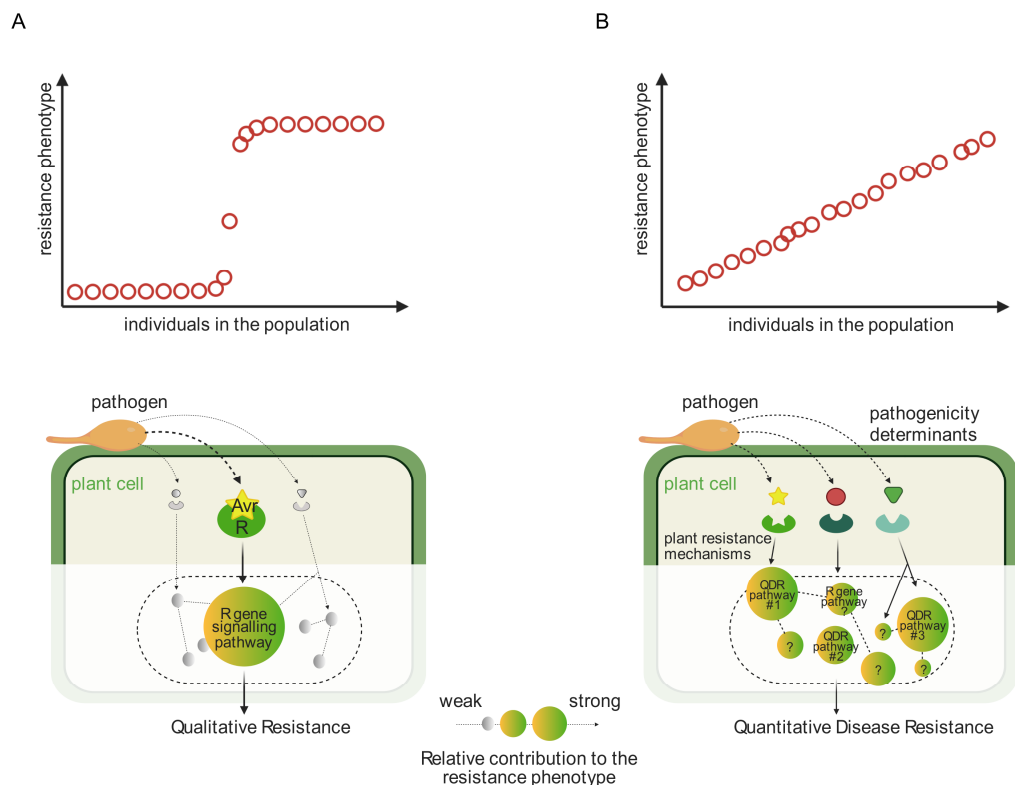


**Figure 1.3. Qualitative versus quantitative plant disease resistance. A) Principles of qualitative disease resistance.** For qualitative resistance, the disease resistance phenotype follows a binary 'susceptible or resistant' distribution, resulting from the perception of a single pathogen effector (Avr) by a plant resistance (R) gene. **B) Principles of quantitative disease resistance.** For quantitative disease resistance (QDR), a continuous distribution from susceptibility towards resistance is observed in the population, which is the result of the integration of multiple perception pathways each having a relatively minor contribution to the overall resistance phenotype. Modified from Roux et al. 2014. Created with BioRender.com.

Current studies in molecular plant pathology have mainly focused on understanding the molecular mechanisms of qualitative resistance, as the large-effect genes are more easily available for detailed molecular analysis. In contrast, mechanisms controlling QDR still remain poorly understood (Poland et al. 2009; Roux et al. 2014; Corwin and Kliebenstein 2017). Even though many QDR loci have been mapped in the past, the underlying complex genetic architecture has limited the molecular characterisation of mechanisms involved (Corwin and Kliebenstein 2017). Still, several QDR genes with various functions have been cloned recently. In several cases, kinases have been shown to play important roles in QDR. Two maize wall-associated kinases, ZmWAK-RLK1 and ZmWAK, confer QDR to Northern leaf blight and head smut, respectively (Zuo et al. 2015; Hurni et al. 2015). Other QDR genes encode putative transporters, the ABC (adenosine triphosphate [ATP]-binding cassette) transporter encoded by Lr34 confers resistance to diverse fungal pathogens in wheat (Krattinger et al. 2009). A caffeoyl-CoA O-methyltransferase connected to lignin production was shown to confer QDR to various necrotrophic pathogens of maize (Yang et al. 2017). Antimicrobial metabolites are implicated in QDR to several pathogens as well. GSH1, a gene involved in the biosynthesis of glutathione, is important for limiting the spread of virulent *P. syringae* and for establishing disease resistance to *Phytophthora brassicae* in *Arabidopsis thaliana* (Parisy et al. 2006). Genes influencing plant growth, development and architecture often also have pleiotropic effects on QDR. For example, genes controlling flowering time have been found to be strongly correlated with QDR to many necrotrophic pathogens and in addition, several developmental stage-specific resistance QTLs have been identified (Thompson and Bergquist 1984; Steffenson et al. 1996; Collins et al. 1999).

Matching defence responses to the lifestyle of the invader is of critical importance. Hence, it is not surprising that also genes involved in the regulation of the SA and JA/ET pathways contribute to QDR. For example the *A. thaliana* WRKY33 gene, encoding a WRKY transcription factor balancing the cross-talk between JA- and SA-regulated disease response pathways, is involved in resistance to *Botrytis cinerea* and *Alternaria brassicicola* (Zheng et al. 2006). Other genes identified in QDR correspond to previously uncharacterised defence genes, such as the soybean wound-inducible domain protein W112, the soybean serine hydroxymethyltransferase RHG4 and the rice proline-containing protein Pi21, which lack similarity to any currently known defence-related genes (Fukuoka et al. 2009; Cook et al. 2012). Additionally, studies of QDR by RNA-Seq approaches indicated highly interconnected and multifaceted defence responses, which were mostly distinct from functions previously identified for plant immunity (Kebede et al. 2018; Pan et al. 2018; Delplace et al. 2020). However, some components of PTI and ETI have also been found to condition quantitative differences in disease resistance. Mutations in the

chitin receptor CERK1 or the flagellin receptor FLS2, which both play essential roles in PTI, have been reported to result in quantitatively reduced resistance to the biotrophic fungal pathogen *Erysiphe cichoracearum* or bacterial colonisation, respectively (Zipfel et al. 2004; Ramonell et al. 2005; Wan et al. 2008). In rare cases, also NLR genes can underlie QDR (Poland et al. 2009; Barbacci et al. 2020), which drives the hypothesis that allelic variants, i.e. weak alleles, of R genes can cause incomplete resistance. This is also supported by the physical co-localisation of resistance QTLs and R genes in genomes of several species, including rice, maize and potato (Wang et al. 1994; Gebhardt and Valkonen 2001; Xiao et al. 2007). Thus, the dichotomy of qualitative versus quantitative disease resistance is obliterated, as strong-effect R genes might be eroded through pathogen evolution, converting them into quantitative resistance genes. Nonetheless, this form of QDR likely primarily accounts for resistance towards biotrophic pathogens for which R gene-mediated defence is mostly effective (Poland et al. 2009). However, QDR against biotrophs is rarely described, and QDR is mostly considered to be the predominant form of defence against generalist necrotrophs such as *Sclerotinia sclerotiorum* and *B. cinerea* (Denby et al. 2004; Perchepped et al. 2010).

Compared to qualitative resistance, the molecular functions underlying QDR are highly diverse and involve aspects such as plant morphology and development, components of signal transduction systems, antimicrobial compounds such as phytoalexins, and other previously unknown factors. In general, even though some mechanisms of QDR were found to overlap with genes mediating qualitative resistance, the predominant mechanisms of QDR extend beyond pathogen recognition (Corwin and Kliebenstein 2017). Due to the high selective pressures exerted by large-effect R genes on adapted pathogens, qualitative resistances are expected to be overcome rapidly in the field. In contrast, breakdown of QDR is considered less likely because of the smaller effects of QDR genes and their presumed broader specificity, rendering QDR more durable and therefore of special interest for sustainable crop protection strategies (Parlevliet 2002; Poland et al. 2009; St.Clair 2010; Roux et al. 2014; Niks et al. 2015).

## 1.2 *Ustilago maydis*: the causative agent of corn smut disease

The biotrophic basidiomycete fungus *Ustilago maydis* causes smut disease in maize (*Zea mays*) and its wild relative teosinte (*Euchlaena mexicana*; Martínez-Espinoza et al. 2002). Characteristic disease symptoms include local tumours in which spores develop and that can be formed on all above-ground organs in less than a week, including leaves, ear and tassel (Figure 1.4f; Basse and Steinberg 2004; Kämper et al. 2006). *U. maydis* has the potential to cause severe yield losses, since stunting, reduction of grain and even death of plants can be the consequences of infection. Nevertheless, smut galls, then named “huitlacoche”, also serve as a delicacy in several regions of the world (Lübberstedt et al. 1998).

### 1.2.1 Pathogenic development of *U. maydis*

As for most smuts, *U. maydis* displays a dimorphic life cycle. Under favourable conditions, the diploid teliospores germinate, undergo meiosis and form a pro-mycelium, in which four haploid nuclei migrate into different compartments (Figure 1.4a; Snetselaar and Mims 1992). Haploid cells then bud off after mitosis and enter the non-pathogenic vegetative state, in which the fungus grows as saprophytic yeast-like sporidia which proliferate via budding (Figure 1.4b; Christensen 1963; Banuett and Herskowitz 1996). The infection cycle is initiated by recognition and fusion of sporidia with compatible mating types on an appropriate host surface, leading to a morphological switch to diploid pathogenic filaments (Figure 1.4c; Bölker et al. 1992; Spellig et al. 1994).

Upon perception of a hydrophobic surface and cutin monomers, the filaments form specialised infection structures, the appressoria, and thereby penetrate the plant epidermis using turgor pressure and lytic enzymes (Figure 1.4d; Mendoza-Mendoza et al. 2009). During colonisation, the fungal hyphae are surrounded by the host plasma membrane and form a tight interaction zone. This interaction zone, the so-called biotrophic interface, is the site of nutrient and signal exchange as well as of effector secretion (Figure 1.4e; Bauer et al. 1997; Brefort et al. 2009; Doehlemann et al. 2009; Lanver et al. 2017). As the infection progresses, the hyphae reach the mesophyll and grow mostly along or inside the vascular bundles, likely to access nutrients (Matei and Doehlemann 2016). The formation of tumours is initiated around 4 days post infection (dpi) on the cellular level and becomes macroscopically visible 5 dpi (Banuett and Herskowitz 1996; Doehlemann et al. 2008a). Tumour development is associated with both plant cell enlargement and an increase of cell divisions (Doehlemann et al. 2008a; Matei et al. 2018). Then, inside the mature tumours, fungal hyphae form large aggregates within

## 1. Introduction

apoplastic cavities and become embedded in a gelatinous polysaccharide matrix (Snetselaar and Mims 1994). After fragmentation of the hyphae, black ornamented teliospores, which mainly perform the dispersal of fungal inoculum, are formed (Figure 1.4f; Banuett and Herskowitz 1996; Begerow et al. 2006).

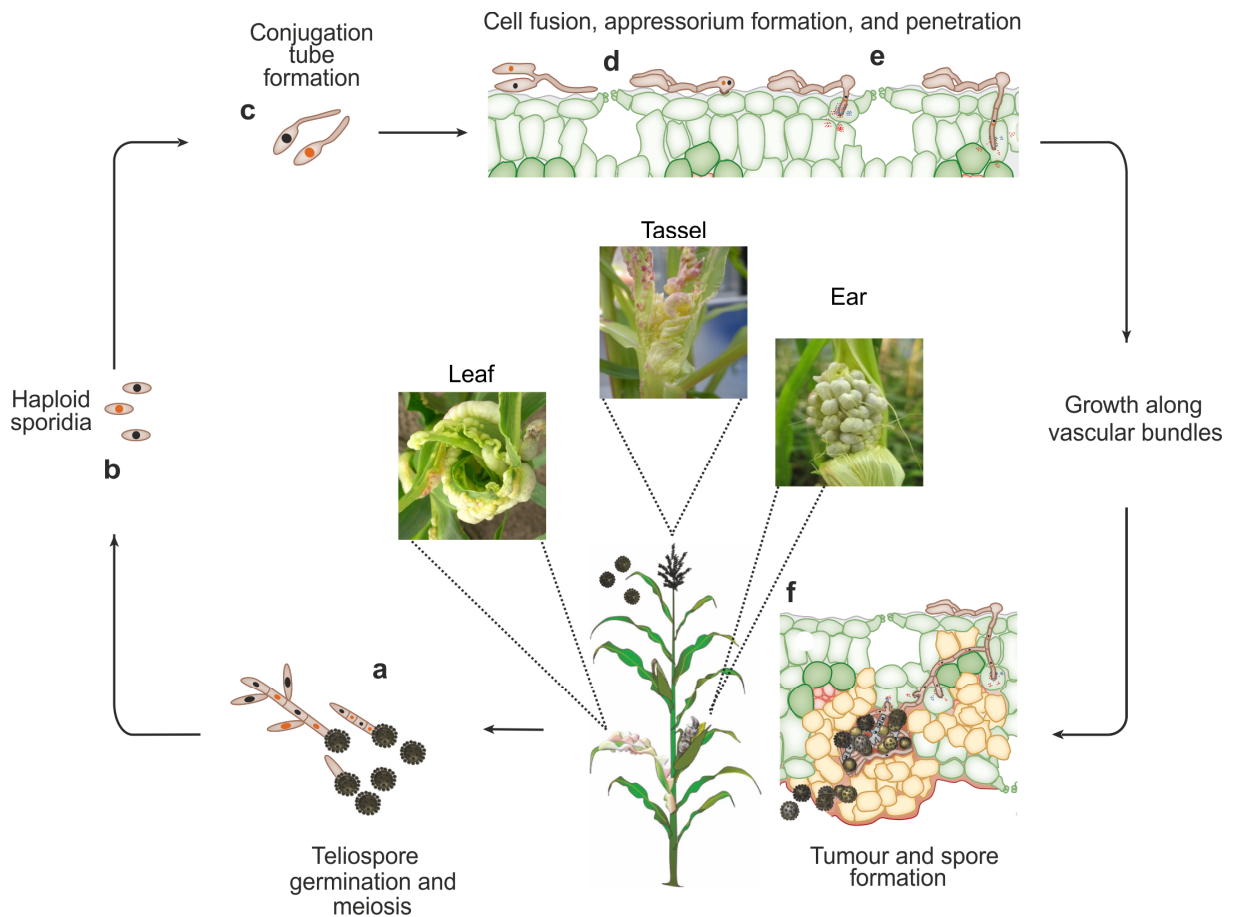


**Figure 1.4. The life cycle of *Ustilago maydis*.** The dimorphic life cycle of *U. maydis* can be divided into a yeast-like saprophytic and filamentous biotrophic phase. Characteristic disease symptoms are tumours that can be formed on all above-ground organs including leaves, ear, and tassel. (a) Teliospores germinate and undergo meiosis to form haploid sporidia, which grow saprophytically (b) until they encounter their compatible mating partners. (c) Cell fusion of two haploid mating types on a host plant leads to the development of infectious dikaryotic hyphae. (d) *U. maydis* forms appressoria to penetrate the host. Biotrophic hyphae grow both inter- and intracellularly, whereas intracellular hyphae are invaginated by the plant plasma membrane building the biotrophic interface. (e) During colonisation, effector proteins are secreted into the host to modulate host defence and metabolism. As the infection progresses, the hyphae reach the mesophyll and mostly grow along vascular bundles. (f) Tumour formation is initiated, and fungal hyphae form large aggregates within them. At the late stage of infection, mature tumours break open and release black teliospores for a new round of infection. Modified from Zuo et al. 2019. Pictures from A. Redkar.

Due to its unique morphological features, rapid symptom development, very compact genome, easy *in-vitro* cultivation and accessibility to genetic manipulation, *U. maydis* has advanced to an important model system for the study of fungal cell biology and biotrophic fungal pathogens (Kämper 2004; Brefort et al. 2009; Dean et al. 2012; Schuster et al. 2016; Zuo et al. 2019; Zuo et al. 2020a). The generation of the solopathogenic strain SG200, which can form infectious filaments without prior mating, has furthermore greatly facilitated the investigation of *U. maydis* pathogenic development (Kämper et al. 2006). Yet, many of the molecular mechanisms that underlie *U. maydis* infection are still not understood.

### **1.2.2 Maize responses to *U. maydis* infection**

On the host side, very early responses to *U. maydis* infection involve the induction of genes with a function in immunity, stress response and redox regulation, showing that *U. maydis* is initially recognised and elicits plant defence reactions. However, already 24 hours post inoculation (hpi) with establishment of the biotrophic interaction, these initial responses are attenuated as several genes involved in redox regulation and defence are downregulated compared to the very early time point. Furthermore, levels of the antioxidant glutathione (GSH) are elevated 24 hpi and increase further during the infection process (Doehlemann et al. 2008a). In addition to its correlation to the induction of PR genes, GSH plays a major role in secondary metabolite synthesis (Loyall et al. 2000; Gomez 2004; Senda and Ogawa 2004). Correspondingly, genes involved in the shikimate and phenylpropanoid pathways are upregulated as well, which goes along with an induction of genes involved in the synthesis of lignin and other phenolic compounds (Doehlemann et al. 2008a; Kretschmer et al. 2017a).

In general, infection leads to establishment of tumour tissue as a strong sink organ for carbohydrates (Horst et al. 2008). In infected tissue, chloroplast and photosynthetic functions are impaired, which is accompanied by a decrease of photosynthetic pigments (Horst et al. 2008; Doehlemann et al. 2008a; Kretschmer et al. 2017a; Matei et al. 2018). The reduction of photosynthetic pigments is likely responsible for prevention of leaf maturation from sink to source organ, resulting in increased carbon supply and enhanced susceptibility to *U. maydis* (Kretschmer et al. 2017a; Kretschmer et al. 2017b; Matei et al. 2018). The changes of carbon allocation can directly promote fungal growth and might also influence plant defence, given the involvement of sugars in plant immunity signalling (Roitsch et al. 2003; Bolouri Moghaddam and Van den Ende 2013; Kretschmer et al. 2017b).



Similarly, amino acid homeostasis is perturbed and nitrogen-rich amino acids substantially increase during tumour formation (Horst et al. 2010). This probably contributes to defence rather than serving as a nitrogen source for the fungus (Kretschmer et al. 2017a). Taken together, a broad reprogramming of maize physiology occurs during *U. maydis* infection, and carbon as well as nitrogen assimilates are rerouted towards the tumour.

Additionally, various phytohormones are altered upon *U. maydis* infection. JA signalling components antagonising the SA pathway and JA defence genes such as defensins and chitinases are upregulated immediately after infection (Doehlemann et al. 2008a). Furthermore, the Bax-inhibitor 1 and cystatin genes are induced, while caspases are repressed, suggesting that *U. maydis* infection goes along with an inhibition of the plant cell death programme (Doehlemann et al. 2008a). Auxin plays an important role during *U. maydis* infection too, as tumours contain elevated auxin levels (Turian and Hamilton, 1960) and auxin synthesis as well as auxin-responsive genes are induced during tumour development (Doehlemann et al. 2008a). Elevated plant-derived auxin levels likely govern the observed cell enlargement in *U. maydis*-induced tumours. In addition, auxins could also play a more direct role in plant resistance by antagonising the SA pathway (Wang et al. 2007).

For leaf tumour formation, *U. maydis* actively triggers DNA synthesis and cell division (Redkar et al. 2015). Bundle sheath cells proliferate and convert to hyperplastic tumour cells, while mesophyll cells enlarge and convert to hypertrophic tumour cells (Matei et al. 2018). In the different tumour cell types, genes involved in the regulation and performance of the cell cycle are differentially regulated, reflecting the distinct cell behaviours (hyperplasia vs hypertrophy; Villajuana-Bonequi et al. 2019). In the tassel however, cell division is already active and tumours largely result from re-channelling of development into a tumour pathway (Gao et al. 2013).

### 1.2.3 Effectors in the *U. maydis*-maize interaction

Throughout the infection cycle, *U. maydis* highly depends on the secretion of effector proteins to mitigate early defence responses as well as in later stages of pathogenesis for tumour formation (Kämper et al. 2006). The *U. maydis* genome is predicted to encode 553 secreted effector proteins, of which the majority is novel and lacks known functional or structural domains (Dutheil et al. 2016; Schuster et al. 2018). A subset of effectors, referred to as core effectors, is shared between species and is thought to facilitate initial host colonisation and target conserved immune responses. In contrast, accessory effectors are more diversified and act in host-, organ- or cell type-specific ways (Schuster et al. 2018; Zuo et al. 2019). Many effectors reside in clusters in the genome, which likely are the result of gene duplications for effector diversification (Kämper et al. 2006). Furthermore, effector genes are encoded in genome regions of low sequence conservation, while the rest of the genome is well-conserved when comparing to related smut fungi, which probably reflects the ongoing co-evolution in the arms race of effectors with their host targets for efficient defence suppression (Schirawski et al. 2010).

Several effectors with virulence functions have been identified, but the molecular mode of action has still only been elucidated in a few cases (Kämper et al. 2006; Lanver et al. 2017; Zuo et al. 2019). In the following, the diverse functions of *U. maydis* effectors that have been characterised so far are described.

As *U. maydis* effectors are crucial during all stages of colonisation, they act in the apoplast as well as within host cells after translocation. The core effector Pep1 for example is essential for successful penetration and suppresses pattern-triggered ROS bursts via inhibition of the apoplastic maize peroxidase POX12 at the very early infection stage (Doehlemann et al. 2009; Hemetsberger et al. 2012). Other apoplastic *U. maydis* effectors protect the fungus from host-derived lytic enzymes. Rsp3 for example binds and shields the fungal cell wall from the antifungal activity of the maize mannose-binding proteins AFP1 and AFP2 (Ma et al. 2018). In addition, Fly1, a fungalyisin metalloprotease, cleaves maize chitinase A to reduce its activity (Ökmen et al. 2018) and the effector Pit2 inhibits papain-like cysteine proteases through a conserved microbial motif to prevent SA signalling during early stages of infection (Doehlemann et al. 2011; Mueller et al. 2013; Misas Villamil et al. 2019). Effectors translocated into the host cell modulate its biology and reprogram different maize metabolic pathways: The chorismate mutase Cmu1, for example, reduces SA biosynthesis via lowering the pool of the SA precursor chorismate (Djamei et al. 2011). More recently, Cmu1 was also found to interact with the defence-related maize kiwellin KWL1, which significantly inhibits the chorismate mutase activity of Cmu1 (Han et al. 2019). Tin2, which is translocated into the host cell as well, reduces

lignin production via stabilisation of the maize protein kinase TTK1, which results in redirection of the lignin biosynthesis pathway towards anthocyanin production (Tanaka et al. 2014). The reactivation of DNA synthesis and cell division in host leaf tissue are essential for tumour formation. These processes are promoted by the intracellular effector See1, which interacts with the maize cell-cycle regulator and host-resistance protein SGT1, preventing its phosphorylation (Schilling et al. 2014; Redkar et al. 2015). In summary, *U. maydis* effectors characterised so far mostly either directly or indirectly suppress plant defence responses.

Overall, *U. maydis* effectors are expressed specifically during biotrophic development compared to axenic culture (Kämper et al. 2006) and are enriched in three distinct co-expressed temporal groups, which correspond to the infection stages on the plant surface, establishment of biotrophy and tumour induction (Lanver et al. 2018). These waves of effector expression are likely key determinants for *U. maydis* virulence. Unlike other smut fungi such as *Sporisorium reilianum* and *Ustilago hordei*, which exclusively cause disease symptoms in the inflorescences (Hu et al. 2002; Schirawski et al. 2010), *U. maydis* can cause disease in different organs of the plant. Accordingly, effector gene expression in *U. maydis* is also specifically tailored to the colonised organ, and several of the organ-specifically expressed effectors, including the leaf-specific effector See1, also have a corresponding organ-specific function for virulence (Skibbe et al. 2010; Schilling et al. 2014). Furthermore, some *U. maydis* effectors are expressed in a cell type-specific manner, as shown by transcriptome profiling of infected mesophyll and bundle sheath cells (Matei et al. 2018). This fine tuning of effector expression to the colonised organ and cell type suggests that the fungus is able to sense differences in its surrounding tissues, however neither the host signals that are perceived nor the transcription factors that could be involved are currently known.

#### 1.2.4 Quantitative disease resistance in the *U. maydis*-maize interaction

Despite *U. maydis* being a predominant model organism of biotrophic plant pathogens, plant resistance to *U. maydis* is rarely described (Lübberstedt et al. 1998; Baumgarten et al. 2007). Unlike in other biotrophic interactions, no gene-for-gene interactions are known in the *U. maydis*-maize pathosystem, although they provide durable resistance to other smut fungi. For example, six avirulence genes with corresponding host resistance genes have been identified in the interaction of *U. hordei* and barley (Tapke 1937; Linning et al. 2004). In contrast, crosses of *U. maydis*-resistant and -susceptible maize lines indicated that *U. maydis* resistance is a polygenic, quantitative trait (Immer 1927; Hoover 1932). Using natural as well as artificial inoculation experiments, several QDR loci that contribute to *U. maydis* infection frequency and severity have been mapped. Equivalent to the organ-specificity of certain *U. maydis* effectors (Skibbe et al. 2010; Schilling et al. 2014), some studies suggested that specific maize loci may contribute to *U. maydis* resistance in an organ-specific manner (Lübberstedt et al. 1998; Baumgarten et al. 2007). Additionally, significant QTL-environment interactions occurred frequently, suggesting that climatic conditions as well as the genetic structure of local *U. maydis* populations can affect *U. maydis* infection (Lübberstedt et al. 1998b; Baumgarten et al. 2007; Ding et al. 2008). In agreement with the absence of major resistance genes in the interaction of maize and *U. maydis*, the identified QTLs explained only a rather small fraction of the resistance phenotype (Lübberstedt et al. 1998; Baumgarten et al. 2007). Interestingly, several QDR loci conferring resistance to *U. maydis* contain genes with a known role in defence against pathogens, such as NLRs, a pathogenesis-related (PR) protein, a chitinase, a basal antifungal protein, and a wound-inducible protein (Baumgarten et al. 2007; Brefort et al. 2009). Yet, it has not been demonstrated whether these genes contribute to the activity of the detected QTLs. Recently, the maize lipoxygenase 3 (LOX3) was identified as an *U. maydis* susceptibility factor (Pathi et al. 2020). *Lox3* mutant plants display quantitatively decreased susceptibility towards *U. maydis* and react with an enhanced PAMP-triggered ROS burst. LOX3 might play a role in JA biosynthesis, as JA levels in leaves of *lox3* mutant maize plants are reduced and, correspondingly, SA levels are increased (Gao et al. 2008). This increase of SA in *lox3* mutant plants might explain the observed impact on *U. maydis* infection.

For one *U. maydis* effector, ApB73, a quantitative maize line-specific reduction of virulence has been observed (Stirnberg and Djamei 2016). This suggests that the fungus' effectors might target certain QTL gene products. However, the molecular basis of QDR in maize and how *U. maydis* interferes with its components is still mostly unknown. Deciphering these molecular mechanisms would greatly help to draw a more

comprehensive picture of the biotrophic interaction of *U. maydis* and maize and furthermore facilitate the efforts to produce *U. maydis*-resistant maize populations.

### 1.3 Aims and objectives of the study

The major aim of this study was to investigate the molecular mechanisms that underlie the interaction of *U. maydis* with maize lines of quantitatively different resistance levels and thereby elucidate whether the fungus' virulence strategy is adapted to different host genotypes. Additionally, this study aimed at identifying host processes involved in QDR to *U. maydis*. Accordingly, the main objectives of this study were:

- (1) To analyse the transcriptome of selected maize lines colonised by *U. maydis* in order to identify fungal effector genes expressed in a maize line-dependent manner as well as of maize genes differentially regulated between maize lines in response to *U. maydis* infection.
- (2) To assess maize line-specific virulence functions of effectors that are differentially expressed between maize lines in order understand if and how *U. maydis* effectors are adapted to the host genotype.
- (3) To identify maize genetic loci quantitatively contributing to QDR towards *U. maydis* via QTL mapping using a population derived from a cross of two maize lines with highly distinct *U. maydis* resistance levels.

## 2 Results

### 2.1 *U. maydis* disease development in different maize lines

To investigate quantitative disease resistance in the maize-*U. maydis* interaction, I first evaluated the susceptibility of different maize lines to *U. maydis* infection. For this, *U. maydis* resistance levels were assessed in the 26 inbred founder lines of the Nested Association Mapping recombinant inbred lines (NAM RILs; Yu et al. 2008; McMullen et al. 2009), a set of maize lines selected to represent world-wide maize diversity. In addition, the sweet corn Early Golden Bantam (EGB) was used, which is the most common maize line in *U. maydis* research (Zuo et al. 2019). Seedling infections were performed in three independent biological replicates under controlled conditions with an average of 102 plants per line being scored for *U. maydis* disease symptoms (Figure 2.1A). In this experimental set-up, resistance levels were highly diverse and ranged from very susceptible to very resistant (>94% vs. <35% tumours, respectively), while no maize line showed complete resistance to *U. maydis* infection (Figure 2.1A). Agglomerative hierarchical clustering of disease indices as a measure of *U. maydis* infection severity identified five susceptibility groups (Figure 2.1B). Two groups consisted only of the most resistant line CML322 and of the most susceptible line Tx303, respectively, and three groups were of comparable sizes, indicating a mostly even distribution of *U. maydis* resistance levels within the NAM founder lines and EGB. The *U. maydis* SG200 strain used in this study was derived from a field isolate from a temperate region (Minnesota, USA; Kämper et al. 2006). Strikingly, among the maize lines with highest susceptibility, most were local to regions close to the origin of SG200 (e.g. Oh43 from Ohio, Mo18w from Missouri, Il14H from Illinois). In contrast, all four most resistant maize lines were of tropical origin (CML322, NC350, NC358, Ki3). Thus, maize lines of close provenance to SG200 were generally more susceptible, indicating a possible adaptation of the local *U. maydis* strain to the local host lines. Based on resistance level, origin, growth soundness and seed production, 1-2 lines were chosen from each group for subsequent investigations (CML322, B73, EGB, Ky21, Oh43 and Tx303).

## 2. Results

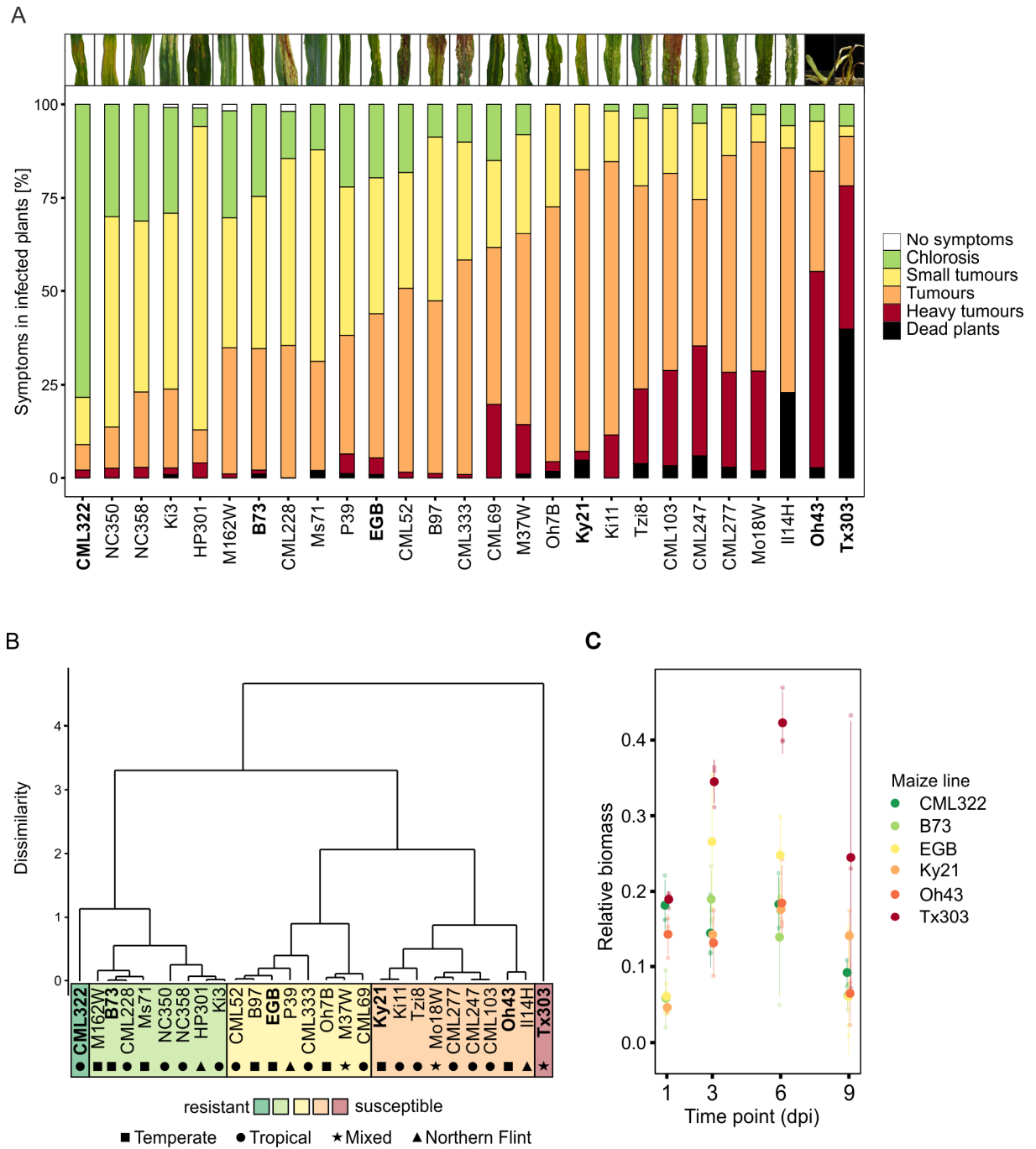


**Figure 2.1. *U. maydis* disease development in the 26 maize NAM founder lines and EGB. A) Disease symptom classification.** Maize seedlings were infected with *U. maydis* SG200 at the three-leaf stage. Three independent experiments were performed, and the average values are expressed as percentage of the total number of infected plants. Disease symptom classification was done 12 days post infection (dpi) as described in Redkar and Doehlemann (2016a). Average number of infected plants per line: 102. Maize lines selected for RNA sequencing are highlighted in bold. Representative pictures of infected leaves at 12 dpi for each maize line are shown at the top. **B) Agglomerative hierarchical clustering of disease indices.** Clustering is based on Euclidean distances of disease indices using complete linkage clustering. Maize lines selected for RNA sequencing are highlighted in bold. The maize lines' provenances are depicted by black symbols. **C) Fungal biomass quantification based on the amount of genomic DNA.** A qPCR with plant-specific (GAPDH) and fungus-specific (ppi) primers was performed at 1, 3, 6, and 9 dpi in the maize lines selected for RNA sequencing. Solid points indicate mean ratios of fungal DNA to plant DNA ( $2^{-\Delta C_t}$ ) of three biological replicates, transparent points indicate individual values, error bars denote the standard deviation.

To further characterise disease progression of *U. maydis* within the different maize lines and to select a time point suitable for transcriptome analysis, relative fungal biomass was assessed by qPCR using genomic DNA (Figure 2.1B) and fungal growth within leaf tissue was visualised by WGA-AF488/propidium iodide co-staining throughout the infection process at 1, 3, 6 and 9 dpi (Figure 2.2). At 1 and 3 dpi, relative fungal biomass did not differ significantly between the maize lines. At 6 dpi however, fungal biomass in Tx303, the most susceptible maize line, was increased approximately two-fold compared to the other maize lines. In line with previous observations, relative fungal biomass decreased at the late infection time point (9 dpi), which might be due to an impaired teliospore formation in the genetically engineered haploid SG200 strain (Lanver et al. 2018).

At the microscopic level, the infection progress was comparable for 1 and 3 dpi in all maize lines as well. At 6 dpi, strong differences could be observed, as for CML322, the most resistant maize line, hyphae were still only mostly proliferating, whereas for the more susceptible maize lines, fungal aggregates, fragmented hyphae and enlarged maize cells were visible. Size and number of fungal aggregates and maize cell enlargements increased with susceptibility levels of the maize lines (Figure 2.2). Based on these fungal quantification and microscopic growth data, the 3 dpi time point was chosen for transcriptome analysis. At this time point, the different maize lines showed comparable growth of biotrophic hyphae while levels of fungal colonisation allowed sufficient coverage of *U. maydis* genes by RNA-Seq.



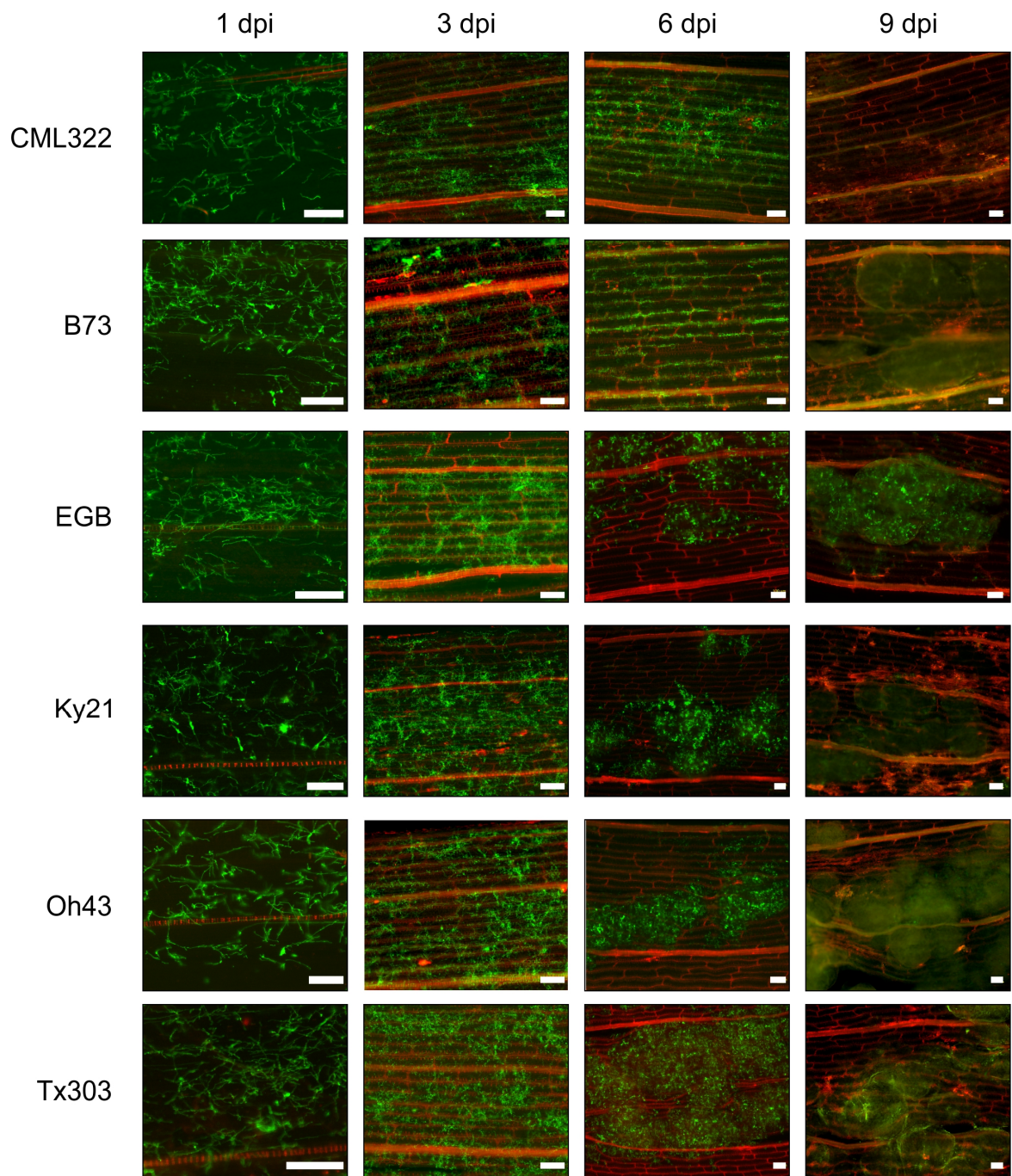


**Figure 2.2. Microscopic disease development in maize lines selected for RNA sequencing.** WGA-AF488/propidium iodide co-stained maize leaves infected with *U. maydis*. Samples were collected at 1, 3, 6, and 9 days post infection (dpi). Fungal hyphae were visualised by staining with WGA-AF488 (green), plant cell walls were visualised by staining with propidium iodide (red). Scale bars = 200  $\mu$ m.

## 2.2 Transcriptome analysis of *U. maydis* infecting maize lines of distinct disease resistance levels

To analyse the gene expression changes induced by different maize lines of distinct resistance levels, maize seedlings of CML322, B73, EGB, Ky21, Oh43 and Tx303 were infected with *U. maydis* SG200 or water (mock control). Infected and mock-treated leaf sections were collected 3 dpi in biological triplicates and their transcriptome was subsequently analysed via RNA-Seq. After filtering for low expression, 6284 of 6766 *U. maydis* genes remained for the analysis (93%). Variability between the samples was evaluated through a multi-dimensional scaling (MDS) plot (Figure 2.3A). To additionally examine whether the infection stage in the different maize lines was comparable and to demonstrate that gene expression differences were not caused by faster infection progression in the more susceptible maize lines, we included transcriptome data previously published by Lanver et al. (2018), where the maize line EGB was infected with the more virulent *U. maydis* wildtype crossing FB1xFB2 and the fungal transcriptome was mapped during different stages of the infection process. All our samples clustered with the 2 dpi samples of Lanver et al. (2018), which likely reflects the slower disease progression of SG200 compared to FB1xFB2. Again, this showed no pronounced differences in infection progression between the different maize lines at the time point tested.

To analyse whether *U. maydis* gene expression is influenced by the colonised maize line, I compared expression in all 15 possible pairs of the six different maize lines. This analysis showed that in total 406 of the 6284 expressed genes (6.4%) were differentially expressed ( $\log_2$  expression fold change  $>0.5$  or  $<-0.5$ , adjusted p value  $<0.05$ ) in at least one of the 15 comparisons. The number of differentially expressed *U. maydis* genes (DEGs) ranged from 0 to 300 genes in the different comparisons and only a few genes were differentially expressed in several of the 15 comparisons (Figure 2.3B, C). The majority of DEGs was only differentially expressed in one to three comparisons (approx. 75%) and only 1% of DEGs was differentially expressed in more than half of the comparisons, which suggests that not a shared set of genes is responsive to different host environments, but that different maize lines lead to rather diverse changes in gene expression.

## 2. Results

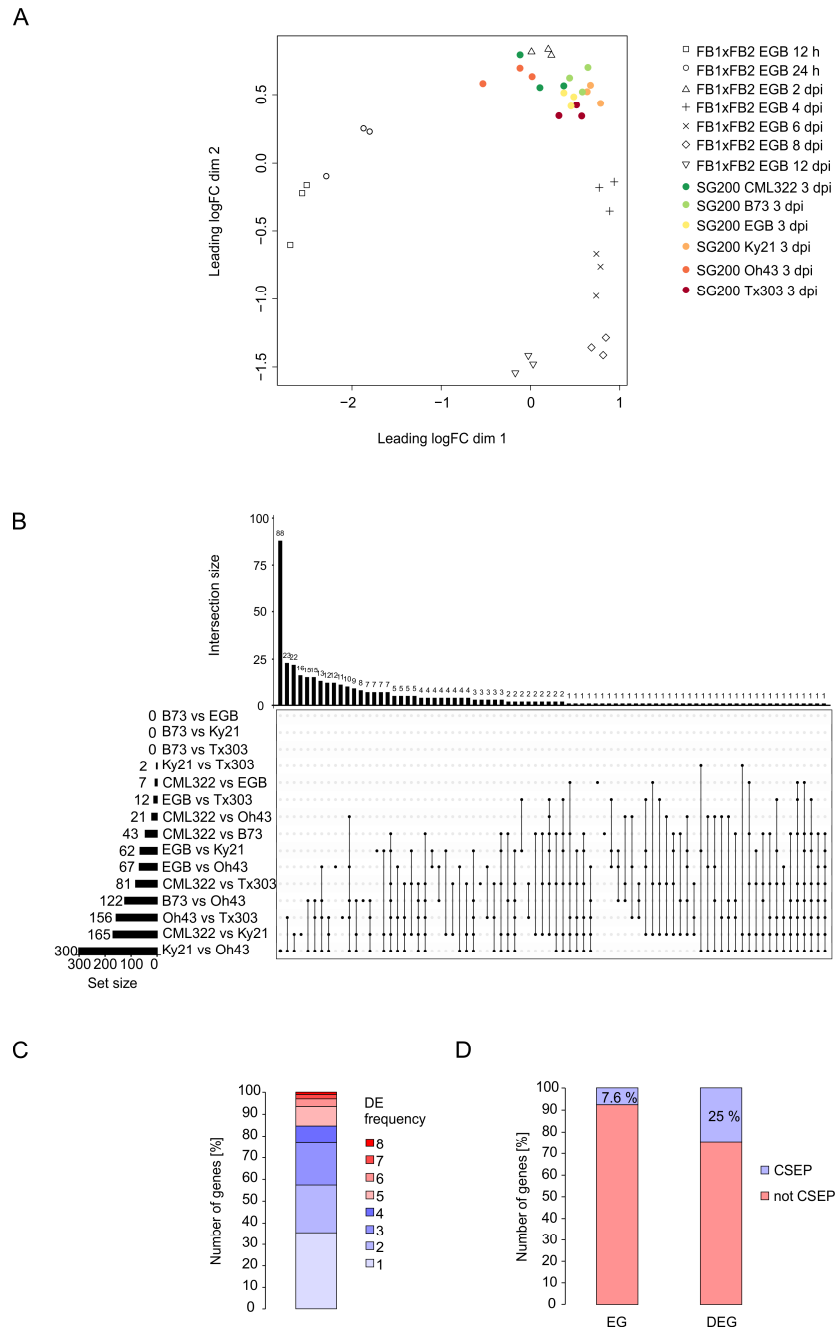


**Figure 2.3. A) Multi-dimensional scaling plot of *U. maydis* RNA sequencing data.** The top 1000 variable genes were used to calculate pairwise distances between the samples. FB1xFB2 RNA-Seq data were previously published and represent different time points in the *U. maydis* disease cycle in EGB (Lanver et al. 2018). **B) UpSet plot of the distribution of differentially expressed *U. maydis* genes across maize lines.** Genes with a  $\log_2$  expression fold change  $>0.5$  or  $<-0.5$  and adjusted p value  $<0.05$  were considered differentially expressed (DE). In total, 406 of 6284 expressed genes were differentially expressed between maize genotypes. Number of DE genes (DEGs) for each of the 15 possible comparisons is shown by set size (horizontal bars). Overlaps of DE genes between comparisons are depicted by connected black dots. Intersection size (vertical bars) indicates the size of overlaps. **C) Number of differentially expressed genes by frequency of differential expression within comparisons.** The categories of the bar plot show the percentage of all DEGs that are DE in the indicated number of comparisons. DE: differential expression. **D) Enrichment of candidate secreted effector proteins in differentially expressed genes.** Frequency of CSEPs in all 6284 expressed *U. maydis* genes compared to the frequency of CSEPs in genes DE between maize genotypes. Within DE genes, CSEPs show a 3.3-fold enrichment (hypergeometric test, p value 5.65e-30). EG: expressed genes. DEG: differentially expressed genes. CSEP: candidate secreted effector protein.

Strikingly, amongst the 406 DEGs, 102 encode candidate secreted effector proteins (CSEPs, Dutheil et al. 2016), which represents a significant 3.3-fold enrichment (hypergeometric p value  $5.65e-30$ , Figure 2.3D). A heatmap based on the expression profiles of the 102 line-specific CSEPs shows distinct groups of CSEPs with similar expression patterns (Figure 2.4). Of the 102 CSEPs, one group of 38 genes is upregulated on the most resistant maize line CML322 and downregulated in more susceptible maize lines, except for Oh43, while another group of 29 CSEPs shows the opposite expression pattern. Besides these two main expression patterns, some CSEPs show no clear correlation to the resistance level. Consequently, a dominant expression pattern that underlies all maize line-specific CSEPs cannot be observed.

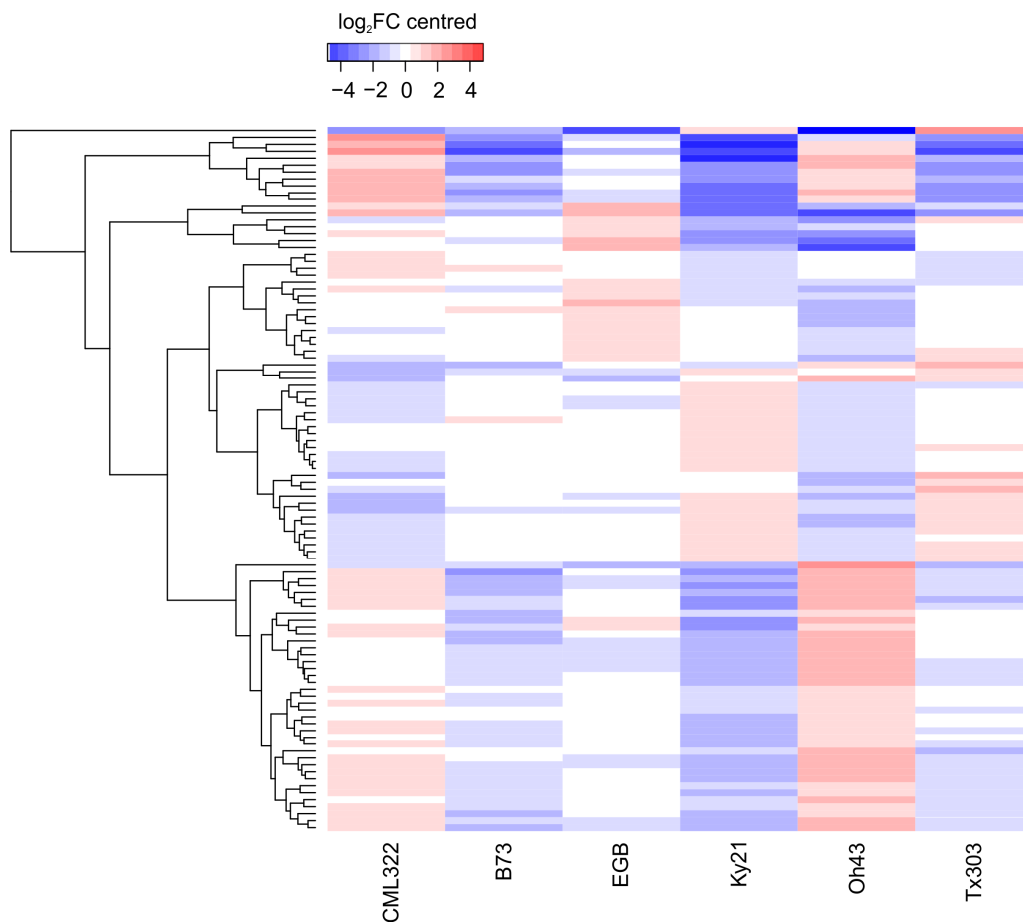


**Figure 2.4. Expression profile of differentially expressed *U. maydis* CSEPs across maize lines.** Heatmap shows log<sub>2</sub> expression fold changes compared to mean expression across all samples. CSEP: candidate secreted effector protein. FC: fold change.

### **2.2.1 Weighted gene co-expression analysis of *U. maydis* genes during infection of maize lines of distinct disease resistance levels**

To elucidate which processes could be involved in colonising maize lines of different resistance levels, the correlation of *U. maydis* gene expression to the resistance level of the colonised maize line was assessed. To this end, first a weighted gene co-expression network analysis (WGCNA) using the *U. maydis* expression data of the different maize lines was performed. WGCNA identifies modules of co-expressed genes and represents the modules by summary expression profiles, referred to as the module eigengene (Zhang and Horvath 2005; Langfelder and Horvath 2008). This analysis identified eleven colour-coded modules with differential expression profiles of the module eigengenes, ranging in size from 1073 ('turquoise') to 65 genes ('purple'; Figure 2.5A). Subsequently, in order to identify modules associated with the severity of the infection, the correlation of each module eigengene with the disease indices of the different maize lines was calculated (referred to as gene significance, GS; Figure 2.5B). The 'purple' module showed a significant positive correlation (GS >0.5, p value <0.05) and the 'greenyellow' module showed a significant negative correlation to the disease index (GS <-0.5, p value <0.05), i.e. expression of genes in the 'purple' module was higher in more susceptible maize lines and expression of genes in the 'greenyellow' module was higher in more resistant maize lines. Expression of the other modules was either independent from the colonised maize line ('green' and 'pink' modules), only differed in one or two maize lines ('black', 'blue', 'brown', 'magenta', 'red' and 'yellow' modules) or was highly variable between maize lines but did not correlate with the infection severity ('turquoise' module).

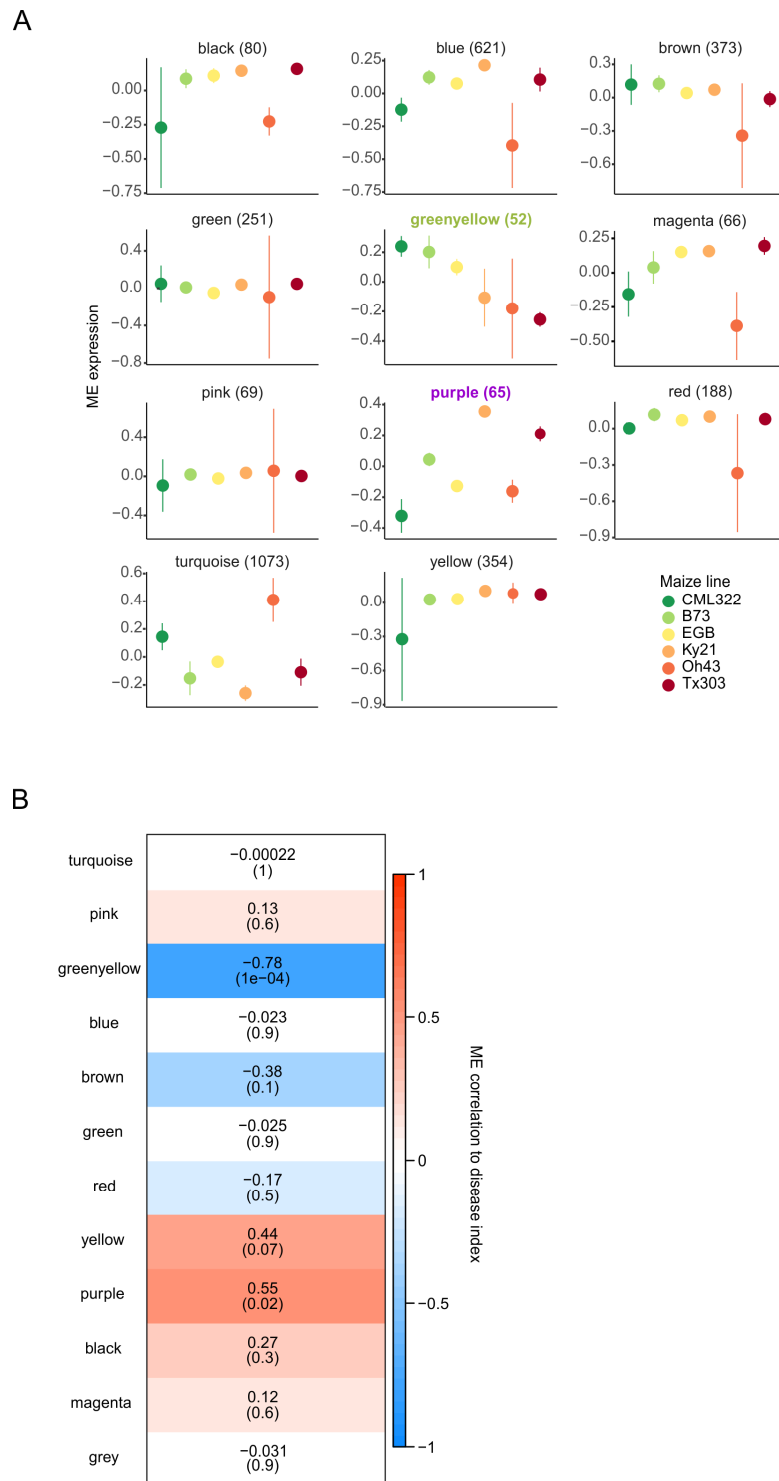


**Figure 2.5. A) Modules of co-expressed *U. maydis* genes across maize lines.** The RNA sequencing data was subjected to weighted gene co-expression network analysis (WGCNA) to detect modules of co-expressed genes. Each plot represents the expression profile of the module eigengene (ME), which can be considered as representative of the expression of the respective co-expression module. Error bars indicate standard deviation of three biological replicates. The modules are named according to their colour, and the size of each module is shown in parentheses. Modules significantly correlated with disease index are highlighted in bold and their respective colour. **B) Module-disease index association.** Correlation of modules of co-expressed genes with the disease index of the colonised maize line. Numbers in the heatmap show the correlations with disease index and p values in parentheses for the respective module eigengene (ME). Correlation was considered significant for correlation  $>0.5$  or  $<-0.5$  and p value  $<0.05$ .

To evaluate which biological processes were associated with the colonisation of more resistant and more susceptible maize lines, the 'purple' and 'greenyellow' modules were subjected to enrichment analysis of Gene Ontology (GO) terms and CSEPs (Ashburner et al. 2000; The Gene Ontology Consortium 2017; Figure 2.6). In summary, mostly ion transport processes were significantly enriched in the 'purple' module. Ion transmembrane transport through H<sup>+</sup>-ATPases is a crucial driving force for nutrient exchange between host plants and fungi (Palmgren 1990; Glaninazzi-Pearson et al. 1991; Sondergaard et al. 2004; Wang et al. 2014). Furthermore, different nutrient transporters were found to be important virulence factors tied to biotrophic development in *U. maydis* (Lanver et al. 2018). As indicated by the enrichment of ion transport processes in the module with higher gene expression in more resistant maize lines, different availability of nutrients in more resistant vs. more susceptible maize lines could therefore be involved in QDR to *U. maydis*. Additionally, 'oxidation-reduction' was the GO term with the most genes. Oxidation-reduction processes are involved in metabolism as well, but can also have a signalling function or be related to detoxification of reactive oxygen species (ROS). In the 'greenyellow' module, all significantly enriched GO terms were related to carbohydrate metabolism. In addition, CSEPs were significantly enriched in this module and represented the biggest category. Carbohydrate utilisation has been directly linked to plant cell wall degradation in other plant pathogenic fungi (Tonukari et al. 2000; Ospina-Giraldo et al. 2003). Since carbohydrate metabolism is enriched in the module with higher gene expression in more resistant maize lines, it could be speculated, that the fungus might need to overcome enhanced cell wall reinforcements as part of increased resistance. The enrichment of CSEPs in this module might represent an attempt of the fungus to suppress enhanced defence mechanisms in more resistant host lines.

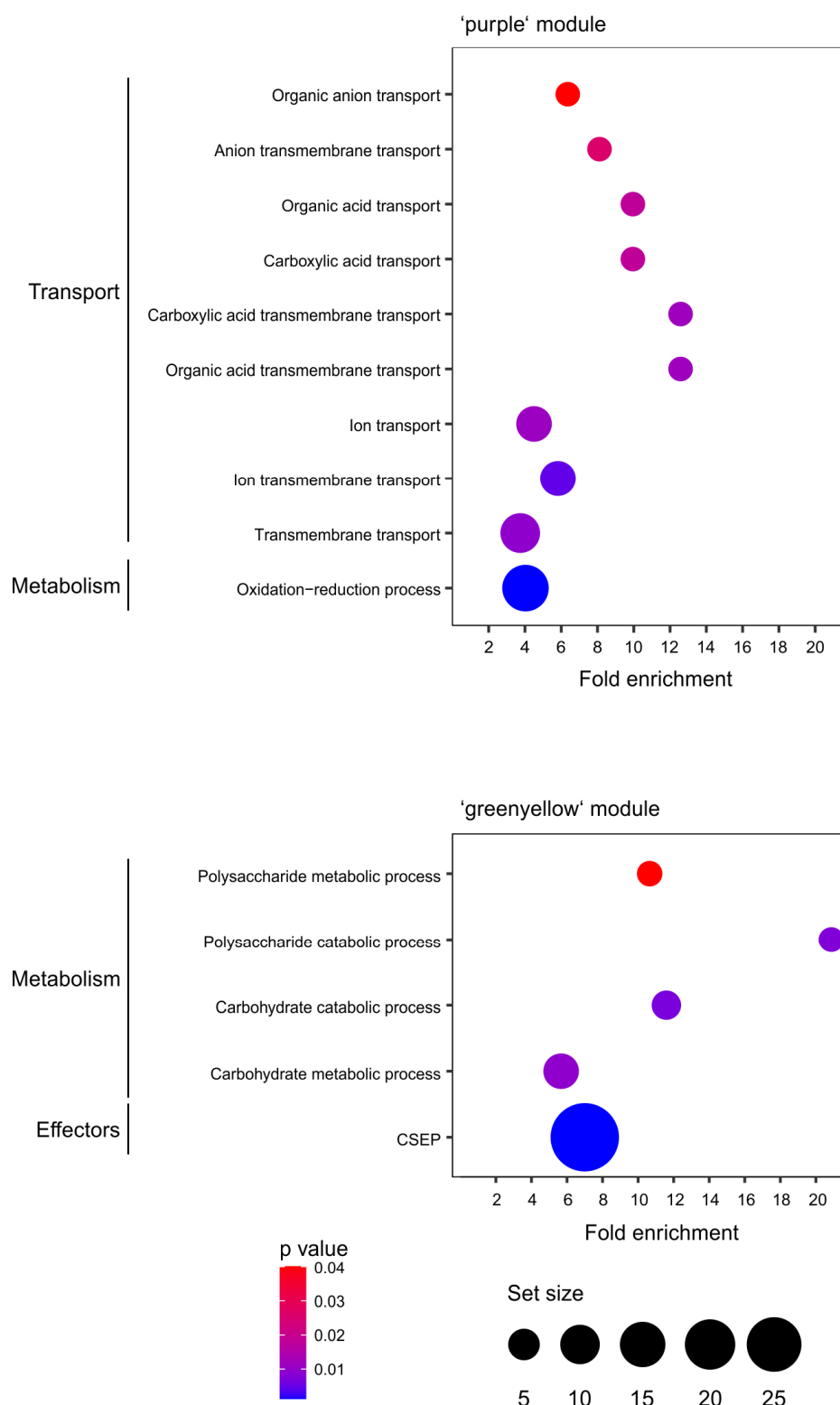


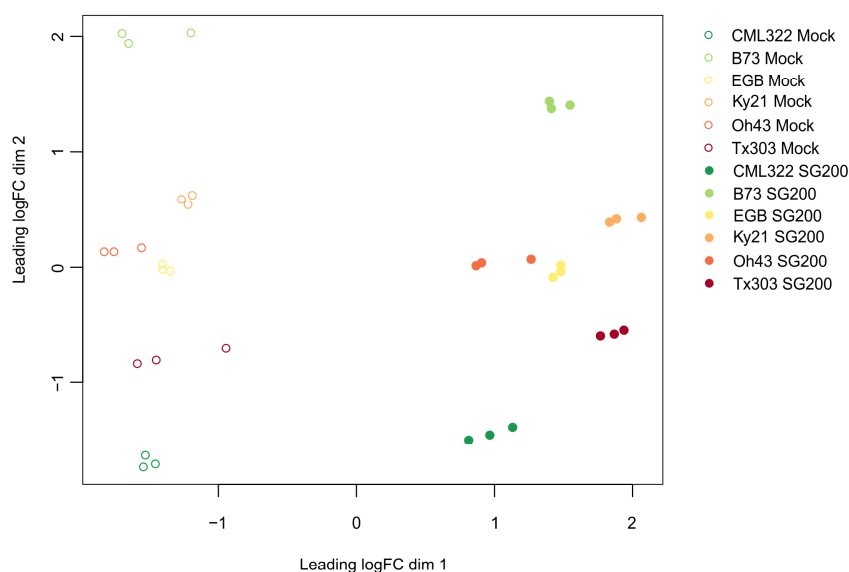
**Figure 2.6. GO and CSEP enrichments in modules correlated with disease index.** GO biological process terms and additionally CSEPs (candidate secreted effector proteins) were tested for significant enrichment in the 'purple' (positive correlation to disease index) and 'greenyellow' (negative correlation to disease index) modules. Gene sets were considered significantly enriched for p value <0.05 (hypergeometric test). Dot size is representative for the number of analysed genes in the respective term. Only genes with a gene significance to disease index of >0.5 ('purple') or <-0.5 ('greenyellow') and p value <0.05 were considered for the analysis and only terms with a set size >3 are shown.



### **2.3 Transcriptome analysis of *U. maydis*-infected maize lines of distinct disease resistance levels**

To identify maize genes involved in QDR to *U. maydis*, maize line-dependent transcriptional changes in response to *U. maydis* were analysed via RNA-Seq. Of all 63477 maize annotated loci, 40056 were expressed in the samples (63%). To assess the variability between the samples a multi-dimensional scaling plot was used (Figure 2.7A). *U. maydis*-infected and control samples formed two distinct groups, within which the samples of each maize line clustered together, indicating both treatment-specific and genotype-specific expression patterns. To identify genes which differentially respond to *U. maydis* infection between maize lines, I compared expression fold changes of the *U. maydis*-infected samples to the respective mock control samples for all 15 possible pairs of six different maize lines (i.e. difference between genotypes in response to infection). This analysis showed that in total 8675 of 40056 transcripts (22%) responded differentially to *U. maydis* infection ( $\log_2$  expression fold change  $>0.5$  or  $<-0.5$ , adjusted p value  $<0.05$ ) in at least one of the 15 comparisons. The number of DEGs ranged from 358 to 1283 genes in the different comparisons and the fraction of genes differentially expressed in several of the 15 comparisons was very small (Figure 2.7B). Around 50% of DEGs were differentially expressed in only one of the comparisons and only 4% of DEGs were differentially expressed in more than half of the comparisons. Together, this shows that genes differentially responding to *U. maydis* infection are highly diverse between maize lines.

A



B

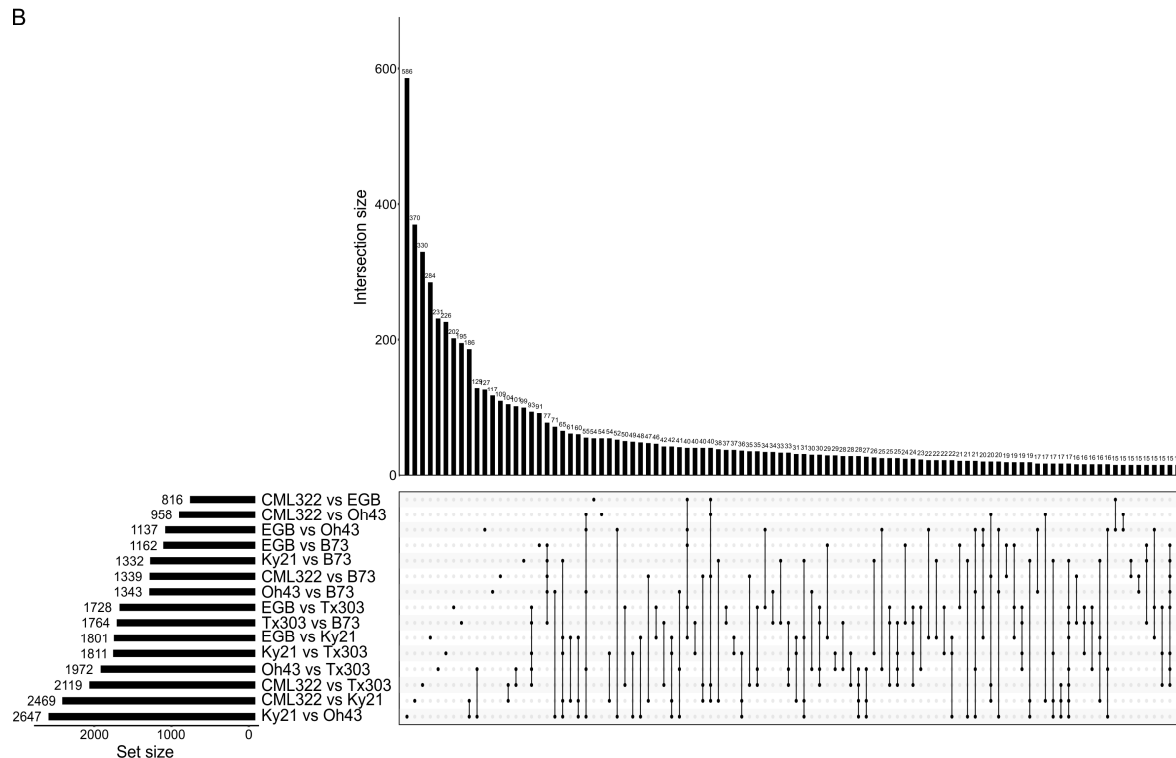
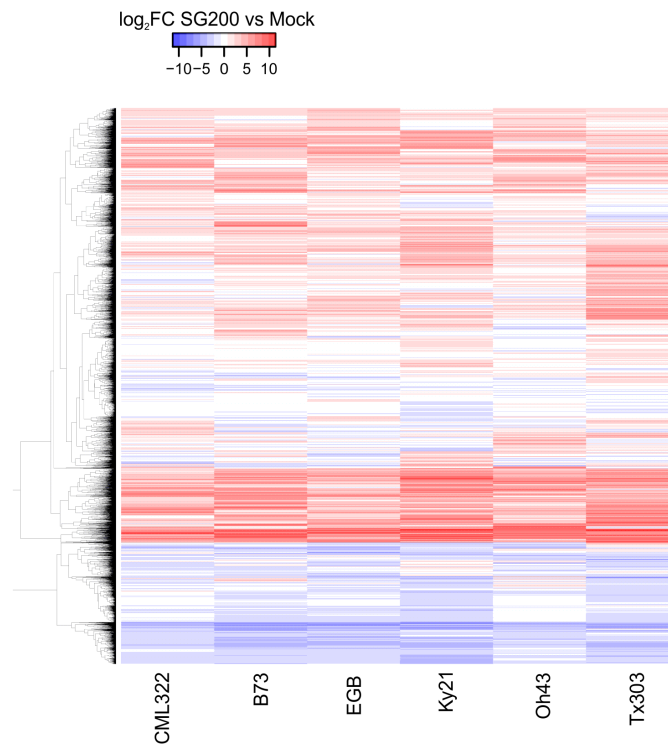


**Figure 2.7. A) Multi-dimensional scaling plot of maize RNA sequencing data.** The top 5000 variable genes were used to calculate pairwise distances between the samples. **B) UpSet plot of the distribution of genes differentially expressed between maize lines in response to *U. maydis*.** Genes with a  $\log_2$  expression fold change  $>0.5$  or  $<-0.5$  and adjusted p value  $<0.05$  were considered differentially expressed (difference between genotypes in response to infection). In total, 8675 of 40056 expressed genes were differentially responding to *U. maydis* between maize genotypes. Number of differentially expressed genes (DEGs) for each of the 15 possible comparisons is indicated by set size (horizontal bars). Overlaps of DEGs between comparisons are depicted by connected black dots. Size of overlaps is indicated by intersection size (vertical bars).

The expression changes between SG200-infected and mock-treated samples of the DEGs are depicted in Figure 2.8A. This illustrated that genes generally upregulated or downregulated in response to *U. maydis* infection are significantly differently expressed between maize lines.

To identify biological processes which were associated with the maize line-specific gene expression responses, all maize DEGs were subjected to enrichment analysis of GO terms (Ashburner et al. 2000; The Gene Ontology Consortium 2017), highlighting processes involved in transport, response to stimulus, cellular processes and metabolism (Figure 2.8B). The GO terms with most genes were 'transmembrane transport' as well as 'oxidation-reduction' and 'protein phosphorylation', which could indicate a special importance of these processes in genes differentially regulated in response to *U. maydis* between maize lines. Transport processes play a pivotal role in signalling, nutrient uptake as well as growth and development. Oxidation-reduction processes are involved in metabolism but can also have a signalling function. Protein phosphorylation occurs during kinase signalling processes. A predominant role of genes related to metabolism as well as kinase-signalling cascades for QDR has been proposed before (Delplace et al. 2020). Taken together, this suggests that maize line-specific responses to *U. maydis* involve various cellular activities, consistent with the complex nature of QDR.

A



B

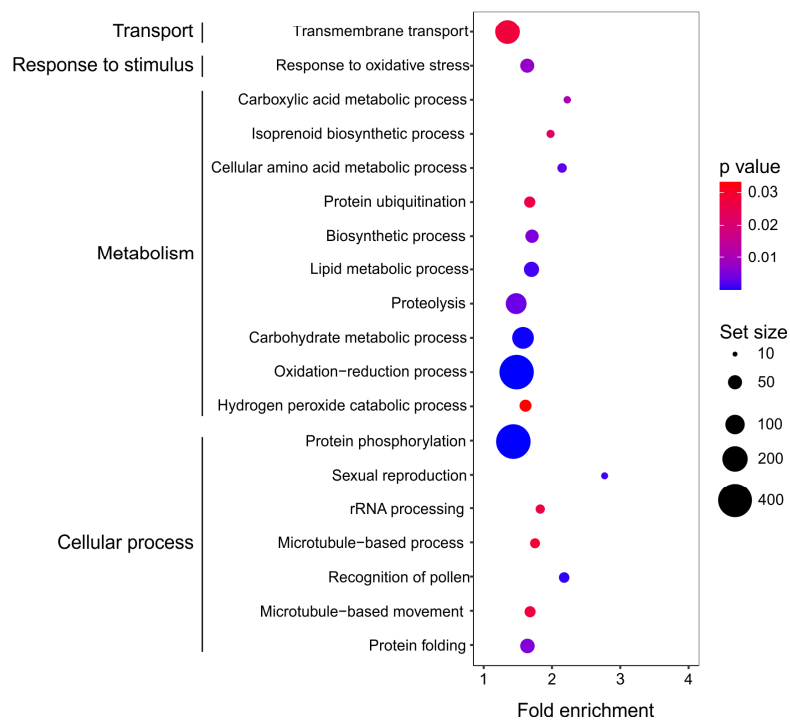


**Figure 2.8. A) Expression profile of differentially expressed maize genes in response to *U. maydis*.** Heatmap shows log<sub>2</sub> expression fold changes of SG200-infected vs mock-treated samples. **B) GO enrichments in differentially expressed maize genes.** GO biological process terms were tested for significant enrichment in all genes differentially expressed between maize lines in response to *U. maydis*.

## 2. Results

Gene sets were considered significantly enriched for p value <0.05 (hypergeometric test). Dot size is representative of the number of analysed genes in the respective term.

To examine, if the maize DEGs include genes associated with other forms of immunity, I compared *A. thaliana* orthologues of the DEGs with *A. thaliana* genes previously found to be linked to PTI and/or ETI responses (Dong et al. 2015; Hatsugai et al. 2017; Mine et al. 2018). Of the 3264 DEG *A. thaliana* orthologues, only about 11% (363 and 360 genes) were found in common with either PTI- and/or ETI-associated genes (Figure 2.9). This result might suggest that processes differentially regulated between maize lines in response to *U. maydis* are likely distinct from canonical PTI and ETI pathways.

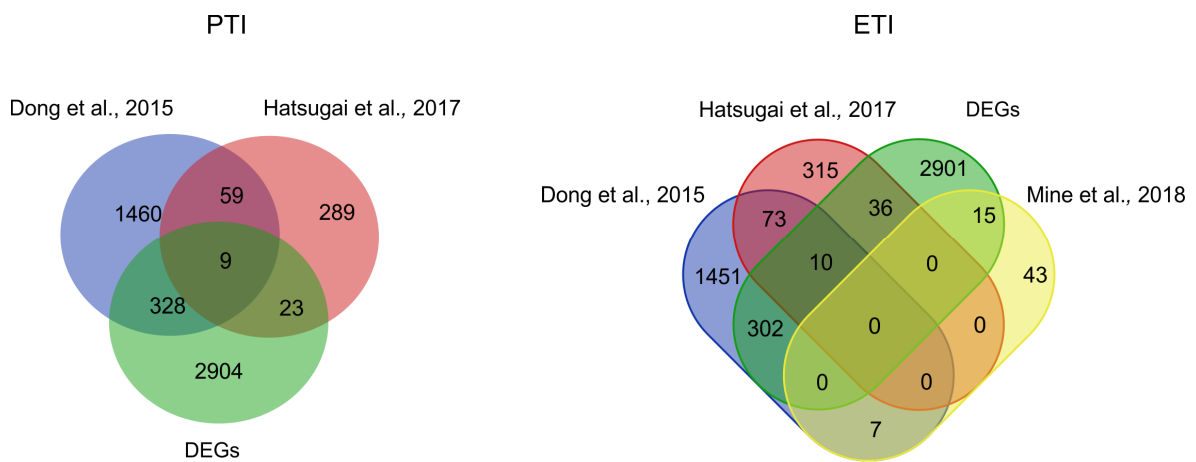
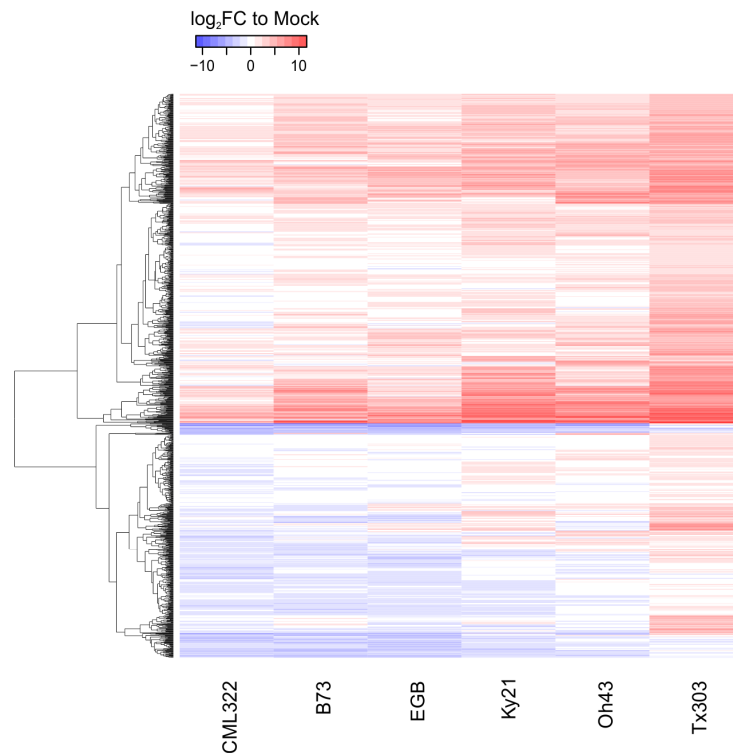


**Figure 2.9. Identification of genes previously associated with PTI or ETI immune responses within maize DEGs.** *A. thaliana* orthologues of maize differentially expressed genes (DEGs) were examined for overlaps to genes previously identified to be associated with PAMP-triggered- (PTI, left) or effector-triggered immunity (ETI, right; Dong et al. 2015; Hatsugai et al. 2017; Mine et al. 2018).

### 2.3.1 Correlation analysis of maize gene expression to disease resistance levels

To assess which processes could be connected to either resistance or susceptibility to *U. maydis*, the correlation of *U. maydis*-induced transcriptional changes to the disease index in the respective maize lines was calculated. All DEGs were then filtered for genes with a significant positive (GS >0.5 and p value <0.05) or negative (GS <-0.5 and p value <0.05) correlation to the disease index. This identified two sets of genes that were either more strongly upregulated in response to infection in the more susceptible maize lines, or more strongly downregulated in response to infection in the more resistant maize lines (positive correlation to disease index, Figure 2.10A), or vice versa (negative correlation to disease index, Figure 2.11A).

A



B

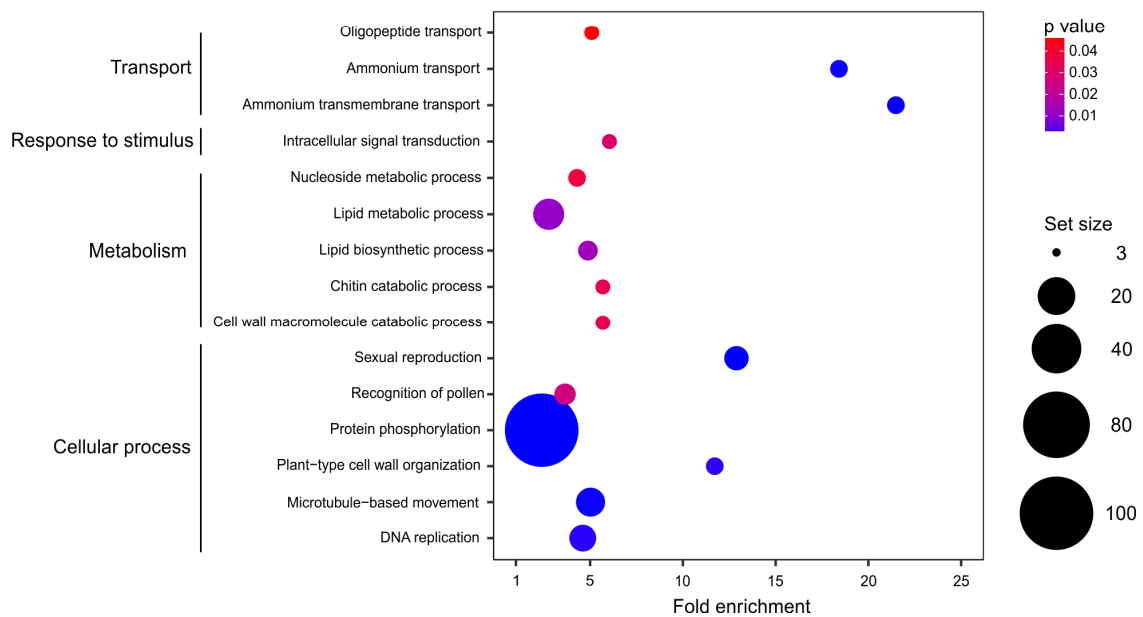
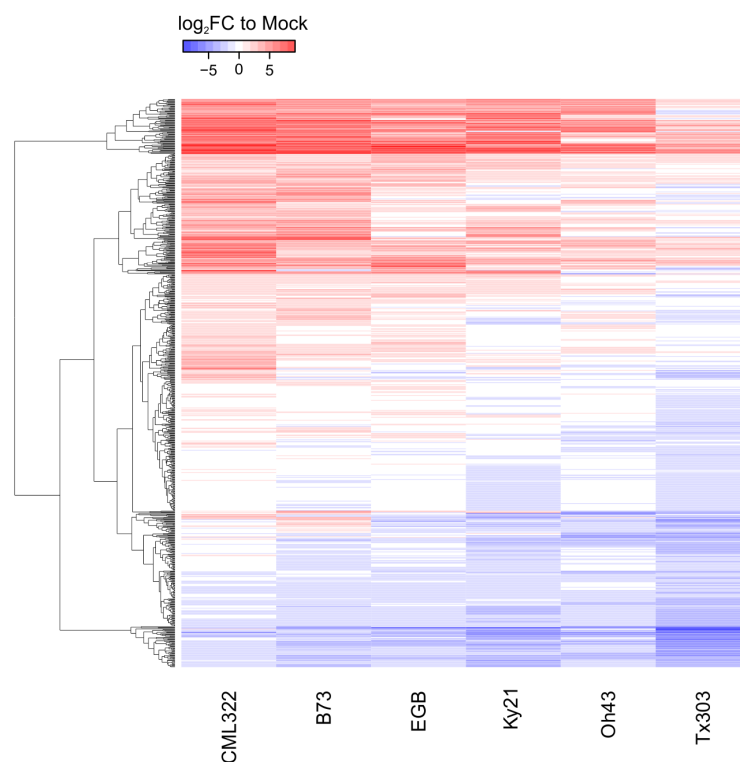


**Figure 2.10. A) Expression profile of genes positively correlated with the disease index.** Genes with a gene significance for the disease index  $>0.5$  and  $p$  value  $<0.05$  were considered significantly positively correlated to the disease index. Heatmap shows log<sub>2</sub> expression fold changes of SG200-infected vs mock-treated samples. **B) GO enrichments of genes positively correlated with the disease index.** GO biological process terms were tested for significant enrichment in all genes differentially expressed between maize lines in response to *U. maydis* and positively correlated to the disease index. Gene sets were considered significantly enriched for  $p$  value  $<0.05$  (hypergeometric test). Dot size is representative of the number of analysed genes in the respective term.

Next, these two gene sets were again subjected to enrichment analysis of GO terms (Figure 2.10B, Figure 2.11B). In the DEGs with positive correlation to the disease index, i.e. upregulated in more susceptible maize lines, enrichments were found in four main cellular activities: cellular processes, response to stimulus, transport, and metabolism (Figure 2.10B). The enriched GO term with the largest number of genes was ‘protein phosphorylation’, one of the most important cellular regulatory mechanisms involved in signal transduction. Furthermore, biological process terms that can be linked to cell division processes (‘DNA replication’, ‘microtubule-based movement’) and ‘sexual reproduction’/‘recognition of pollen’ were significantly enriched. In DEGs negatively correlated to the disease index, i.e. genes upregulated in the more resistant maize lines, enrichments were found in transport and metabolism (Figure 2.11B). The enriched GO term with the largest number of genes was ‘translation’, and a process that could be involved in photosynthesis (‘porphyrin-containing compound biosynthetic process’) was most strongly enriched.

The re-activation of cell division processes including DNA replication are crucial for formation of *U. maydis*-induced tumours (Doehlemann et al. 2008b; Redkar et al. 2015; Matei et al. 2018; Villajuana-Bonequi et al. 2019). Hence, enrichment of such processes in more susceptible maize lines is not surprising since there, *U. maydis* induces more and larger tumours compared to the more resistant lines. Suppression of photosynthesis-associated genes is a typical process in *U. maydis*-infected tissue, where the normal development from sink to source is prevented (Doehlemann et al. 2008a). The finding that processes related to photosynthesis were enriched within maize genes upregulated in more resistant maize lines indicates that here, the induction of such genes could be less reduced by *U. maydis* infection.

A



B

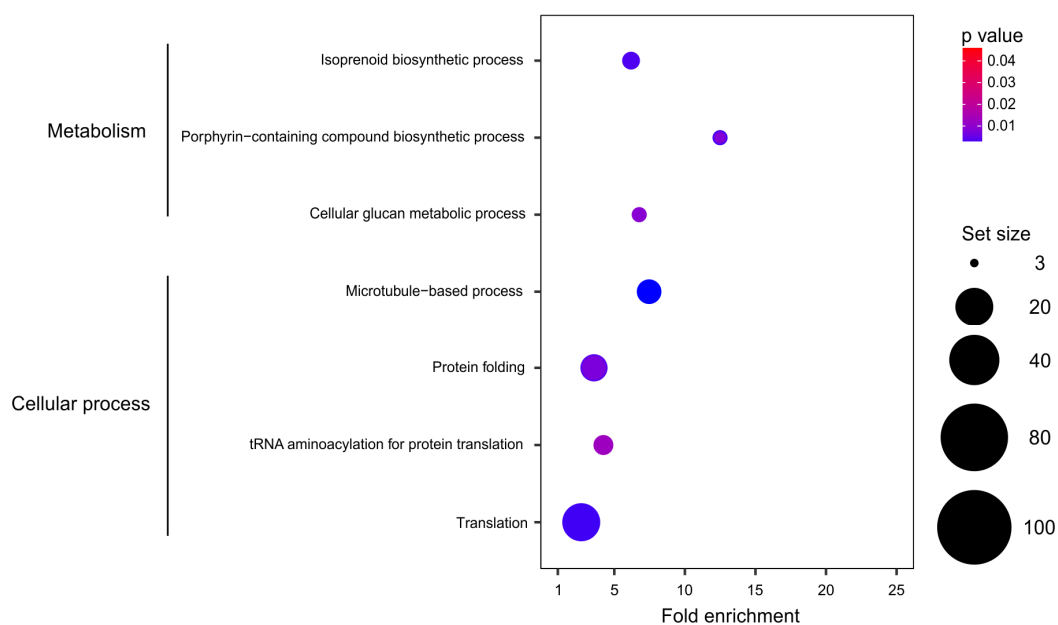


**Figure 2.11. A) Expression profile of genes negatively correlated with the disease index.** Genes with a gene significance for the disease index  $<-0.5$  and p value  $<0.05$  were considered significantly negatively correlated to the disease index. Heatmap shows log<sub>2</sub> expression fold changes of SG200-infected vs mock-treated samples. **B) GO enrichments of genes negatively correlated with the disease index.** GO biological process terms were tested for significant enrichment in all genes differentially expressed between maize lines in response to *U. maydis* and negatively correlated to the disease index. Gene sets were considered significantly enriched for p value  $<0.05$  (hypergeometric test). Dot size is representative of the number of analysed genes in the respective term.



## 2.4 Identification of *U. maydis* CSEPs targeting components of quantitative disease resistance

As *U. maydis* genes encoding CSEPs were enriched both in genes differentially expressed between maize lines, as well as in the co-expression module correlated to infection severity, I decided to investigate whether line-specifically expressed CSEPs also have line-specific functions for virulence. To this end, 12 candidate maize line-specific (MIs) CSEP genes were selected from all 102 differentially expressed CSEPs based on a high  $\log_2$  expression fold change and an expression pattern with higher expression in resistant and lower in susceptible maize lines or vice versa (sum of  $\log_2$  expression fold change across all samples  $>2$ ; Figure 2.12A). CSEPs with similar expression patterns were targeted for simultaneous knock-out (KO) in the SG200 background using the CRISPR/Cas9 system (Figure 2.12A,B, Schuster et al., 2016).

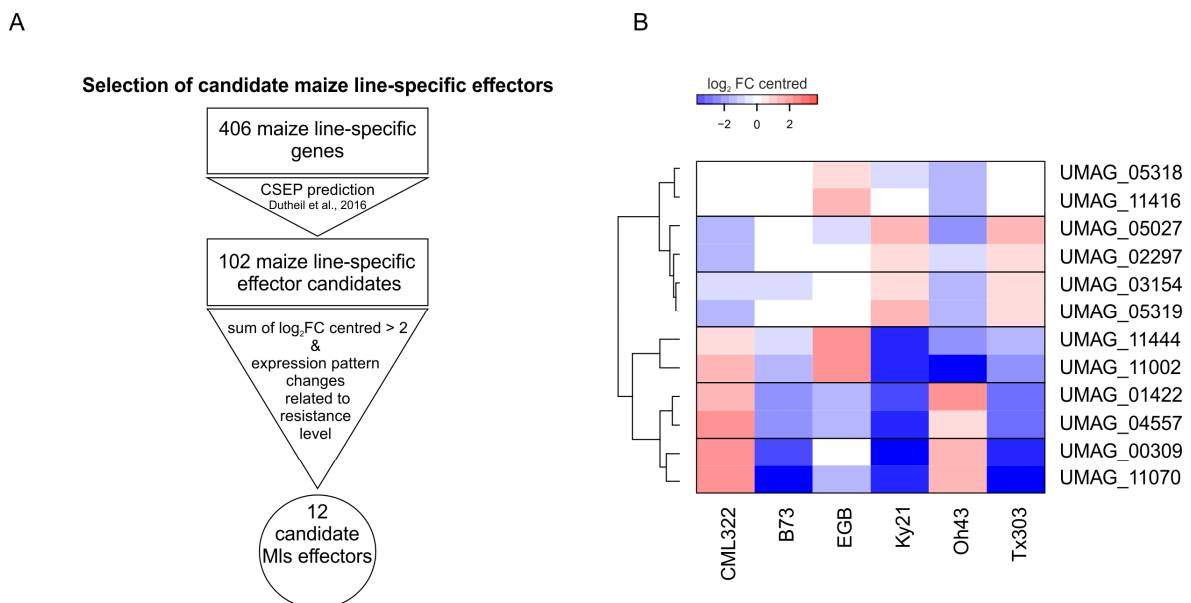


**Figure 2.12. A) Selection of maize line-specific effector candidates for functional characterization.** CSEP: candidate secreted effector protein. MIs: maize line-specific. **B) Expression profile of selected maize line-specific effector candidates across maize lines.** Heatmap shows  $\log_2$  expression fold changes compared to mean expression across all samples.

In addition to the first set of candidates (Figure 2.12A), further criteria were applied to all differentially expressed CSEPs. As the high variance of expression fold changes used for the first set of candidates resulted in a slight bias towards genes with low expression values, the second set of candidates was selected only from the top 50% of highest expressed maize line-specific CSEPs and by filtering for genes with an average  $\log_2$  expression fold change across all maize lines of 0.5 (i.e. with a sum of  $\log_2$  expression fold change across all samples  $>3$ ; Figure 2.13A). Furthermore, CSEPs of which all paralogues were among the maize line-specific genes (Figure 2.13B) and CSEPs from virulence clusters (Kämper et al. 2006) with a large number of maize line-specific genes (Figure 2.13C) were selected as interesting candidates for further analysis because such genes could result from effector diversification in order to adapt to different host genotypes. As for the first set of candidates, CSEPs with similar expression patterns were targeted for simultaneous knock-out in the SG200 background using the CRISPR/Cas9 system (Schuster et al., 2016).

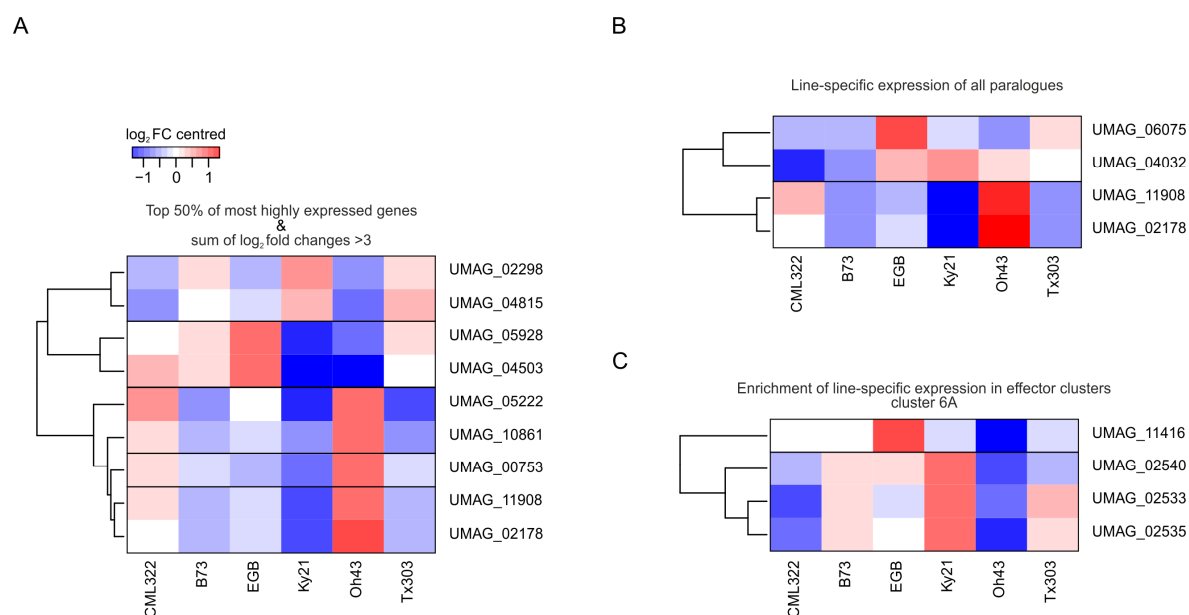


**Figure 2.13. Expression profiles of additional maize line-specific effector candidates. A) Expression profile of highly expressed candidate maize line-specific effectors.** Candidate genes were selected within the 50% most highly expressed maize line-specific CSEPs which displayed total  $\log_2$  fold changes across all samples  $>3$ . Heatmap shows  $\log_2$  expression fold changes compared to mean expression across all samples. **B) Expression profiles of paralogue candidate maize line-specific effectors.** Candidate genes were selected based on maize line-specific expression of all CSEP paralogues. Heatmap shows  $\log_2$  expression fold changes compared to mean expression across all samples. **C) Expression profiles of cluster candidate maize line-specific effectors.** Candidate genes were selected within virulence clusters (Kämper et al. 2006) enriched for maize line-specifically expressed CSEPs. Heatmap shows  $\log_2$  expression fold changes compared to mean expression across all samples. CSEP: candidate secreted effector protein.

## 2. Results

---

Plant infections with the generated *U. maydis* mutant strains identified line-specific virulence functions for the CSEP genes UMAG\_02297 and/or UMAG\_05027. While virulence of the double mutant KO\_UMAG\_02297/ KO\_UMAG\_05027 was not reduced on B73 or EGB, a significant reduction was observed on CML322 and Oh43. For reasons of seed availability, subsequent analyses of the mutants were focussed on the maize line CML322. Here, the virulence defect could be restored by introducing single copies of both genes into the *ip* locus of the double mutant strain, demonstrating specificity of the observed virulence reduction (Figure 2.14).

Furthermore, a maize line-specific virulence function was observed for UMAG\_05318 and/or UMAG\_11416 (Figure 2.14). Here, the double mutant KO\_UMAG\_05318/ KO\_UMAG\_11416 showed reduced virulence on EGB, but not B73. Re-introducing single copies of the KO genes into the *ip* locus of the double KO strain restored the virulence defect here as well (Figure 2.14), confirming specificity of the observed phenotypes. As the single KO strain KO\_UMAG\_11416 did not show any virulence defect (Supplementary Figure 6.3) and a reduction of virulence on EGB for a UMAG\_05318 deletion strain had already been reported previously (Schilling et al. 2014), these CSEPs were not further investigated. For all other tested mutants of the first candidate set, either no reduction of virulence (KO\_UMAG\_01422/ KO\_UMAG\_04557, KO\_UMAG\_11070/ KO\_UMAG\_00309, KO\_UMAG\_11444/ KO\_UMAG\_11002) or a reduction of virulence on all tested maize lines was observed (KO\_UMAG\_05027/ KO\_UMAG\_02297/ KO\_UMAG\_05319/ KO\_UMAG\_03154, Figure 2.14).

For reasons of seed availability, virulence of the additional set of KO mutants was assessed in plant infections of different maize lines in only one biological replicate (Supplementary Figure 6.4). Preliminary data suggested a maize line-specific reduction of virulence for KO\_UMAG\_02178/ KO\_UMAG\_11908 and KO\_UMAG\_10861/ KO\_UMAG\_05222 (virulence reduction on EGB, but not on Ky21 or Oh43) as well as for KO\_UMAG\_05928/ KO\_UMAG\_04503 (virulence reduction on B73 and EGB, but not on Ky21). For KO\_UMAG\_00753 and KO\_UMAG\_02533/ KO\_UMAG\_02535/ KO\_UMAG\_02540, a strong reduction of virulence was observed on all tested maize lines. KO\_UMAG\_02298/ KO\_UMAG\_04815 virulence levels were comparable to SG200. Due to the lack of replicates, these results require further validation.

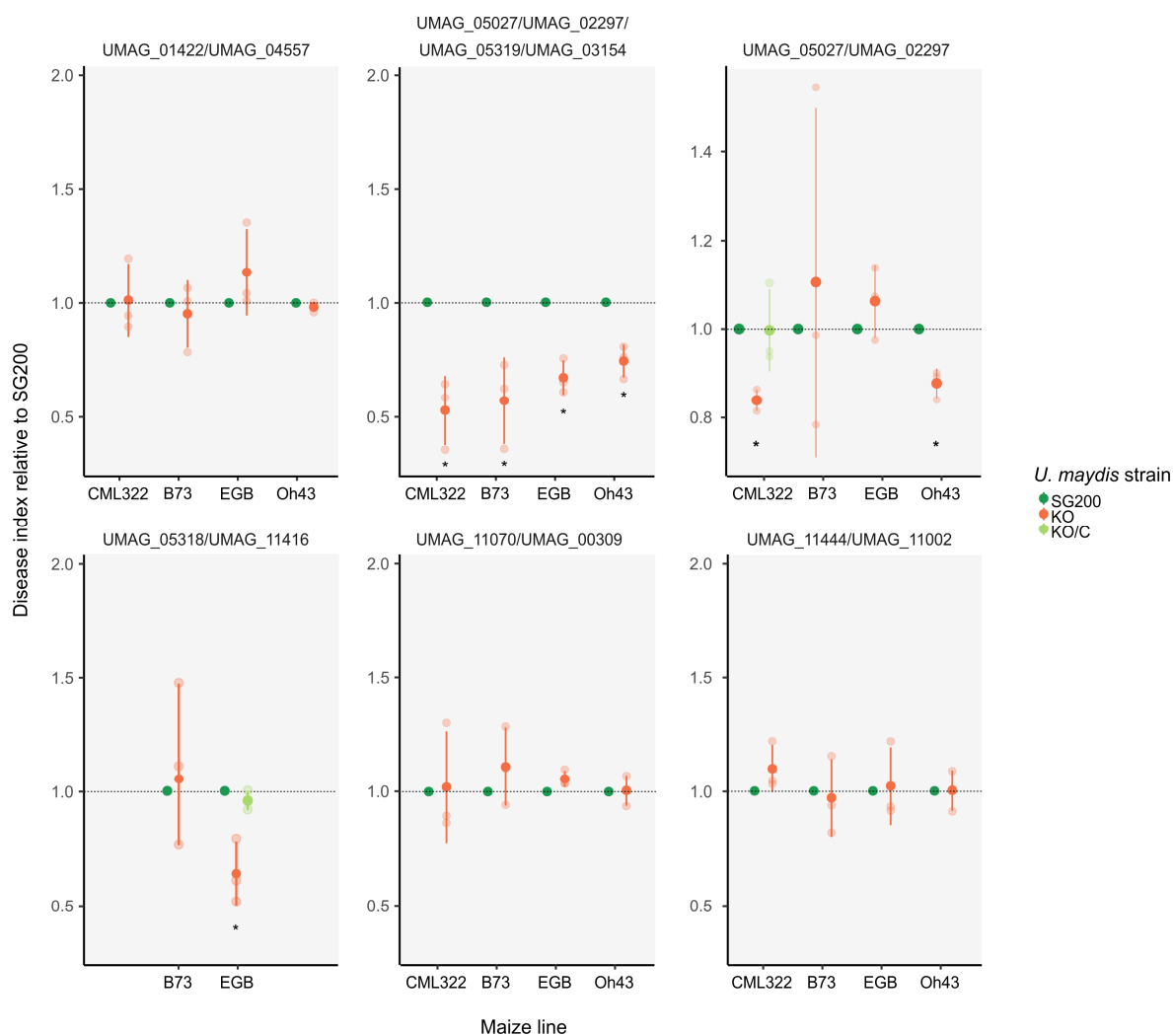


**Figure 2.14. Virulence functions of candidate maize line-specific effectors.** Double and quadruple knock-out (KO) mutant strains of selected maize line-specific effectors were injected into maize seedlings of the indicated line and symptoms were scored 12 days post infection (dpi). Gene names are shown at the top. KO refers to the respective CRISPR/Cas9 KO strain. Gene names separated by slash indicate double KO of these genes. KO/C indicates that a single copy of the respective genes was introduced into the KO strain for complementation. Disease indices reflect disease symptom severity and are shown in relation to SG200, which was set to unity. Asterisks label significant reduction in disease index compared to SG200 (student's t-test, p value < 0.05). All experiments were performed in three independent biological replicates. Average number of infected plants per strain and maize line: 89.

To assess if both or only one of the genes contribute to maize line-specific virulence of KO\_UMAG\_05027/ KO\_UMAG\_02297 on CML322, single KO mutants of UMAG\_02297 and UMAG\_05027 were tested for virulence on EGB and CML322. This experiment showed that UMAG\_02297 alone, but not UMAG\_05027, was necessary for full virulence on CML322. The virulence defect of KO\_UMAG\_02297 could be restored by introducing a single copy of UMAG\_02297 into the *ip* locus of the mutant strain (Figure 2.15A). To gain more detailed insight into the expression profile of UMAG\_02297 during infection progression, relative expression levels were analysed via qRT-PCR on the six different maize lines (Figure 2.15B). Interestingly, UMAG\_02297 was expressed at lowest levels on CML322 throughout the infection process, the maize line on which it was required for full virulence. Hence, high expression levels do not seem to determine the function for virulence. To investigate the relation of expression level of the effector and *U. maydis* virulence, I generated a strain in which UMAG\_02297 was expressed under control of the promoter *ppit2*, which is highly active throughout the infection process (Mueller et al. 2013), leading to a strong overexpression of the gene. EGB and CML322 seedlings were infected with *Ppit2:UMAG\_02297* single and multiple integration strains (Figure 2.15C). Interestingly, the overexpression strain showed a maize line-specific virulence defect as well: on CML322, but not on EGB, the multiple integration strain was significantly reduced in virulence compared to strain SG200. This shows that an adjusted expression level of UMAG\_02297 is required for virulence on maize line CML322. The finding that neither KO, nor overexpression of UMAG\_02297 had a significant effect on virulence on EGB suggests that the host targets of this effector might either not be present, or not involved in QDR to *U. maydis* in this maize line.

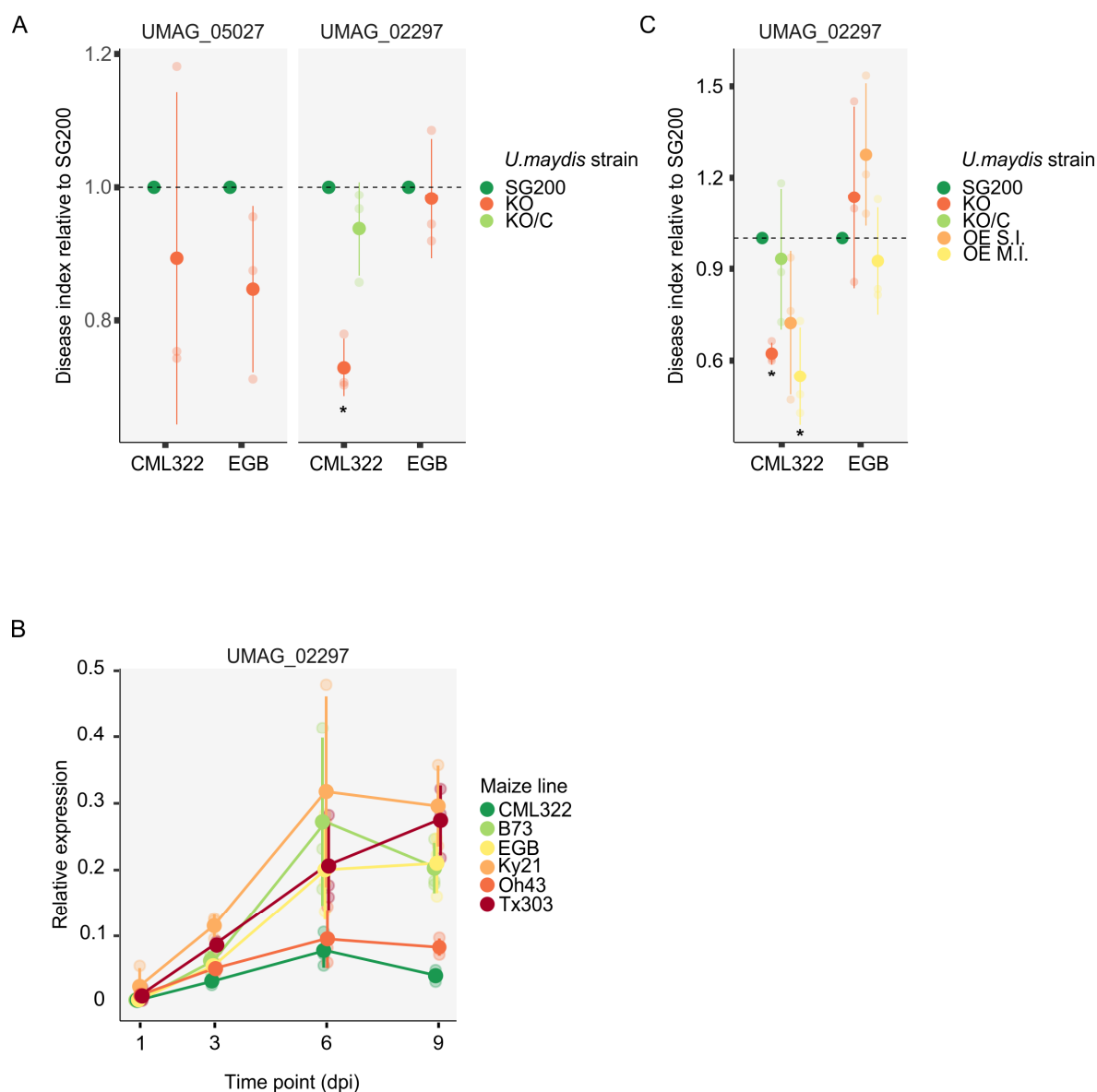


**Figure 2.15. A) Virulence functions of candidate maize line-specific effectors.** Single knock-out (KO) mutant strains of selected maize line-specific effectors were injected into maize seedlings of the indicated line and symptoms were scored 12 days post infection (dpi). Gene names are shown at the top. KO refers to the respective CRISPR/Cas9 KO strain. KO/C indicates that a single copy of the respective gene was introduced into the KO strain for complementation. Disease indices reflect disease symptom severity and are shown in relation to SG200, which was set to unity. Asterisks label significant reduction in disease index compared to SG200 (student's t-test, p value <0.05). All experiments were performed in three independent biological replicates. Average number of infected plants per strain and maize line: 88. **B) Expression of UMAG\_02297 during disease progression in different maize lines.** UMAG\_02297 relative expression was quantified during infection progression at 1, 3, 6, and 9 days post infection (dpi) via qRT-PCR. Solid points indicate mean ratios of UMAG\_02297 to ppi ( $2^{-\Delta Ct}$ ) of three biological replicates. Transparent points indicate individual values; error bars denote the standard deviation. **C) Impact of UMAG\_02297 overexpression on virulence.** SG200, KO\_UMAG\_02297, KO\_UMAG\_02297/C and OE\_UMAG\_02297 strains were injected into CML322 and EGB seedlings and symptoms were scored 12 dpi. OE: overexpression. S.I.: single integration. M.I.: multiple integration. Disease indices reflect disease symptom severity and are shown in relation to SG200, which was set to unity. Asterisks label significant reduction in disease index compared to SG200 (student's t-test, p value <0.05). All experiments were performed in three independent biological replicates. Average number of infected plants per strain and maize line: 86.

### 2.4.1 Intraspecific variation of UMAG\_02297

Allelic variation between host genotypes in genes that contribute to resistance or susceptibility is assumed to build the genetic basis of QDR (Niks et al. 2015). Consequently, to maintain efficient interaction with their targets, pathogen effectors targeting components of QDR are expected to display allelic variation as well. Therefore, the intraspecific sequence variation of the maize line-specific effector UMAG\_02297 was analysed. To this end, the amino acid sequences of UMAG\_02297 from all publicly available *U. maydis* genomes (Kämper et al. 2006; Zuo et al. 2020; <https://www.ncbi.nlm.nih.gov/assembly/organism/5270>) and from genomes of a collection of field isolates from different regions of Mexico (Kahmann et al., unpublished) were compared with each other (Table 2.1, Figure 2.16).

**Table 2.1. Origins of sequenced *U. maydis* strains.** Geographic origins of the *U. maydis* strains used for sequence variation analysis of UMAG\_02297 (Figure 2.16).

Strain	Origin
SG200	Minnesota, USA
521	USA
A, B, C, D, E	Irapouto, Mexico
F, G, H, I, J	Oaxaca, Mexico
K, L, M, N, O	Pachuca, Mexico
P, Q, R	Sinaloa, Mexico
S, T, U, V	Toluca, Mexico
ASM166006	Marburg, Germany
ASM166200	Marburg, Germany
ASM173615	Marburg, Germany
ASM173618	Düsseldorf, Germany
ASM173621	Marburg, Germany
JCM2005	Japan

This identified four different UMAG\_02297 orthologues, with amino acid identities ranging from 99.3% to 98.6%. The first orthologue was present in three strains originating from different geographic locations in Mexico (strains B, Q, V from Irapouto, Sinaloa and Toluca, respectively). The second orthologue was present in all other Mexican strains as well as the Japanese strain JCM2005. SG200 and 521, both from the USA, and three strains from different German locations (ASM166200, ASM173621 from Marburg and ASM173618 from Düsseldorf) carried a third UMAG\_02297 orthologue. Two other strains collected in Marburg, Germany (ASM173606 and ASM173615) shared a fourth orthologue. In summary, some strains that originated from highly distinct geographic locations had identical UMAG\_02297 sequences, while other strains from similar locations displayed different UMAG\_02297 sequences. This implies that geographic origin is not the main determinant of UMAG\_02297 sequence variation and one could therefore speculate that the host genotype plays a larger role in UMAG\_02297 sequence variation. It could therefore be insightful to compare from which maize lines the different strains were isolated. However, such information is not available for the analysed strains. Nevertheless, it should also be noted that conclusions drawn from variation in only one gene are rather limited. Therefore, for future studies, a detailed analysis of variation in all effector genes in different *U. maydis* strains would provide a more comprehensive view of adaptation of *U. maydis* to different environments.





Furthermore, to compare the extent of variation in UMG\_02297 to overall variation in *U. maydis* effector genes, the fraction of non-synonymous substitutions per non-synonymous site was calculated as a measure of sequence diversification for all effector genes. Then, based on the calculated values, the effectors were ranked from low variance to high variance. Here, UMG\_02297 was ranked in the top 15% of genes with highest variation, i.e. displayed higher sequence variation than most other *U. maydis* effectors (Figure 2.17). As stated above, high rates of sequence variation between genotypes are expected for genes involved in QDR. Together with the maize line-specific virulence function of the KO and the overexpression of UMG\_02297, this further indicates that UMG\_02297 could target components of QDR.

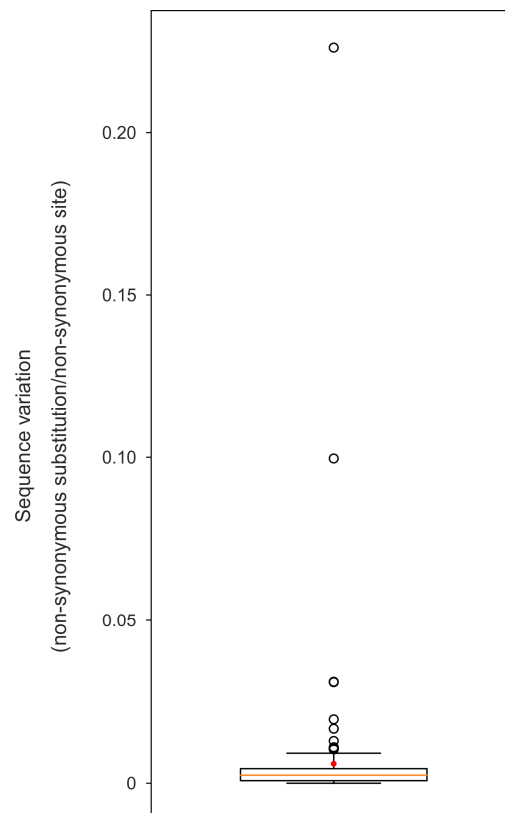


**Figure 2.17. Intraspecific sequence variation within *U. maydis* effector genes.** Boxplot of sequence variation between different *U. maydis* genotypes as the fraction of non-synonymous substitutions per non-synonymous site. Sequence variation was calculated for effectors of all publicly available *U. maydis* genomes and a collection of field isolates from different regions of Mexico (Table 2.1). Orange dot highlights UMG\_02297, orange line represents the median.

### 2.5 Host transcriptional changes induced by UMAG\_02297

To investigate, which host processes might be influenced by the maize line-specific effector UMAG\_02297, leaf samples of CML322 maize seedlings infected with SG200 and KO\_UMAG\_02297 were analysed by RNA-Seq at 3 dpi. Of all 63477 maize annotated loci, 30637 were expressed in these samples (48%). Variability between the samples was assessed in a multidimensional scaling plot (Figure 2.18A). Both *U. maydis*-infected samples formed one cluster highly distinct from the mock-treated samples, indicating that maize gene expression was mostly influenced by infection in general, rather than by the different *U. maydis* strains.

To identify genes which were uniquely responsive to infection with SG200 or the UMAG\_02297 KO strain, expression fold changes to the CML322 mock sample of the different infected samples were compared ( $\log_2$  expression fold change  $>0.5$  or  $<-0.5$ , adjusted p value  $<0.05$ ). This analysis identified the highest number of DEGs in comparison with the SG200-infected sample (6046 genes upregulated and 3646 genes downregulated compared to mock). The KO strain induced slightly milder transcriptional changes (5699 genes upregulated and 3212 genes downregulated compared to mock), which is in line with its reduced virulence. Most of the DEGs were jointly regulated: 91% of the upregulated genes (5486) and 81% of the downregulated genes (2962) were equivalently regulated in response to both strains. Only around 9% and 4% (560 and 213 genes) were uniquely upregulated in response to SG200 or KO, respectively, and around 19% and 8% (684 and 250 genes) were uniquely downregulated in response to SG200 or KO, respectively. Taken together, this indicates that maize gene expression is slightly and specifically altered by UMAG\_02297.

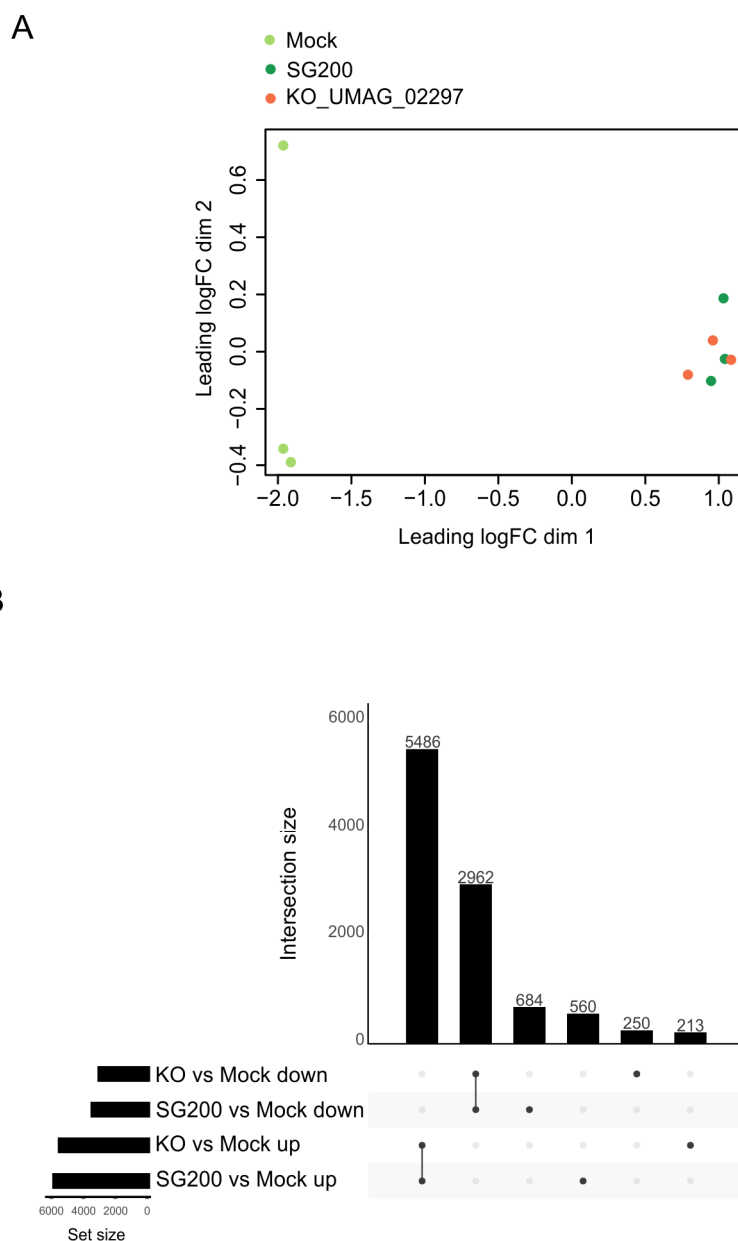


**Figure 2.18. Maize gene expression changes in response to *U. maydis* KO\_UMAG\_02297 and SG200.** The transcriptome of CML322 maize seedlings infected with SG200, KO\_UMAG\_02297 and mock was analysed via RNA sequencing 3 days post infection (dpi). KO: knock-out. **A) Multi-dimensional scaling plot of maize RNA sequencing data.** The top 5000 variable genes were used to calculate pairwise distances between the samples. **B) UpSet plot of maize genes differentially expressed in response to SG200 and KO\_UMAG\_02297 infections in comparison to mock.** Genes with a  $\log_2$  expression fold change  $>0.5$  or  $<-0.5$  and adjusted p value  $<0.05$  were considered differentially expressed (DE). In total, 10155 of 30637 expressed genes were DE. Number of differentially expressed genes (DEGs) for each of the 15 possible comparisons is indicated by set size (horizontal bars). Overlaps of DEGs between comparisons are depicted by connected black dots. Size of overlaps is indicated by intersection size (vertical bars).

## 2. Results

To gain insight into which host processes could be targeted by UMAG\_02297, genes uniquely responsive to each of the strains were additionally filtered for genes that were differentially expressed in response to *U. maydis* SG200 infection between CML322 and EGB, where UMAG\_02297 was not found to have a function for virulence (426 genes). Within these, genes predicted to encode auxin efflux transporters were strongly enriched (12-fold enrichment, hypergeometric p value 0.002). Interestingly, additionally several other genes predicted to be related to auxin were found within these (Figure 2.19). The auxin-efflux carrier *pin12* (GRMZM2G160496\_P01) and auxin-responsive SAUR32 (GRMZM2G466229\_P01) were similarly regulated in CML322 in response to KO and in EGB in response to SG200, while SAUR56 (GRMZM2G414727\_P01) and the auxin-efflux carrier *pin5* (GRMZM2G025742\_P01) differed more strongly between the maize lines (SG200- and KO-infected CML322 vs SG200-infected EGB). This observed specific regulation of auxin-related genes identifies the manipulation of the auxin pathway as a potential maize line-specific target of UMAG\_02297.

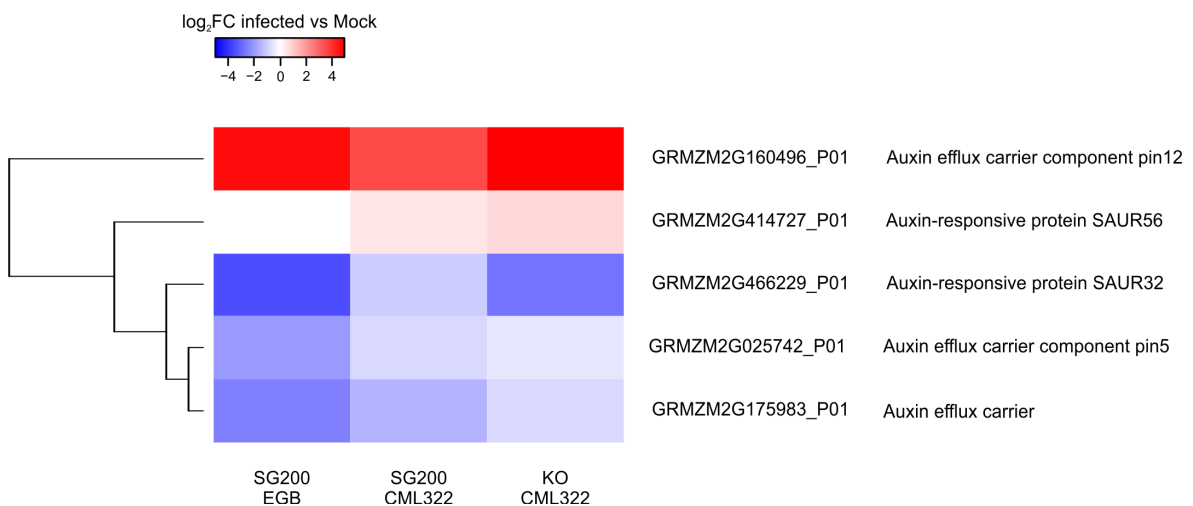


**Figure 2.19. Expression profile of auxin-related maize genes in response to *U. maydis* SG200 and KO\_UMAG\_02297 in EGB and CML322.** Heatmap shows log<sub>2</sub> expression fold changes of infected vs mock-treated samples.

## 2.6 QTL mapping for *U. maydis* disease resistance

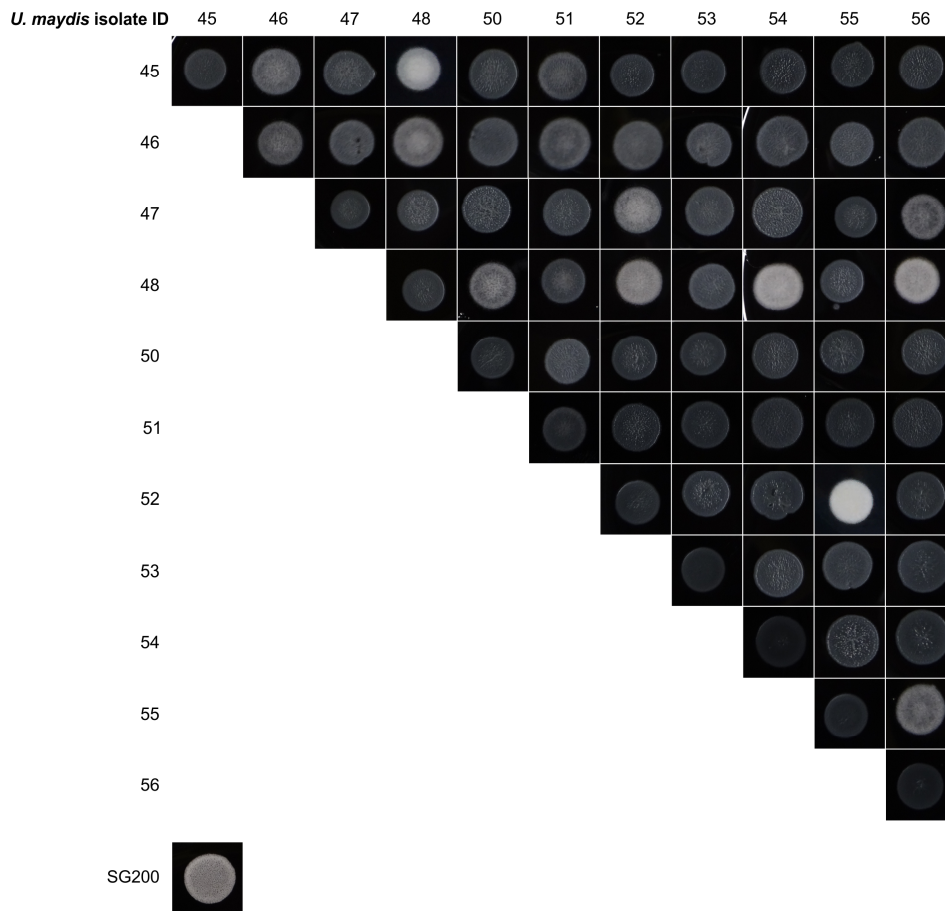
### 2.6.1 Identification of local compatible *U. maydis* field isolates

To identify genetic loci contributing to QDR towards *U. maydis* in maize seedlings, a QTL mapping experiment was conducted. For this, the third filial generation ( $F_3$ ) of a cross of B73 and Tx303, maize lines which displayed highly distinct *U. maydis* disease resistance phenotypes (Figure 2.1A), was used. As the number of plants needed for this study would have surmounted the greenhouse space available, the experiment was conducted in the field. Since only local wildtype strains were permitted to be used in field trials, suitable wildtype strains needed to be identified first. To this end, field isolates collected in the Marburg area in Germany (strain IDs 45-50) and in Luxemburg (strain IDs 51-56) were tested for compatibility. All possible strain combinations were dropped on PD-charcoal plates to assess filament formation (Figure 2.20A). Filamentation is manifested by white, fuzzy colonies and indicates successful mating in compatible mixtures. As control, all strains alone and the solopathogenic SG200 strain were used.

In mixtures 45x48, 47x52, 48x52, 48x54, 48x56 and 52x55 filament formation was visible. From these, 45x48 and 52x55 were selected for virulence assessment, as these were the only compatible mixtures of the same geographic origin. For this, B73 and Tx303 seedlings were inoculated with 45x48 and 52x55 in the greenhouse and symptoms were scored 12 dpi (Figure 2.20B). On B73, infection of both wildtype mixtures resulted in 42-62% of dead plants. The remaining plants displayed mostly chlorosis and normal tumours. Almost 95% of Tx303 plants infected with 45x48 and 52% of those infected with 52x55 were dead 12 dpi. In most remaining plants heavy tumours were observed. Taken together, this shows that both strain mixtures are highly virulent, and that the previously observed difference in resistance between Tx303 (highly susceptible) and B73 (relatively resistant) is also apparent using the tested wildtype mixtures. Because of closer origin of 45x48 to the location of the field, these isolates were selected for the QTL mapping experiment.

## 2. Results

A



B

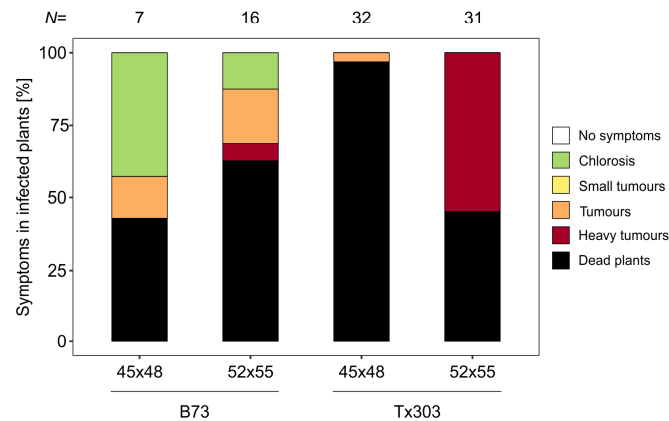


**Figure 2.20. Mating and virulence of *U. maydis* field isolates. A) Mating test of *U. maydis* field isolates.** Filamentation of mixtures of *U. maydis* field isolates was assessed by dropping 2.5  $\mu$ l of culture mixtures on PD charcoal plates. The solopathogenic SG200 strain was used as control. Strains 45-50 were collected from a maize field in the Marburg area, Germany. Strains 51-56 were collected from a maize field in Luxembourg. **B) Disease symptom classification of *U. maydis* field isolates.** B73 and Tx303 maize seedlings were inoculated with the indicated mixtures of compatible *U. maydis* isolates at the three-leaf stage. Disease symptom classification was done 12 days post infection (dpi) as described in Redkar and Doehlemann (2016a) and values are expressed as percentage of the total number of infected plants. *N*: number of infected plants.

## 2.6.2 Genetic map construction

To identify correlations between genetic loci and *U. maydis* resistance by QTL mapping, first the B73xTx303 segregating progeny were genotyped. For this, 111 molecular markers evenly distributed across the genome that were polymorphic and showed no heterozygosity between the parental lines were selected from single nucleotide polymorphisms (SNPs) identified by Ganai et al. (2011). The selected SNP markers were genotyped by competitive allele-specific PCR (KASP) on a bulk of five plants per F<sub>3</sub> family derived from the B73xTx303 cross. Markers that were monomorphic and with more than 30% missing data and families with more than 20% missing data were omitted (Supplementary Figure 6.5) as well as markers with strong segregation distortion (p value <10<sup>-15</sup>), leaving 76 markers and 93 families for the analysis. Segregation distortion, also referred to as meiotic drive, leads to strong deviation from the expected genotypes and often indicates problematic markers, as unlinked markers appear to be linked. The genetic map was constructed chromosome-wise by checking all possible orders of markers in a sliding window approach. Finally, the marker orders that minimised the obligate number of crossovers were chosen. The resulting genetic map displayed a total size of 1812 cM, with an average marker spacing of 27.5 cM (Table 2.2 and supplementary Figure 6.6).

**Table 2.2. Genetic map properties.** Number of markers, length and spacing of markers within chromosomes and the complete genome. Chr: Chromosome. No.: Number. The genetic map was constructed with R/qtl v1.46-2 (Broman et al. 2003) using Haley-Knott regression in collaboration with Benjamin Stich.

Chromosome	No. of markers	Length [cM]	Average spacing [cM]	Maximum spacing
1	12	252.5	23.0	82.6
2	8	286.1	40.9	92.8
3	6	245.2	49.0	154.8
4	7	97.4	16.2	22.3
5	9	193.1	24.1	79.6
6	7	110.1	18.4	49.6
7	5	174.5	43.6	82.3
8	8	137.3	19.6	58.3
9	8	162.4	23.2	36.2
10	6	153.6	30.7	49.1
all	76	1812.3	27.5	154.8

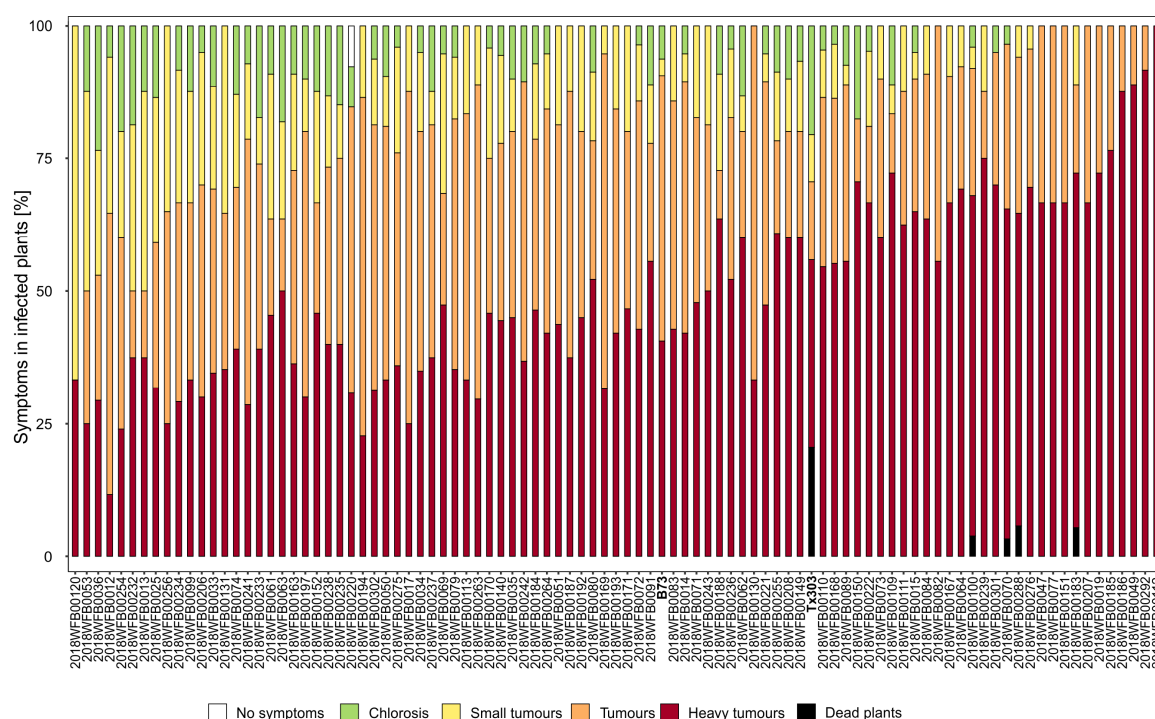


### 2.6.3 QTL analysis

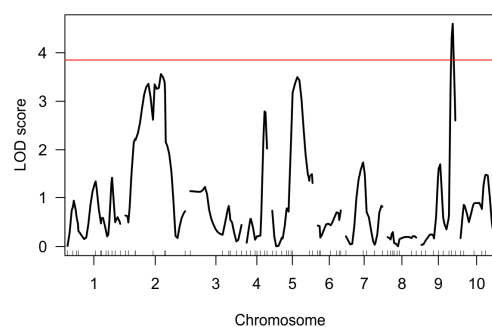
For the phenotypic analysis of the B73xTx303 segregating progeny, approximately 20 seedlings of 100 B73 x Tx303 F<sub>3</sub> families and of the parental lines were inoculated with *U. maydis* 45x48 in two independent biological replicates in the field. Because of the extraordinarily strong virulence of the selected strains, the inoculum was reduced to 50% (OD<sub>600</sub> of inoculum was 0.5 instead of OD<sub>600</sub> 1). Disease symptoms were scored 11 dpi (Figure 2.21A). QTL detection identified the marker PZE-109112175 on chromosome 9 to significantly contribute to heavy tumour formation (Figure 2.21B,  $\alpha = 0.05$ ). The QTL was extended to the neighbouring markers and spanned a 10.89 Mb region containing 884 predicted genes. Figure 2.21C depicts the effect of the genotype of the identified marker on heavy tumour frequency. In families carrying the B73 allele at the identified marker (AA), heavy tumours were slightly reduced compared to families carrying the Tx303 allele (BB). Families that were heterozygous at the identified marker showed heavy tumour levels comparable to those homozygous for the B73 allele, suggesting a dominant negative effect on heavy tumour formation of the B73 allele. For the other symptom categories as well as for the disease index, no significant QTL was identified.

QTL mapping was repeated in two additional biological replicates in the subsequent year. Due to high variation of the observed phenotypes between replicates, results from the first year could not be confirmed, indicating a strong influence of environmental factors on *U. maydis* resistance (results not shown). Therefore, QTL mapping should be repeated using more plants per family and/or more stable conditions to validate the identified QTL. Comparison with the transcriptome data of different maize lines infected with *U. maydis* revealed 34 genes within the QTL being differentially expressed between B73 and Tx303 in response to *U. maydis* (Chapter 2.3). In case the identified QTL will be confirmed in subsequent analyses, these genes would represent promising candidates that could underlie the effect of the QTL on *U. maydis* resistance.

A



B



C

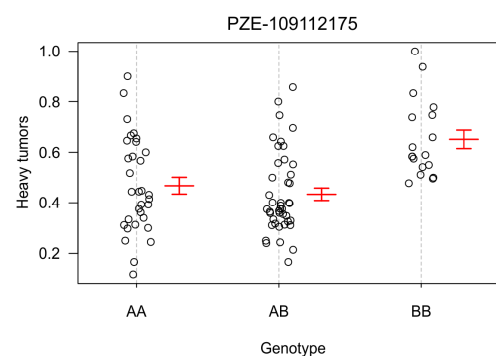


**Figure 2.21. QTL mapping for *U. maydis* disease resistance. A) Symptom scoring of B73xTx303 F<sub>3</sub>-families and parental lines.** Seedlings grown in the field were inoculated with *U. maydis* 45x48 wildtype isolates at the three-leaf stage in two independent biological replicates in 2018. Disease symptom classification was done 11 days post infection (dpi) as described in Redkar and Doehlemann (2016a) and values are expressed as percentage of the total number of infected plants. Average number of infected plants: 18. Benjamin Stich generated the F<sub>3</sub>-families and kindly provided seeds. **B) LOD scores for heavy tumours.** LOD scores are a measure of the likelihood of linkage of loci to the quantitative trait. LOD threshold for  $\alpha = 0.05$  is indicated by red line ( $\approx 3.85$ ). LOD: logarithm of the odds. **C) Effect plot for genotypes at the identified marker.** AA corresponds to the B73 allele and BB corresponds to the Tx303 allele. Adjusted entry means (aems) for the shown genotypes for heavy tumours are indicated by the y axis. Means of the aems are indicated by red lines and error bars indicate the standard error  $\pm$  1. QTL detection was done in collaboration with Benjamin Stich.

### 3 Discussion

The maize pathogen *U. maydis* serves as a model system to study the molecular mechanisms of biotrophic plant-pathogen interactions and causes important yield losses in the world's major crop maize. Unlike in most biotrophic interactions, resistance of maize to *U. maydis* is a polygenic, quantitative trait. However, the molecular basis of QDR in the *U. maydis*-maize interaction is mostly unknown. Therefore, the molecular mechanisms underlying QDR in maize and how *U. maydis*' virulence strategy is adapted to different host genotypes were investigated in this study.

#### 3.1 *U. maydis* resistance levels of diverse maize lines

Plant inoculation experiments revealed that *U. maydis* resistance levels of the NAM founder lines and EGB are highly diverse, which further corroborates the quantitative nature of the *U. maydis*-maize interaction and indicates that several genes are involved in determining resistance or susceptibility. Resistance levels of the NAM founder lines to other diseases such as Northern leaf blight or aphids have been previously analysed, which showed distinct patterns from the *U. maydis* resistance levels observed in this study. B73 for example is highly susceptible to Northern leaf blight, while CML322 is very resistant and Ky21, Oh43 and Tx303 showed medium susceptibility levels (Poland et al. 2011). Aphid resistance is high on Tx303, Oh43 and Ky21, whereas CML322 is highly susceptible and B73 displays medium aphid susceptibility (Meihls et al. 2013). For *U. maydis*, CML322 displayed highest resistance levels, followed by B73, and Ky21, Oh43 and Tx303 were moderately to highly susceptible. This suggests that specific defence mechanisms rather than general disease robustness determine the outcome of maize interactions with different pathogens and pests.

Furthermore, maize lines of tropical origin were generally more resistant, while maize lines of temperate origin, i.e. of close provenance to SG200, were generally more susceptible. This could indicate that the local *U. maydis* strains might adapt to the local host lines. However, this is based on the observation of the maize resistance phenotypes towards only one *U. maydis* strain. Tropical maize lines might also display higher resistance levels to *U. maydis* infection in general, as pressure from pathogens and pests tends to be higher in such habitats, which probably results in a stronger focus on disease resistance breeding in tropical regions (Schemske et al. 2009; Rasman and Agrawal 2011). Hence, investigating the resistance levels of different maize lines towards *U. maydis* strains of

diverse geographical origins is required to clarify possible mechanisms of geographic adaptation.

### 3.2 Maize processes involved in QDR against *U. maydis*

To elucidate the molecular mechanisms underlying the quantitative maize-*U. maydis* interaction, I performed an RNA-Seq analysis of maize lines of distinct resistance levels colonised by *U. maydis*. Investigations of the genotype-dependent transcriptional changes in maize in response to *U. maydis* aimed at identifying host processes involved in QDR to *U. maydis*.

In general, maize responses towards *U. maydis* infection involve a broad physiological reprogramming, which includes suppression of photosynthesis-associated genes in infected leaves (Horst et al. 2008; Doehlemann et al. 2008a). This is accompanied by an increase of free hexose levels and a decrease in chlorophyll content, reflecting that the fungus blocks the transition to a photosynthetically active source tissue (Doehlemann et al. 2008a; Matei et al. 2018). Free hexoses within tumour cells are thought to serve as an easily accessible carbon source for the fungus, as well as help to build up osmotic pressure for tumour cell-expansion (Horst et al. 2008; Horst et al. 2010). Infection experiments using maize mutants with distorted starch metabolism furthermore showed that alterations in carbon allocation are an important factor influencing *U. maydis* growth and plant defence (Kretschmer et al. 2017b). Similarly, *U. maydis* infection goes along with redirection of nitrogen-rich amino acids towards tumour tissues, where they are thought to contribute to defence rather than serving as nutrients for the fungus (Horst et al. 2010; Kretschmer et al. 2017a). Changes in phytohormones such as JA, SA and auxin are also associated with *U. maydis* infection (Turian and Hamilton 1960; Doehlemann et al. 2008a). Additionally, the fungus actively triggers cell division and reactivates DNA synthesis for tumour formation in leaves, which goes along with cell type-specific alterations of genes involved in cell-cycle regulation (Redkar et al. 2015; Matei et al. 2018; Villajuana-Bonequi et al. 2019).

Of these general *U. maydis*-induced host responses, several were identified to be specifically altered depending on the maize line. Correlation analysis of gene expression to resistance levels via WGCNA identified genes involved in photosynthesis to be upregulated in the more resistant maize lines. This suggests that there, the induction of photosynthesis is not as strongly suppressed as in the more susceptible maize lines by *U. maydis*. Inefficient suppression of photosynthesis might result in changes in carbon allocation and consequently lead to a reduced fungal proliferation, either directly through

limitation of nutrient supply for the fungus or indirectly via alterations in plant defence signalling (Roitsch et al. 2003; Bolouri Moghaddam and Van den Ende 2013; Kretschmer et al. 2017a).

Furthermore, cell division processes were upregulated in response to *U. maydis* in the more susceptible maize lines. In the *A. thaliana-Plasmodiophora brassicae* interaction, which is also accompanied by gall formation, genes involved in cell proliferation are associated with QDR as well (Jubault et al. 2013). In addition to the obvious involvement in tumour formation, cell-cycle deregulation can also have an impact on expression of R genes and thereby modulates plant defence (Bao et al. 2013). Thus, one could speculate that genes involved in cell division might also play a role in QDR against *U. maydis*. However, based on the available data one cannot exclude that the positive correlation of photosynthesis-repression and cell division with fungal infection could also be consequence rather than cause of an enhanced susceptibility. Nevertheless, as the developmental stages of the fungus in all my samples were comparable, it is likely that the observed resistance level-specific transcriptional changes directly contribute to the outcome of the quantitative interaction with *U. maydis*.

Within all genes differentially regulated between maize lines in response to *U. maydis* infection, the major functional classes were related to 'transmembrane transport' as well as 'oxidation-reduction' and 'protein phosphorylation'. Protein phosphorylation through kinases is a central process for signal transduction in immune responses. Interestingly, kinases have been shown to play important roles in QDR in several cases. Two maize wall-associated kinases, ZmWAK-RLK1 and ZmWAK, confer QDR to Northern leaf blight and a close relative of *U. maydis*, *S. reilianum*, respectively (Zuo et al. 2015; Hurni et al. 2015). Transport processes are essential for plant responses during interactions with pathogens, and several QDR genes encode putative transporters. For example, the ABC transporter encoded by Lr34 confers resistance to diverse fungal pathogens in wheat (Krattinger et al. 2009). Hence, this suggests a possible role for kinases as well as transport processes also in QDR against *U. maydis*.

Together, the analyses of maize line-dependent transcriptional changes induced by *U. maydis* show that genes associated with QDR to *U. maydis* involve genes of various functional classes. Furthermore, the finding that only a small fraction of the maize line-specifically expressed genes was shared with genes previously found to be associated with PTI and ETI in *A. thaliana* (Dong et al. 2015; Hatsugai et al. 2017; Mine et al. 2018), assuming conservation of PTI and ETI between the different plant species, suggests that QDR mechanisms are mostly distinct from canonical PTI and ETI gene networks. This is in line with the generally complex nature of QDR and the idea that QDR extends beyond pathogen perception (Corwin and Kliebenstein 2017).

### 3.3 Maize line-specific gene expression in *U. maydis*

The major aim of this study was to elucidate whether the virulence strategy of *U. maydis* is adapted to different host genotypes. To this end, I investigated changes in *U. maydis* gene expression patterns induced by the interaction with maize lines of distinct disease resistance levels via RNA-Seq.

WGCNA identified several modules of co-expressed genes, and two of them were significantly correlated to the resistance level of the colonised maize line. In the co-expression module positively correlated to colonisation of more resistant maize lines, enriched biological processes included mechanisms connected to carbohydrate metabolism, which has been directly linked to plant cell wall degradation in plant pathogenic fungi (Tonukari et al. 2000; Ospina-Giraldo et al. 2003). During *U. maydis* infection, degradation of cell walls is essential at very early stages to allow initial penetration and intracellular growth, as well as in later stages when plant cell walls need to be loosened to enable cell enlargement for tumour formation, rather than being used as a nutrient source (Doehlemann et al. 2008b; Lanver et al. 2018). Furthermore, changes in cell wall lignification play an important role in the restriction of *U. maydis*-induced tumour formation (Tanaka et al. 2014; Matei et al. 2018). Consequently, one could speculate that enhanced cell wall reinforcements or different cell wall compositions might be an additional obstacle the fungus needs to overcome when colonising host lines of higher resistance levels. Several studies have suggested differences in cell wall composition as factors in other host-pathogen interactions as well (Vorwerk et al. 2004; Bacete et al. 2020). *A. thaliana* mutants of the GPI-anchored putative pectate lyase PMR6 are highly resistant to powdery mildew (Vogel et al. 2002). In wheat, variation in pectin composition has been associated with resistance to the stem rust fungus *Puccinia graminis* (Wiethölter et al. 2003). In maize, significant differences in cell wall composition between maize lines have been reported (Hazen et al. 2003). A detailed cell wall carbohydrate profiling of all NAM founder lines would allow investigating if more resistant or more susceptible maize lines share similar cell wall compositions and would thereby help to answer the question to which extent natural variation in cell wall composition affects pathogen resistance.

Transport reactions are essential in all living cells to transfer metabolites or nutrients and to interact with their environment. In *U. maydis*, different nutrient transporters are important virulence factors tied to biotrophic development (Wahl et al. 2010; Horst et al. 2012; Schuler et al. 2015). The previously described high-affinity sucrose transporter Srt1 (Wahl et al. 2010), hexose transporter Hxt1 (Schuler et al. 2015) and nitrogen transporter Nit2 (Horst et al. 2012) were not differentially expressed between maize lines. However, nutrient uptake is not only dependent on specific nutrient transporters, but most

importantly driven by an ion gradient which is produced by the activity of plasma membrane H<sup>+</sup>-ATPases that transport ions through the membrane (Palmgren 1990; Gianinazzi-Pearson et al. 1991; Sondergaard et al. 2004; Wang et al. 2014). For example during mycorrhizal symbiosis, plant H<sup>+</sup>-ATPases were found to energise nutrient uptake in rice and *Medicago truncatula* (Wang et al. 2014). Within the co-expression module positively correlated to the disease index, i.e. that contains genes generally upregulated during infection of more susceptible maize lines, one significantly enriched functional group is linked to ion transport processes and contains a putative H<sup>+</sup>-ATPase that could be involved in nutrient uptake. Consequently, this could indicate that different availability of nutrients in more resistant vs. more susceptible maize lines might influence *U. maydis* growth and disease development, and thereby contribute to the observed resistance phenotypes.

In general, the *U. maydis*-maize interaction follows a two-phased model, where first the establishment of the interaction depends on universal pathogenicity factors that suppress conserved plant defences (Skibbe et al. 2010). In the second phase, the fungus encounters different cell types or cells of diverse physiological and nutritional stages, probably depending on the plant organ, tissue, or genotype. Thus, a more adapted and refined response, including highly specific regulation of CSEPs, is required upon disease progression (Walbot and Skibbe 2010; Skibbe et al. 2010; Gao et al. 2013; Matei et al. 2018). So far, organ-specific as well as cell type-specific CSEP expression patterns have been identified (Skibbe et al. 2010; Matei et al. 2018).

Within *U. maydis* genes being differentially expressed between host genotypes, CSEPs were significantly enriched. Additionally, CSEPs were significantly enriched in the co-expression module that was negatively correlated to the disease index, i.e. within genes that were upregulated in the more resistant maize lines as well. Both these findings indicate a predominant role of CSEPs in colonising host lines of different resistance levels and point to an important involvement of CSEPs in targeting components of QDR. Also in other pathogens, such as *B. graminis* ssp. *hordei* and *Z. tritici*, regulation of effector genes was found to be dependent on the host genotype (Hacquard et al. 2013; Kellner et al. 2014).

Accordingly, in addition to organ- and cell type-specific regulation, *U. maydis* CSEPs are also specifically regulated depending on the colonised maize line, which adds another layer of specificity into this pathogenic interaction. How CSEP expression is altered according to the plant organ, tissue or genotype remains unclear. In general, expression of CSEPs can be regulated by a variety of mechanisms, including specific transcription factors. In *U. maydis*, so far only infection stage-specific transcription factors have been characterised (reviewed in Lanver et al. 2017). Hence, identifying the transcription factors

or signals that could be involved in fine-tuning CSEP expression patterns would give valuable insights into the highly sophisticated virulence strategy of *U. maydis*.

### 3.4 Maize line-specific activity of *U. maydis* CSEPs

It has been hypothesized that allelic variation between plant genotypes in genes contributing to resistance or susceptibility likely builds the molecular basis of QDR (Niks et al. 2015). This can lead to altered expression patterns or different modes of defence reactions. If these QDR genes represent effector targets, allelic variation can also influence the efficiency an effector can interact with and thereby manipulate its respective host target. Therefore, the targets of pathogen effectors which quantitatively contribute to virulence are potential candidates contributing to QDR in the host and thus, the identification of these effectors and subsequently, their respective targets, can help to elucidate the diverse genetic basis of QDR. One example which strongly supports the hypothesis that allelic variations in effector targets may be the basis of QDR came from the *Phytophthora infestans* effector EPIC1, which inhibits the papain-like cysteine protease (PLCP) RCR3 in tomato and potato (Song et al. 2009). Comparative analysis with the *Phytophthora mirabilis* EPIC1 homolog, PmEPIC1, identified host-specific abilities to suppress RCR3. PmEPIC1 failed to suppress potato and tomato RCR3, but was highly effective in inhibiting an RCR3-like protease in *Mirabilis jalapa*. These different specificities resulted from single amino acid polymorphisms in both the host target and the pathogen effectors (Dong et al. 2014). Similarly, one *U. maydis* effector conserved across different species, Pit2, shows gradual adaptation to the host target (Misas Villamil et al. 2019). There, the *S. reilianum* Pit2 orthologue can only partially complement the virulence defect of an *U. maydis* Pit2 KO mutant. Furthermore, the KO mutant of another *U. maydis* effector, ApB73, displays a strongly reduced virulence phenotype in the maize line B73, while in the more susceptible maize line EGB the virulence defect is less pronounced (Stirnberg and Djamei 2016). The cause of this quantitative difference in virulence is unclear. Taken together, these observations underpin the importance of effector diversification and their possible quantitative influence on pathogen virulence.

Based on the enrichment of CSEPs in maize line-specifically expressed *U. maydis* genes, the virulence functions of selected maize line-specifically expressed sets of CSEPs were assessed in different maize lines to further investigate the importance of maize line-specific adaptation of *U. maydis* effectors. By this, I identified two sets of effectors which specifically contribute to *U. maydis* virulence depending on the maize line (UMAG\_02297/UMAG\_05027 and UMAG\_05318/UMAG\_11416). Subsequent analysis of



single CSEP mutants isolated UMAG\_02297 as the gene that underlies the maize line-specific virulence reduction of the UMAG\_02297/UMAG\_05027 KO mutant. Preliminary data additionally suggest a maize line-specific virulence function for the CSEP sets UMAG\_02178/UMAG\_11908 and UMAG\_10861/UMAG\_05222. The other maize line-specifically expressed sets of CSEPs either contribute to virulence in none or all the tested maize lines. Hence, maize line-specific expression patterns do not always result in maize line-specific function. Overall, the identification of several sets of CSEPs with maize line-specific virulence functions further substantiates the importance of effectors in targeting components of QDR and suggests specific adaptation of *U. maydis* effectors to different host genotypes.

#### **3.5 The maize line-specific effector UMAG\_02297**

In this study, I identified a maize line-specific virulence function for the effector gene UMAG\_02297. Unexpectedly, UMAG\_02297 is required for full virulence in the maize line in which expression levels are lower than in the maize lines where it does not affect virulence throughout the infection. Furthermore, overexpression of UMAG\_02297, similar to its KO, resulted in a maize line-specific virulence defect. Both these findings underline that manipulation of host processes by effectors requires a fine-tuned adaptation to the host genotype. Similarly, in the barley pathogen *Rhynchosporium commune*, effector transcript levels and functional importance do not always coincide either. Here, the three necrosis-inducing effectors NIP1, NIP2, and NIP3 were found to impact virulence differently depending on the host genotype, and NIP1 transcript levels did not correlate with its functional importance (Kirsten et al. 2012).

These findings suggest that the specific functions of effectors do not only depend on their expression levels, but could also be a consequence of functional specialisation that did not necessarily require adaptation on the transcriptional level. Correspondingly, cross-species analyses between *U. maydis* and *S. reilianum* effector orthologues highlighted that adaptation of effector genes can be caused by changes on the transcriptional level as well as through neo-functionalisation of the effector proteins (Zuo et al. 2020b). This is furthermore supported by the observation that ApB73, which has a maize line-specific function for virulence in *U. maydis* (Stirnberg and Djamei 2016), is not differentially expressed between maize lines, at least not at the time point tested in this study. Additionally, presence or variation of the respective effector host target probably also strongly determine effector function. This is endorsed by the finding that UMAG\_02297 is upregulated in EGB, where it did not contribute to virulence, and that overexpression of

UMAG\_02297 in EGB did not affect virulence in this maize line. The relatively high expression level of UMAG\_02297 in EGB could represent an attempt of the fungus to compensate loss of function by overexpression. Moreover, the *S. reilianum* ApB73 orthologue is able to complement the *U. maydis* ApB73 mutant phenotype in B73, even though sequence identity is only about 44% (Stirnberg and Djamei 2016), suggesting that interaction with the respective B73 target does not strongly depend on the particular effector sequence, but that in fact, the effector target might be highly variable between B73 and EGB, where ApB73 only has a minor contribution to virulence. Hence, variation in effector host targets, in addition to variation in effectors themselves, plays an important role in determining effector virulence function.

### 3.5.1 Sequence variation in UMAG\_02297 orthologues

It is assumed that effectors involved in QDR exhibit sequence diversification, since allelic variation in their respective targets probably forms the basis of QDR (Niks et al. 2015). The identification of pathogen race-specific resistance QTLs in rice against the blast fungus *Magnaporthe grisea* further substantiate the importance of allelic variation in both the host and the pathogen in QDR (Talukder et al. 2004). In *U. maydis*, a hint that variation between factors which target QDR components significantly influences QDR came from the finding that some maize resistance QTLs were only functional in a specific environment (Lübberstedt et al. 1998a). There, a QTL mapping approach using natural *U. maydis* infections showed that the resistance phenotype of the same host genotype is dependent on the supposedly variable locally prevalent *U. maydis* genotypes.

Comparison of the protein sequences of the maize line-specific effector UMAG\_02297 from different *U. maydis* isolates identified four variable amino acid positions. One of these variable positions lies within the signal peptide and might affect secretion of the effector. Two other amino acid changes are conservative, the fourth change in contrast (proline to asparagine) could influence protein function. Even though variation within UMAG\_02297 is rather limited (with minimal sequence identity of 98.3%), it ranked within the top 15% of variable effectors in the investigated strains, meaning that effector variation in general is very low in *U. maydis*. The low diversity of amino acid sequences observed between isolates could be explained by the fact that evolutionary pressure is sometimes exerted on only a few and precise amino acid positions involved in the interaction of the protein with its target (Morales et al. 2020).

Still, single amino acid changes can have immense impact on protein function, as it is demonstrated by e.g. the different inhibition specificities of the abovementioned EPIC1 effector from two different *Phytophthora* species. Here, a single amino acid polymorphism

in the host protease and a reciprocal single amino acid change in the pathogen effectors resulted in the host-specific inhibition of their target protease, underlining the importance of ecological effector diversification (Dong et al. 2014). Furthermore, in the *P. infestans* avirulence protein Avr3a, as little as one or two amino acid variations determine the avirulence or virulence phenotype of the respective strain (Armstrong et al. 2005).

Strikingly, some strains from geographically distant origin displayed identical UMAG\_02297 sequences, while other strains from closer origin differed in their UMAG\_02297 sequence. In many sexual pathogens, as *U. maydis*, better-adapted genotypes often emerge locally through recombination instead of gene flow through immigrants, as it was shown for *Leptosphaeria maculans* and *Z. tritici* (Daverdin et al. 2012). Accordingly, it could be speculated that the different UMAG\_02297 variants were independently established in similar host backgrounds where they were better adapted to their target, as the strains that carry the advantageous allele in the respective maize line would probably predominate other strains in the field. Unfortunately, correlation of the effector variants to the maize lines from which the respective strains were isolated is not possible due to the lack of such information. As a next step, it would therefore be of interest to investigate whether the different variants of UMAG\_02297 are functional in different host genotypes.

To conclude, the relatively high level of intraspecific variation of UMAG\_02297 compared to overall effector diversity within *U. maydis* strains further strengthens its putative role in targeting components of QDR. Overall, it has become clear that natural variation in both pathogen and host are important factors that quantitatively influence the outcome of plant-pathogen interactions.

### 3.5.2 Manipulation of host gene expression by UMAG\_02297

The analysis of transcriptional changes induced by the UMAG\_02297 KO mutant in comparison to wildtype infections identified auxin-related processes being a possible target of this effector. In general, auxins play a cardinal role in controlling plant growth and development. Additionally, auxin can act as an antagonist of the SA pathway in plant defence, and thereby could promote fungal growth and disease development (Kazan and Manners 2009). Previous studies have identified many auxin-related genes that underlie QDR. For example in the soybean-*Phytophthora sojae* interaction, auxin catabolite accumulation differed between a relatively resistant and a more susceptible soybean cultivar, and the ability of resistant cultivars to cope with auxin accumulation could play an important role in QDR in this pathosystem (Stasko et al. 2020). In maize, cloning of the causal gene of the Giberella stalk rot resistance QTL *qRfg2* identified ZmAuxRP1, which encodes a plastid stroma-localized auxin-regulated protein, presumably modulating auxin biosynthesis (Ye et al. 2019). Furthermore, increased auxin levels can generally lead to enhanced susceptibility to several biotrophic pathogens (Navarro et al. 2006; Wang et al. 2007; Mutka et al. 2013) and a few pathogen effectors that target auxin-related processes have been identified so far. The *P. syringae* effector AvrRpt2 for example initiates auxin signalling through degradation of auxin/IAA proteins (Cui et al. 2013), and the effector PSE1 from *Phytophthora parasitica* modulates local auxin levels through altered distribution of auxin efflux transporters (Evangelisti et al. 2013).

For *U. maydis*, it has been proposed that auxin plays an important role in cell enlargement during tumour formation, as auxin synthesis and auxin-responsive genes are induced during this process (Turian and Hamilton 1960; Doehlemann et al. 2008a). Furthermore, several gall-producing bacteria secrete auxins into the host to enable tumour or gall formation and infection (Fu and Wang 2011; Patten et al. 2013). Hence, in addition to its role in plant defence, regulation of developmental changes by auxin might be an important factor during *U. maydis* disease development.

More precisely, the auxin-related genes that are possibly influenced by UMAG\_02297 are predicted to encode SAUR (small auxin up-regulated RNA) family proteins and PIN (PIN-FORMED) auxin efflux transporters. Due to their extensive genetic redundancy, the functions of most SAUR genes have remained elusive. Several lines of evidence suggest that SAURs can positively and as well negatively regulate plant growth through controlling cell expansion or division (Ren and Gray 2015). In addition, SAUR proteins might provide a functional link between  $\text{Ca}^{2+}$  and auxin responses (Ren and Gray 2015) and could thereby also be involved in defence signalling processes. The correct localisation and patterning of auxin levels is crucial for auxin-regulated processes, and the PIN family

plays an important role in polarised auxin export (Ng et al. 2015). The inhibition of auxin transport can differentially affect resistance to different pathogens (Kazan and Manners 2009), and the cyst nematode *Heterodera schachtii* was found to hijack the host's PIN-modulated auxin distribution network to facilitate infection and gall formation (Grunewald et al. 2009).

Taken together, this renders auxin-related processes an interesting and promising target of UMAG\_02297, which however requires further functional validation. Protein-interaction studies of UMAG\_02297 as well as comparison of auxin-levels in tissues infected by the UMAG\_02297 KO strain and SG200 could further strengthen the hypothesis that this effector might target auxin-related processes. Auxin measurements in infected tissues of different maize lines would furthermore provide more general insights into the possible roles of auxin in maize QDR against *U. maydis*.

#### **3.5.3 Model for the maize line-specific function of UMAG\_02297**

The observations on the maize line-specific function of UMAG\_02297 can be summarised in a tentative model (Figure 3.1). The KO of UMAG\_02297 resulted in a specific reduction of virulence in the maize line CML322, but not in EGB. Hence, in CML322, UMAG\_02297 successfully contributes to virulence probably via interaction or modification of its maize target. In EGB, the respective maize target could display allelic variation, thereby inhibiting UMAG\_02297 to enhance fungal virulence. The finding that UMAG\_02297 expression was higher in EGB than CML322 throughout the infection could indicate that expression of UMAG\_02297 is upregulated in EGB as an attempt to compensate loss-of-function. It could also be speculated whether the expression of the functional effector is suppressed by the host in CML322, but that the remaining expression level is still sufficient to contribute to virulence. However, the results from the UMAG\_02297 overexpression experiment do not support this hypothesis.

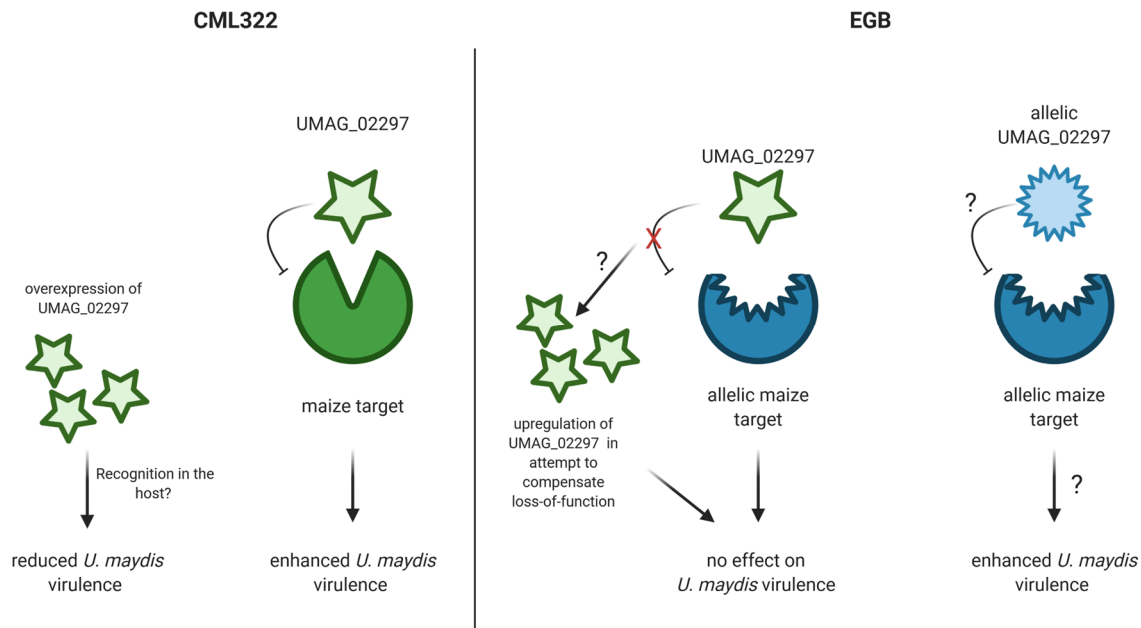


**Figure 3.1. Model for the maize line-specific function of UMAG\_02297.** In CML322, UMAG\_02297 can successfully interact with its maize target and contributes to virulence. In EGB, through presumed allelic variation in the host target, the function of UMAG\_02297 is inhibited. Loss of effector function might induce overexpression of UMAG\_02297 in EGB, without affecting virulence. In CML322, overexpression of UMAG\_02297 reduced fungal virulence potentially by recognition of the over-abundant effector. Allelic variation in UMAG\_02297 could in turn allow interaction with the allelic maize target.

In CML322, overexpression of UMAG\_02297 resulted in a similar virulence defect as the KO, rather suggesting that the effector might be recognised at higher abundance by the host, which could be why expression levels are kept low. Furthermore, highly specific tailoring of UMAG\_02297 expression is necessary for correct virulence function. In EGB, overexpression did not result in any changes of fungal virulence, further underlining that UMAG\_02297 is not functional or recognised in that maize line.

The identification of UMAG\_02297 allelic variants in different *U. maydis* strains might point towards a diversification of this effector to maintain its function for virulence in different host genotypes. It could be speculated whether an allelic variant might in turn be successful to interact or specifically modify its maize target in another maize line, e.g. EGB, and thereby restore its function for virulence.

#### 3.6 QTL mapping for *U. maydis* resistance in maize seedlings

QTL mapping approaches have been successfully employed to ultimately identify genes controlling complex, multigenic traits (e.g. Cook et al. 2012; Hurni et al. 2015; Zuo et al. 2015). Therefore, as an additional approach to the transcriptome analysis, I performed a QTL mapping experiment to study the genetic basis of QDR in the maize-*U. maydis* interaction. Using a segregating population derived from a B73xTx303 cross, this identified one QTL on chromosome 9 that contributed to heavy tumour formation in two biological replicates.

In previous studies, several QTLs associated with *U. maydis* disease resistance have been identified. Using natural infections in different European locations, 19 distinct QTLs distributed over all 10 chromosomes were mapped (Lübberstedt et al. 1998a). In addition, 12 QTLs contributing to frequency or severity of *U. maydis* infection across the entire plant as well as in an organ-specific manner were found on all chromosomes except chromosome 6 in field inoculation experiments (Baumgarten et al. 2007). Furthermore, additive-effect QTLs on chromosomes 3, 5 and 8 were detected to influence *U. maydis* infection frequency (Ding et al. 2008). All these QTLs explained only 3.2% to 58% of the phenotypic variation, which further underlines the multigenic basis of *U. maydis* disease resistance. Comparison of the genetic locations of the QTLs across these studies showed some consistency, however no QTL was identified in all of them, and none of the QTLs discussed above localised to the same genetic region as the one identified in the present study.

Similar inconsistencies were reported for other complex maize traits, such as resistance against grey leaf spot (Bubeck et al. 1993) or *Puccinia sorghi* (Lübberstedt et al. 1998b). The lack of consistent QTLs could be explained by different sets of polymorphic detectable QTLs in the different populations, low power of QTL detection, epistasis between non-allelic genes or interactions with the environment. In small populations of about 100 families, as it was the case also in the present study, the power of QTL detection is low even for traits with high heritability, and the probability of the simultaneous detection of the same QTL is estimated to be only about 10% (Utz et al. 1994). Furthermore, the experimental set-up of the different QTL mapping experiments was substantially different. In the discussed QTL studies, relatively mature plants were used, and often only presence/absence of infection was scored rather than severity of symptoms. In my approach, seedlings were used, and infection severity was assessed using a quantitative scoring system. Plant stage-dependent phenotypic expression has been commonly observed for various QTLs associated with plant disease resistance and could explain the observed sparsity of overlapping QTLs. In barley for example, the QTL

*Rphq2* is effective in resistance against *Puccinia hordei* only in seedlings but not in adult plants, while the QTL *Rphq4* is effective only at the adult plant stage (Qi et al. 1998; Wang et al. 2010). The plant stage-specific effect of QTLs might in part be caused by changes in growth-regulating phytohormones, which are involved in plant development as well as defence pathways, however the exact mechanisms remain enigmatic (Develey-Rivière and Galiana 2007; Chung et al. 2008; Wang et al. 2010).

It should be mentioned that the identified QTL was not confirmed in the third and fourth biological replicates in the subsequent year, and hence must be regarded as preliminary. The observed phenotypes were highly variable between the years and between both replicates of the second year, possibly due to large differences in weather conditions during the experiments.

A strong influence of the environment on resistance to *U. maydis* was observed in all other QTL mapping studies as well, where the effect of approximately 50% of QTLs was significantly variable in different environments (Lübberstedt et al. 1998a; Baumgarten et al. 2007; Ding et al. 2008), and variations in precipitation and temperature have been shown to affect *U. maydis* infection in maize fields in general (Christensen 1963; Kostandi and Geisler 1989). Different weather conditions might have influenced the expression of QTLs involved in developmental, morphological, and chemical characteristics affecting resistance against *U. maydis*, and also probably directly affected the fitness of the fungal inoculum and fungal growth rate in the field. Hence, it is obvious that the environment plays an important role in the complex nature of *U. maydis* resistance in the field.

Another factor that could have accounted for the high variance between the replicates was the low number of plants per family for each replicate (on average 9), which was due to low or irregular germination rates and damage caused by animal feeding. Even under controlled greenhouse conditions, the phenotypes of individual maize plants of the same genotype are highly variable. Therefore, generally around 30 plants per replicate are used to generate reliable results. Increasing the amount of plants and stabilising the environmental conditions might help to improve consistency between replicates and enhance the power of QTL detection.



#### 3.7 Concluding remarks and perspectives

In recent years, even though fundamental progress in the field of plant-pathogen interactions has been achieved through reductionist approaches, the need for more comprehensive studies taking into account natural variation in both pathogen and host has become more and more clear. In this study, the influence of different host genotypes on *U. maydis* virulence was investigated, which revealed that activity and function of effector genes are specifically dependent on the host line. Furthermore, transcriptome analysis of six *U. maydis* infected maize lines of different resistance levels offered unprecedented insights into the transcriptional changes associated with host disease resistance.

Although it has been known for long that *U. maydis* effector gene expression is a highly specific and adapted process, the cues and mechanisms determining the different specialised expression patterns remain elusive. It would therefore be of particular interest to investigate which signals or transcription factors might be involved in adaptation of the particular 'effector cocktail' to the colonised maize line, organ, or tissue.

Carbohydrate metabolism genes were upregulated during colonisation of more resistant maize lines, suggesting that different cell wall compositions might affect *U. maydis* disease resistance. This is in line with the finding, that differences in cell wall composition strongly influence disease resistance of maize to various pests and other diseases (Santiago et al. 2013). A detailed cell wall carbohydrate profiling of the NAM founder lines and correlation of these results with *U. maydis* disease resistance phenotypes could help to address the question how natural variation in cell wall composition affects *U. maydis* resistance. It could also be speculated whether eminent differences in cell wall composition between maize lines might represent a signal perceived by the fungus that could specifically influence gene expression.

Differences in nutrient availability might also play a role in QDR to *U. maydis*, as indicated by the enrichment of ion-transport processes within *U. maydis* genes being upregulated during colonisation of the more susceptible maize lines. On the maize side, inefficient suppression of photosynthesis was suggested to take place in the more resistant maize lines. This would result in changes in carbon allocation and influence nutrient availability as well. Accordingly, determining how nutrient content differs between the maize lines during *U. maydis* infection could help to further support these findings.

A maize line-specific virulence function was identified for the effector gene UMAG\_02297, and transcriptome data suggested auxin-related processes as a possible target. Furthermore, preliminary data indicated maize line-specific virulence functions for several other maize line-specific effector candidates. Further functional characterisation of these

candidates as well as the validation of auxin-related processes as a target of UMAG\_02297 will provide more insights into the molecular mechanisms underlying QDR in the maize-*U. maydis* interaction and how *U. maydis* interferes with them. Auxin measurements in different *U. maydis*-infected maize lines could shed light on the possible roles of auxin in maize QDR against *U. maydis*.

As an additional approach to identify maize genes involved in QDR against *U. maydis*, a QTL mapping experiment was performed in the field. The lack of reproducibility of results in the subsequent season highlighted the influence of environmental conditions on *U. maydis* infection. Stabilising the conditions as well as increasing the amount of plants tested per family would most likely enhance QTL detection power and help generate more reliable results in follow-up experiments.

In the present study, the importance of variation in the host in the maize-*U. maydis* interaction was investigated. For future studies it will be of great interest to also examine natural variation on the fungal side in more detail. UMAG\_02297 displays allelic variation between different *U. maydis* strains, and it would consequently be of special interest to determine whether different variants of the same effector are functional in different host genotypes. Genome sequences from additional strains originating from highly diverse backgrounds will be crucial to broaden the understanding on *U. maydis* effector diversity and adaptation. As genetic diversity is generally higher in natural populations of the host plants and pathogens (Forbes et al. 2013), it would be sensible to include strains from more natural environments, i.e. that would be isolated from the wild maize relative teosinte. Taken together, this would further help elucidate how a highly specific, biotrophic pathogen like *U. maydis* co-adapts with its host maize in different ecologic backgrounds.

## 4 Materials and Methods

The used materials and methods are summarised in the following.

### 4.1 Materials and source of supply

#### 4.1.1 Chemicals

All chemicals used in this study were acquired from Biozym (Hessisch Oldendorf, Germany), Difco (Augsburg, Germany), GE Healthcare Life Science (Freiburg, Germany), Invitrogen (Carlsbad, USA), Merck (Darmstadt, Germany), Roche (Mannheim, Germany), Roth (Karlsruhe, Germany), and Sigma-Aldrich (St. Louis, USA) unless stated otherwise.

#### 4.1.2 Buffers and solutions

All buffers, media and solutions were prepared with H<sub>2</sub>O<sub>bid.</sub> unless stated otherwise and autoclaved for 5 min at 121 °C. Heat-sensitive solutions were filter-sterilised (0.2 µm pore size, GE Health Care Life Science, Freiburg, Germany). The composition of all buffers, media and solutions are indicated in the respective methods.

#### 4.1.3 Enzymes, antibodies, and additional materials

The restriction enzymes used in this study were purchased from New England Biolabs (Ipswich, USA). DNA polymerases used in this study were Phusion<sup>®</sup> High Fidelity DNA Polymerase, Q5<sup>®</sup> High Fidelity DNA Polymerase (New England Biolabs, Ipswich, USA) or GoTaq<sup>®</sup> Green Master Mix (Promega GmbH, Madison, USA). Ligation of DNA molecules was performed with T4 DNA ligase (New England Biolabs, Ipswich, USA). Gibson assembly of DNA fragments was done using NEBuilder<sup>®</sup> HiFi DNA Assembly Master Mix (New England Biolabs, Ipswich, USA). For the enzymatic degradation of fungal cell walls Novozyme234 (Novo Nordisk, Copenhagen, Denmark) was used. Additionally used enzymes are indicated in the respective method sections. Antibiotics and size markers used in this study are shown in Table 4.1 and Figure 4.1, respectively.

GeneRuler 1 kb DNA Ladder

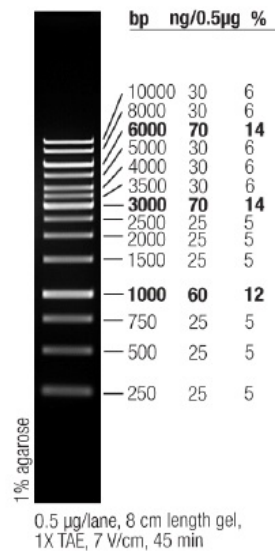


**Figure 4.1. Standard marker used in this study.** Thermo Scientific™ GeneRuler™ 1 kb DNA ladder (Thermo Fisher Scientific, Waltham, USA) used for size determination of DNA fragments on an agarose gel.

**Table 4.1. Antibiotics used in this study.**

Antibiotic	Usage	Working concentration [µg/ml]
Carbenicillin	<i>E. coli</i>	100
Kanamycin	<i>E. coli</i>	40
Carboxin	<i>U. maydis</i>	2
Hygromycin	<i>U. maydis</i>	200

#### 4.1.4 Commercial kits

Plasmid DNA extraction was done using the NucleoSpin® Plasmid Kit (Macherey-Nagel, Düren, Germany). PCR clean-up and gel-extraction of nucleic acids was performed using the NucleoSpin® gel and PCR Clean-up kit (Macherey-Nagel, Düren, Germany). Isolation of genomic DNA from maize material was performed using the MasterPure™ Complete DNA and RNA Purification Kit from Epicentre (Madison, USA). Enzymatic degradation of DNA was done using the TURBO DNA-free™ Kit (Ambion®/ Thermo Fisher Scientific, Waltham, USA). Synthesis of cDNA was performed using RevertAid H Minus First Strand cDNA Synthesis Kit (Thermo Fisher Scientific, Waltham, USA).

## 4.2 Media and cultivation methods for microorganisms

### 4.2.1 Media

The composition of the media used for cultivation of microorganisms used in this study is shown in Table 4.2. The media were autoclaved at 121 °C for 5 min before use, unless stated otherwise.

**Table 4.2: Composition of media.**

<b>Name</b>	<b>Composition</b>
dYT liquid (Sambrook et al. 1989)	1.6% (w/v) Tryptone 1.0% (w/v) Yeast extract 0.5% (w/v) NaCl
YT solid	0.8% (w/v) Tryptone 0.5% (w/v) Yeast extract 0.5% (w/v) NaCl 1.5% (w/v) Agar
YEPS <sub>light</sub>	1.0% (w/v) Yeast extract 0.4% (w/v) Peptone 0.4% (w/v) Sucrose
Potato-Dextrose-Agar (PD)	2.4% (w/v) Potato-Dextrose Broth 2.0% (w/v) Agar
PD-Charcoal Agar	addition of 1.0% (w/v) activated charcoal to the PD-Agar medium
Regeneration Agar (Schulz et al. 1990)	1 M Sorbitol 1.0% (w/v) Yeast extract 0.4% (w/v) Peptone 0.4% (w/v) Sucrose 1.5% (w/v) Agar

### 4.2.2 Cultivation of *E. coli*

*E. coli* was used for amplification of plasmid DNA. It was cultivated at 37 °C either on YT solid medium or in dYT liquid medium with shaking at 200 rpm. Glycerol stocks for long term storage of cultures were prepared by adding 25% (v/v) glycerol to a thickly grown overnight culture in a total volume of 1.8 ml and stored in a screw cap vial at -80 °C. For selection, media were supplied with carbenicillin (100 µg/ml) or kanamycin (40 µg/ml).

### 4.2.3 Cultivation of *U. maydis*

*U. maydis* liquid cultures were cultivated in YEPS<sub>light</sub> at 28 °C with shaking at 200 rpm. Solid cultures of *U. maydis* were cultivated on Potato Dextrose (PD) Agar at 28 °C. Glycerol stocks for long term storage of cultures were prepared by adding 25% (v/v) glycerol to a culture with a OD<sub>600</sub>= 0.6-1.0 in a total volume of 1.8 ml and stored in a screw cap vial at -80 °C. After transformation of *U. maydis*, regeneration agar was used. For selection, the media was supplied with 2 µg/ml carboxin.

### 4.2.4 Determination of cell density

To determine cell density, absorption at 600 nm (OD<sub>600</sub>) was measured in a Genesis 10S VIS spectrophotometer (Thermo Fisher Scientific, Waltham, USA) by taking the corresponding medium as reference. To ensure a linear dependence of the measurements, cultures were diluted to absorption values below 0.8. For *U. maydis*, an absorption of 1 at OD<sub>600</sub> accounts for ~1.5 x10<sup>7</sup> cells. For *E. coli*, an absorption of 1 at OD<sub>600</sub> accounts for ~1 x10<sup>9</sup> cells.

## 4.3 Microbial strains, plasmids, and oligonucleotides

The organisms used for this study are listed in the following with their characteristics and references.

### 4.3.1 *E. coli* strains

For plasmid amplification during routine cloning procedures, *E. coli* K-12 Top10/DH10β [F-mcrA Δ (mrr-hsd RMS-mcrBC) Φ80lacZΔM15 ΔlacO74 recA1 araΔ139 Δ (ara98leu) 7697 galU galK rpsL (StrR) endA1 nupG] (Grant et al. 1990; Invitrogen, Carlsbad, USA) and *E. coli* K-12 DH5α [F- Φ80d lacZ ΔM15 Δ (lacZYA-argF) U169 deoR recA1 endA1 hsdR17 (rK-, mK+) phoA supE44 λ- thi-lgyr A96 relA1] (Hanahan 1983; GibcoBRL, Eggenstein, Germany) were used.

**4.3.2 *U. maydis* strains**

The *U. maydis* SG200 strain (Kämper et al. 2006) was used for most *U. maydis* experiments. All plasmids generated for transformation of this strain as well as the plasmids used for generation of the knock-out strains derived from this initial strain are listed in chapter 4.3.4. As a summary, all *U. maydis* strains produced in this study are listed in Table 4.3. For field experiments, compatible *U. maydis* wildtype isolates were used (Table 4.4).

**Table 4.3. *U. maydis* strains used in this study.**

Strain (Genotype)	Usage	Reference
SG200	Maize infection	Kämper et al. 2006
SG200_KO_UMAG_11444_KO_UMAG_11002	Maize infection	Schuster et al. 2018
SG200_KO_UMAG_05027_KO_UMAG_02297	Maize infection	This study
SG200_KO_UMAG_11070_KO_UMAG_00309	Maize infection	This study
SG200_KO_UMAG_05318_KO_UMAG_11416	Maize infection	This study
SG200_KO_UMAG_01422_KO_UMAG_04557	Maize infection	This study
SG200_KO_UMAG_05027_KO_UMAG_02297_KO_UMAG_05319_KO_UMAG_03154	Maize infection	This study
SG200_KO_UMAG_02178_KO_UMAG_11908	Maize infection	This study
SG200_KO_UMAG_10861_KO_UMAG_05222	Maize infection	This study
SG200_KO_UMAG_02533_KO_UMAG_02535_KO_UMAG_02540	Maize infection	This study
SG200_KO_UMAG_00753	Maize infection	This study
SG200_KO_UMAG_02297	Maize infection	This study
SG200_KO_UMAG_05027	Maize infection	This study
SG200_KO_UMAG_02297_Ppit2::UMAG_02297::Tnos	Maize infection, overexpression	This study
SG200_KO_UMAG_02297_Ppit2::UMAG_02297-mCherry-HA::Tnos	Maize infection, localization	This study
SG200_KO_UMAG_02178_KO_UMAG_11908/C	Maize infection, complementation	This study
SG200_KO_UMAG_10861_KO_UMAG_05222/C	Maize infection, complementation	This study
SG200_KO_UMAG_05027/C	Maize infection, complementation	This study
SG200_KO_UMAG_05027_KO_UMAG_02297/C	Maize infection, complementation	This study
SG200_KO_UMAG_05318_KO_UMAG_11416/C	Maize infection, complementation	This study
SG200_KO_UMAG_02297/C	Maize infection, complementation	This study

**Table 4.4: *U. maydis* wildtype isolates used in this study.**

ID	Name	Location
45	<i>Ustilago maydis</i> Wandertag #1	Marburg area, Germany
46	<i>Ustilago maydis</i> Wandertag #2	Marburg area, Germany
47	<i>Ustilago maydis</i> Wandertag #3	Marburg area, Germany
48	<i>Ustilago maydis</i> Wandertag #4	Marburg area, Germany
49	<i>Ustilago maydis</i> Wandertag #5	Marburg area, Germany
50	<i>Ustilago maydis</i> Wandertag #6	Marburg area, Germany
51	<i>Ustilago maydis</i> Luxemburg #1	Luxemburg
52	<i>Ustilago maydis</i> Luxemburg #2	Luxemburg
53	<i>Ustilago maydis</i> Luxemburg #3	Luxemburg
54	<i>Ustilago maydis</i> Luxemburg #4	Luxemburg
55	<i>Ustilago maydis</i> Luxemburg #5	Luxemburg
56	<i>Ustilago maydis</i> Luxemburg #6	Luxemburg

### 4.3.3 Oligonucleotides

All oligonucleotides used in this study were purchased from Sigma-Aldrich (St. Louis, USA) and are listed in Table 4.5, Table 4.6 and Table 4.7.

**Table 4.5: General oligonucleotides used in this study. KO: knock-out.**

Name	Sequence	Purpose of use
ptRNA-Gly_scaf_F	CGGTGCTTTTTTTGTGGTACACCTCAGA CCAAGCGTGAAC	Cloning of CRISPR/Cas9-KO plasmid
scaffold_R_Acc65I	GCGTTCGACTCTTGGCAGGTGGTACCA CAAAAAAAGCACCGACTC	Cloning of CRISPR/Cas9-KO plasmid
pLeuFScaf	CGGTGCTTTTTTTGTGGTACTCGATGTG TGCACAAATC	Cloning of CRISPR/Cas9-KO plasmid
SeqF_UMAG_00793	CTATCAGCCCGTTCAGCCTC	KO verification
SeqR_UMAG_00793	CTTGCTCCATGTCCTACAAC	KO verification
SeqF_UMAG_11416	GGCCAAGTCCATCATTCTCC	KO verification
SeqR_UMAG_11416	CTTGACCAGCGCGAGAAATC	KO verification
SeqF_UMAG_11070	TTCGTTGATCGCCTCGGTTC	KO verification
SeqR_UMAG_11070	GTAGCTCCCTGCCAGATTAG	KO verification
SeqF_UMAG_00309	TGTCAGGACCAGGGATTACG	KO verification
SeqR_UMAG_00309	CTGCGTGTTGGAGGAGCTTC	KO verification
SeqF_UMAG_01422	AGCTGCTGCCATCTACTGAG	KO verification



#### 4. Materials and Methods

Name	Sequence	Purpose of use
SeqR_UMAG_01422	GCATTCTTGAGCGCAGTCAC	KO verification
SeqF_UMAG_04557	CTTGCAAAGTGCATCCTACC	KO verification
SeqR_UMAG_04557	GCGGTTTCAGCTACTGTAGGC	KO verification
SeqF_UMAG_05222	ATCGCAGGCTTATTCGCTAC	KO verification
SeqR_UMAG_05222	GATGCGCGAAGCAGATCCAG	KO verification
SeqF_UMAG_02533	CTGACCTCCTCACTACTAAG	KO verification
SeqR_UMAG_02533	CTCTCCTTCTTCGCGTGTAG	KO verification
SeqF_UMAG_02535	TGCGTCCAGAGATTGTTAGG	KO verification
SeqR_UMAG_02535	CCTCATCGGGCAATTAACAC	KO verification
SeqF_UMAG_02540	ATGTCCATCCTCGTCATCAG	KO verification
SeqR_UMAG_02540	TGATGCCGTCAATCTTGGTC	KO verification
SeqF_UMAG_05027	TCAGCTTGGGACGAAAGTAG	KO verification
SeqR_UMAG_05027	CCAAACGCAAAGTCACTCCTC	KO verification
SeqF_UMAG_02297	AGCAGCGATCATTCCAAACC	KO verification
SeqR_UMAG_02297	GTCTCAGCGTTGATCATTGC	KO verification
SeqF_UMAG_03154	AGCTCGACTGTGATGTGATG	KO verification
SeqR_UMAG_03154	GCGTGTGCTGAAATGTAGTG	KO verification
SeqF_UMAG_05319	TTAGTGCGAGTAGGGCTTC	KO verification
SeqR_UMAG_05319	GCACGAGTTTGTGTCTGTTG	KO verification
SeqF_UMAG_05319	AGTGGGAGTATCGAGTCAAG	KO verification
SeqR_UMAG_05319	GAAACCAAGAGATCGAGACG	KO verification
SeqF_UMAG_11444	CGCTTTCCACCCAGTATACC	KO verification
SeqR_UMAG_11444	GCCACTGATATGGGCTTTCC	KO verification
SeqF_UMAG_11002	GAGCACTGGGATGTGTATGG	KO verification
SeqR_UMAG_11002	CGATCGCCACAGCATTTGAC	KO verification
SeqR_UMAG_02525_new	GGGTATTGAGGCTCACTCAC	KO verification
SeqF_UMAG_02525_new	ACTGGCTCTCGTGCATTTG	KO verification
UMAG_02298_SeqF	TTGGCTCTCCGGCATTGCTC	KO verification
UMAG_02298_SeqR	TTCGGACGTGGTGCCACTTC	KO verification
UMAG_AG_04815_SeqF	CGAGCTAGCATCTTTGACAC	KO verification
UMAG_04815_SeqR	CCGAAGAAGGTAGCGAAGTC	KO verification
UMAG_05928_SeqF	ACGAGCTGACAAGACGAAGG	KO verification
UMAG_05928_SeqR	GCCGTTTCGCTAGAAGAAG	KO verification
UMAG_04503_SeqF	CTCCTGGCATGGGATTCAAC	KO verification
UMAG_04503_SeqR	ATTGCGCCGAAACGAGTAGG	KO verification
UMAG_10861_SeqF	CCCTGCTTTCACAGCTAGAC	KO verification
UMAG_00753_SeqF_new	CTTCCGTAGCTGTCGTTGTC	KO verification
UMAG_10861_SeqR	CCGACTTTGGTGTGAGTTTC	KO verification
UMAG_02178_SeqF	AACTACGCCTGCACTCATAC	KO verification
UMAG_02178_SeqR	GCTGGTAGTATTGCGAAGAG	KO verification
UMAG_11908_SeqF	CTTGCTTCCAATACCATCC	KO verification
UMAG_11908_SeqR	TTTGACGCTTCTGGTGTGAG	KO verification
UMAG_05027_compl_fw	CTTTCACAGCGCCAACTTTC	Cloning of complementation

Name	Sequence	Purpose of use
		plasmid
UMAG_05027_compl_rev	GAACTCGAGCAGCTGAAGCTGGAGGAA GAAGGAGCTCAAG	Cloning of complementation plasmid
UMAG_02297_compl_fw	GAAAGTTGGCGCTGTGAAAGGTTGGGC GTTGACGAATGAC	Cloning of complementation plasmid
UMAG_02297_compl_rev	CGAGTTTAAGCCGCCCAATG	Cloning of complementation plasmid
UMAG_03154_compl_fw	CGGATCTGCTCGACTTTCTG	Cloning of complementation plasmid
UMAG_03154_compl_rev	CATTGGGCGGCTTAAACTCGACTGAGTA AGCGCGTTTCAC	Cloning of complementation plasmid
UMAG_05319_compl_fw	CAGAAAGTCGAGCAGATCCGGAGCATC TTAGTCCGTTAGC	Cloning of complementation plasmid
UMAG_05319_compl_rev	CGATCTGCAGCCGGGCGGCCCTACTCT TGCGCGTGTCTCG	Cloning of complementation plasmid
UMAG_02297_compl2_rev	CGATCTGCAGCCGGGCGGCCCGAGTTT AAGCCGCCCAATG	Cloning of complementation plasmid
UMAG_03154_compl2_rev	GAACTCGAGCAGCTGAAGCTACTGAGTA AGCGCGTTTCAC	Cloning of complementation plasmid
UMAG_05027_compl1_fw	CGATCTGCAGCCGGGCGGCCCTTTTCAC AGCGCCAACCTTC	Cloning of complementation plasmid
UMAG_02297_compl1_fw	GAACTCGAGCAGCTGAAGCTGTTGGGC GTTGACGAATGAC	Cloning of complementation plasmid
UMAG_02297_compl1_rev	CGATCTGCAGCCGGGCGGCCCGAGTTT AAGCCGCCCAATG	Cloning of complementation plasmid
UMAG_03154_compl1_fw	CGATCTGCAGCCGGGCGGCCCGGATCT GCTCGACTTTCTG	Cloning of complementation plasmid
UMAG_03154_compl1_rev	GAACTCGAGCAGCTGAAGCTACTGAGTA AGCGCGTTTCAC	Cloning of complementation plasmid
UMAG_05319_compl1_fw	GAACTCGAGCAGCTGAAGCTGAGCATC TTAGTCCGTTAGC	Cloning of complementation plasmid
UMAG_04557_compl_F	GGCCTTCAGGTGACAGTCAG	Cloning of complementation plasmid
UMAG_04557_compl_R	CGATCTGCAGCCGGGCGGCCTCCCACG GCTCGTCTTTTCAC	Cloning of complementation plasmid
UMAG_01422_compl_F	CTGACTGTCACCTGAAGGCCTCGGGTG ATGGATTCATACG	Cloning of complementation plasmid
UMAG_01422_compl_R	ACTCGAGCAGCTGAAGCTGGAGGCGAT GCGCACGAACAAG	Cloning of complementation plasmid

#### 4. Materials and Methods

<b>Name</b>	<b>Sequence</b>	<b>Purpose of use</b>
UMAG_00793_compl_F	GTGGATCGCGAAGGAGATGAAGGGAGT TGGGGGAAACAG	Cloning of complementation plasmid
UMAG_00793_compl_R	CGATTCAATGATGCAGAGGCGATAAACT TGGGCTCGCTAC	Cloning of complementation plasmid
UMAG_11416_compl_F	TCATCTCCTTCGCGATCCAC	Cloning of complementation plasmid
UMAG_11416_compl_R	CGATCTGCAGCCGGGCGGCCGCTCCG GCCTGCTACATAAG	Cloning of complementation plasmid
UMAG_05318_compl_R	GCCTCTGCATCATTGAATCG	Cloning of complementation plasmid
UMAG_00793_compl2_R	ACTCGAGCAGCTGAAGCTGGGATAAACT TGGGCTCGCTAC	Cloning of complementation plasmid
UMAG_02297_compl_F2	GAAAGTTGGCGCTGTGAAAGATGTTGG GCGTTGACGAATG	Cloning of complementation plasmid
UMAG_02297_compl_R2	CGATCTGCAGCCGGGCGGCCTGGGACC ACTTAACTTGTTTC	Cloning of complementation plasmid
UMAG_02178_compl_fw	ACGACGATGTCTGGGTTCTC	Cloning of complementation plasmid
UMAG_02178_compl_rev	GAACTCGAGCAGCTGAAGCTGACATGC CCCACAGATAC	Cloning of complementation plasmid
UMAG_11908_compl_fw	GAGAACCCAGACATCGTCGTCATCGCAT GCATCACGATTC	Cloning of complementation plasmid
UMAG_11908_compl_rev	CGATCTGCAGCCGGGCGGCCTTCCAGC AGAGGCAATTTCC	Cloning of complementation plasmid
UMAG_00753_compl_F	GAACTCGAGCAGCTGAAGCTGGCGGCC ATTGTTCAATTC	Cloning of complementation plasmid
UMAG_00753_compl_R	CGATCTGCAGCCGGGCGGCCATGCCAT CTTCAGCACCATC	Cloning of complementation plasmid
UMAG_05928_compl_F	GTTCTGTTGCACGTTGTAGGCGCATA CTTGAGTTCTCC	Cloning of complementation plasmid
UMAG_05928_compl_R	ACTCGAGCAGCTGAAGCTGGCTTTCCAT TAGTGCGTGTG	Cloning of complementation plasmid
UMAG_04503_compl_F	TACAACGTGCAACCAGGAAC	Cloning of complementation plasmid
UMAG_04503_compl_R	CGATCTGCAGCCGGGCGGCCATTGTTG GCTCAGGTCTCAC	Cloning of complementation plasmid
UMAG_10861_compl_F	GATGTAGAGGGTTAGGAGCGTTCAACAA CCCGCTTCAGAG	Cloning of complementation plasmid
UMAG_10861_compl_	GAACTCGAGCAGCTGAAGCTGCGAGAA	Cloning of

Name	Sequence	Purpose of use
R	CTGGTGAGAAATG	complementation plasmid
UMAG_05222_compl_F	CGCTCCTAACCTCTACATC	Cloning of complementation plasmid
UMAG_05222_compl_R	CGATCTGCAGCCGGGCGGCCTCCCGGA ACTGCTGACATAC	Cloning of complementation plasmid
UMAG_02297_F_Ppit 2	ACGACCAAACGCAGCACCGCATGAAGC TATCCCGCATGTT	Overexpression
UMAG_02297_R_mCh	GTGGCGATCGAGCGTTCTAGCTGTGAG TCTAATACGGGC	Overexpression with mCherry tag
UMAG_02297_R_Tnos	CGATCTGCAGCCGGGCGGCCCTACTGT GAGTCTAATACGG	Overexpression

**Table 4.6: Oligonucleotides used as sgRNA for CRISPR/Cas9-mediated KO in this study. sgRNA spacer sequence is underlined.**

Target gene	Sequence	Comments
UMAG_00793	TCGAATCCCGTCTGGTCAAGGTGGCGACGACCAGCAAGGGTT TTAGAGCTAGAAATAGC	ptRNA <sup>Leu</sup> overhang
UMAG_11416	TCGATTCCCGTTCGATGCAGTTTCTCTGGCAAAAAGTGCCTTT TAGAGCTAGAAATAGC	ptRNA <sup>Gly</sup> overhang
UMAG_05318	CAAAATTCCATTCTACAACGACTGGTTTACGCCGATAGTGTTT TAGAGCTAGAAATAGC	pU6 overhang
UMAG_11070	CAAAATTCCATTCTACAACGATCCATACGGTAGCAACGTGTTT TAGAGCTAGAAATAGC	pU6 overhang
UMAG_00309	TCGAATCCCGTCTGGTCAAGTTCGAGGCCGGGTTCCGCCGTT TTAGAGCTAGAAATAGC	ptRNA <sup>Leu</sup> overhang
UMAG_01422	CAAAATTCCATTCTACAACGTTCCCGGAACCAGAAGAATGTTT TAGAGCTAGAAATAGC	pU6 overhang
UMAG_04557	TCGAATCCCGTCTGGTCAAGCTCAACCAGCAGCTCGCCTGTTTTAGAGCTAGA AATAGC	ptRNA <sup>Leu</sup> overhang
UMAG_05222	TCGATTCCCGTTCGATGCAGCAGCTCGTAGCCACCAGTGGTT TTAGAGCTAGAAATAGC	ptRNA <sup>Gly</sup> overhang
UMAG_05027	CAAAATTCCATTCTACAACGCCATTGCTGGGCCTTTCGTGTTT TAGAGCTAGAAATAGC	pU6 overhang
UMAG_02297	TCGAATCCCGTCTGGTCAAGTCACTGGGGCCTCAGACACGTT TTAGAGCTAGAAATAGC	ptRNA <sup>Leu</sup> overhang
UMAG_05319	CAAAATTCCATTCTACAACGGAAAATGCAGCTAGGCAGAGTTT TAGAGCTAGAAATAGC	pU6 overhang
UMAG_03154	TCGAATCCCGTCTGGTCAAGGACAAGCGACGCTGGAAAAGTT TTAGAGCTAGAAATAGC	ptRNA <sup>Leu</sup> overhang
UMAG_02533	CAAAATTCCATTCTACAACGCTCTCGCCACTAAATCCAT GTTTTAGAGCTAGAAATAGC	pU6 overhang
UMAG_02535	CAAAATTCCATTCTACAACGTTCCGAGAAGCGTCCTGATGGTTT TAGAGCTAGAAATAGC	pU6 overhang
UMAG_02540	CAAAATTCCATTCTACAACGTATCACGTCGCTCGTATCGTTTTA GAGCTAGAAATAGC	pU6 overhang
UMAG_02297	CAAAATTCCATTCTACAACGCTCACTGGGCCTCAGACACGTTT TAGAGCTAGAAATAGC	pU6 overhang
UMAG_03154	CAAAATTCCATTCTACAACGCTGCAAAGCGAGACAGCGTGTTT TAGAGCTAGAAATAGC	pU6 overhang
UMAG	CAAAATTCCATTCTACAACGCGAGGCGAACAGAGGTTTGAGTTT	pU6 overhang

#### 4. Materials and Methods

Target gene	Sequence	Comments
_00793	TAGAGCTAGAAATAGC	
UMAG_11444	CAAAATTCCATTCTACAACGGGTGCATGCTACGAAGAGAGTTT TAGAGCTAGAAATAGC	pU6 overhang
UMAG_11002	CAAAATTCCATTCTACAACGCATACACCTGCGCAGAGAGTTT TAGAGCTAGAAATAGC	pU6 overhang
UMAG_11416	CAAAATTCCATTCTACAACGTTTCTCTGGCAAAAAGTGCCTTTT AGAGCTAGAAATAGC	pU6 overhang
UMAG_02298	CAAAATTCCATTCTACAACGCCTCCCAGAAATTGTCGCCGTTT TAGAGCTAGAAATAGC	pU6 overhang
UMAG_04815	TCGATTCCCCGTCGATGCAGATCCTGGTGTGCTCAACATGTTT TAGAGCTAGAAATAGC	ptRNAGly overhang
UMAG_05928	CAAAATTCCATTCTACAACGATCTGCACCTTTGCCGGAAGTTT TAGAGCTAGAAATAGC	pU6 overhang
UMAG_04503	TCGATTCCCCGTCGATGCAGCTCTTCATTCCCCGAAGGAAGTTT TAGAGCTAGAAATAGC	ptRNAGly overhang
UMAG_10861	CAAAATTCCATTCTACAACGCTGTTCCGACTACAAGCCACGTTT TAGAGCTAGAAATAGC	pU6 overhang
UMAG_02178	CAAAATTCCATTCTACAACGTGCACTGGCGTGTCCGGCGGTTT TTAGAGCTAGAAATAGC	pU6 overhang
UMAG_11908	TCGATTCCCCGTCGATGCAGGCGTATGTTGTGCCTTTCCGTTT TAGAGCTAGAAATAGC	ptRNAGly overhang
UMAG_00753	CAAAATTCCATTCTACAACGCGATCAACAAGCTCACCGGGTTT TAGAGCTAGAAATAGC	pU6 overhang

**Table 4.7: Oligonucleotides used for quantitative PCR in this study.**

Target gene	Name	Sequence
UMAG_00793	UMAG_00793_qPCR_F	CAAGGATTCCGCTGGAAAG
UMAG_00793	UMAG_00793_qPCR_R	CATCCATCGGAAGCTCTTG
UMAG_11416	UMAG11416_qPCR_F	TACTCGGCGATATTCAGCAC
UMAG_11416	UMAG11416_qPCR_R	GCGAAGCCTTTGACAAGAG
UMAG_05318	UMAG_05318_qPCR_F	ACCTTTGGCGGAACATACG
UMAG_05318	UMAG_05318_qPCR_R	GAAGGTCGAGTATGCAAAGG
UMAG_01422	UMAG_01422_qPCR_F	CAAACCTGGCTCTCCCTCTTC
UMAG_01422	UMAG_01422_qPCR_R	TTCACCTGGGAATCGTTGAG
UMAG_04557	UMAG_04557_qPCR_F	GCTCGACGACAAGATCAAG
UMAG_04557	UMAG_04557_qPCR_R	CTGTCGAACTTGGGCTTGAG
UMAG_05027	UMAG_05027_qPCR_F	GCTCTCGCTCTACCTCTTTC
UMAG_05027	UMAG_05027_qPCR_R	TGATTCACCCGCGTAGTTG
UMAG_02297	UMAG_02297_qPCR_F	ACTTGATGCTCCTGTGTCTG
UMAG_02297	UMAG_02297_qPCR_R	GCCGAAGGGTCATATTGGAG
UMAG_02297	UMAG_02297_qPCR_F2	CTCTGGCAGCCGAGTAAATC
UMAG_02297	UMAG_02297_qPCR_R2	CTGTCAGAGGTGCTAGGATG
UMAG_05027	UMAG_05027_qPCR_F2	CAATGGCGGTGCAAACACTAC
UMAG_05027	UMAG_05027_qPCR_R2	GCTCGTGATGGATCCGTAG
UMAG_00753	UMAG_00753_qPCR_F	GACGCGATCAACAAGCTCAC
UMAG_00753	UMAG_00753_qPCR_R	CCGAGGACGAGTTGTTCTTG
UMAG_11908	UMAG_11908_qPCR_F	CTCGTCACTTCAGGCGTATG
UMAG_11908	UMAG_11908_qPCR_R	TCTTGTAGACGGGCACAGAC

Target gene	Name	Sequence
UMAG_02178	UMAG_02178_qPCR_F	TTCAGAAGCGATCCGTTGTC
UMAG_02178	UMAG_02178_qPCR_R	TACGTTGGTGAGCCATGTAG
UMAG_05928	UMAG_05928_qPCR_F	TTGTATCAGAGGCGCGAATC
UMAG_05928	UMAG_05928_qPCR_R	TCTGTGCCCAATACACATGC
UMAG_04503	UMAG_04503_qPCR_F	GCCATCCTCAGTGCTACAAG
UMAG_04503	UMAG_04503_qPCR_R	CAGAAGCATCACGGCTAGTC
UMAG_10861	UMAG_10861_qPCR_F	GCTCTCGTCGTCGTACAATC
UMAG_10861	UMAG_10861_qPCR_R	GTCTTAGCGTCACGGTCTAC
UMAG_05222	UMAG_05222_qPCR_F	TTCAACGCGGATGACGATAC
UMAG_05222	UMAG_05222_qPCR_R	TGGCACATCTTGCACGTTAG
UMAG_03175 (pit2)	pit2_RT_for	CAAGAATCCGCCTGCCAAC
UMAG_03175 (pit2)	pit2_RT_rev	AGGATCTGTCCGCATGACC
ppi	RT_ppi_F	ACATCGTCAAGGCTATCG
ppi	RT_ppi_R	AAAGAACACCGGACTTGG
ZmGAPDH	GAPDH-RT-for	CTTCGGCATTGTTGAGGGTTTG
ZmGAPDH	GAPDH-RT-rev	TCCTTGGCTGAGGGTCCGTC

#### 4.3.4 Plasmids for transformation of *U. maydis*

All plasmids used in this study were tested via restriction enzyme digest. In case of insertion of plasmid parts that were generated by PCR, the newly generated sequence was verified via sequencing (Eurofins Genomics, Luxembourg, Luxembourg).

For CRISPR/Cas9 plasmid construction, 59 nt oligomers containing the specific spacer sequence and an upstream 19 nt overlap to the corresponding promoter and a 20 nt overlap downstream to the scaffold sequence were assembled with the Cas9 plasmid backbone via Gibson assembly. The sgRNA spacer sequences were designed by E-CRISP (<http://www.e-crisp.org/E-CRISP/>, Heigwer et al. 2014, Table 4.5) using the “medium” setting and purchased from Sigma-Aldrich (St. Louis, USA). The plasmid backbones used for cloning are listed below. The plasmids used for transformation of *U. maydis* are given in Table 4.8.

##### **pMS73** (Schuster et al. 2016; Schuster et al. 2018)

Self-replicating plasmid containing a codon-optimised Cas9 under control of the *U. maydis* hsp70 promoter, *U. maydis* U6 promoter for expression of sgRNA and cbx resistance marker for selection of *U. maydis* transformants. Transient expression of all CRISPR components from this plasmid allowed easy clean-up of Cas9 from transformed cells. For multiplexing sgRNAs, the *U. maydis* tRNA-Gly and tRNA-Leu promoters derived from pMS77 (Schuster et al. 2018) were used.

#### 4. Materials and Methods

##### **pCas9HF1** (Zuo et al. 2020a)

Self-replicating plasmid derived from pMS73, in which Cas9 was replaced by the high-fidelity variant Cas9HF1.

##### **p123** (Aichinger et al. 2003)

Plasmid backbone used for cloning of complementation constructs containing cbx resistance and enabling integration into the *U. maydis ip* locus via homologous recombination. For this, the plasmids were linearised via *SSpl* or *XcmI* before transformation of *U. maydis*.

**Table 4.8: Plasmids used for transformation of *U. maydis*.**

Backbone	Construct	Reference
pMS73	pCas9_pU6::sgRNA_UMAG_11070_ptRNA <sub>Leu</sub> ::sgRNA_UMAG_00309	This study
pMS73	pCas9_pU6::sgRNA_UMAG_01422_ptRNA <sub>Leu</sub> ::sgRNA_UMAG_04557	This study
pMS73	pCas9_pU6::sgRNA_UMAG_05318_ptRNA <sub>Leu</sub> ::sgRNA_UMAG_00793_ptRNA <sub>Gly</sub> ::sgRNA_UMAG_11416	This study
pMS73	pCas9_pU6::sgRNA_UMAG_05027_ptRNA <sub>Leu</sub> ::sgRNA_UMAG_02297	This study
pMS73	pCas9_pU6::sgRNA_UMAG_05319_ptRNA <sub>Leu</sub> ::sgRNA_UMAG_03154	This study
pMS73	pCas9_pU6::sgRNA_UMAG_02533_ptRNA <sub>Leu</sub> ::sgRNA_UMAG_02535_ptRNA <sub>Gly</sub> ::sgRNA_UMAG_02540	This study
pMS73	pCas9_pU6::sgRNA_UMAG_05027	This study
pMS73	pCas9_pU6::sgRNA_UMAG_05318	This study
pMS73	pCas9_pU6::sgRNA_UMAG_11416	This study
pCas9HF1	pCas9HF1_pU6::sgRNA_UMAG_02297	This study
pCas9HF1	pCas9HF1_pU6::sgRNA_UMAG_00753	This study
pCas9HF1	pCas9HF1_pU6::sgRNA_UMAG_02178_ptRNA <sub>Leu</sub> ::sgRNA_UMAG_11908	This study
pCas9HF1	pCas9HF1_pU6::sgRNA_UMAG_02298_ptRNA <sub>Leu</sub> ::sgRNA_UMAG_04815	This study
pCas9HF1	pCas9HF1_pU6::sgRNA_UMAG_05928_ptRNA <sub>Leu</sub> ::sgRNA_UMAG_04503	This study
pCas9HF1	pCas9HF1_pU6::sgRNA_UMAG_10861_ptRNA <sub>Leu</sub> ::sgRNA_UMAG_05222	This study
pCas9HF1	pCas9HF1_pU6::sgRNA_UMAG_00753	This study

Backbone	Construct	Reference
p123	p123_pnat::UMAG_05027::Tnat_pnat::UMAG_02297::Tnat	This study
p123	p123_pnat::UMAG_05318::Tnat_pnat::UMAG_11416::Tnat	This study
p123	p123_pnat::UMAG_02178::Tnat_pnat::UMAG_11908::Tnat	This study
p123	p123_pnat::UMAG_02297::Tnat	This study
p123	p123_pnat::UMAG_00753::Tnat	This study
p123	p123_pnat::UMAG_10861::Tnat_pnat::UMAG_05222::Tnat	This study
p123	p123_pnat::UMAG_05027::Tnat	This study
p123	p123_pnat::UMAG_05928::Tnat_pnat::UMAG_04503::Tnat	This study
p123	p123_ppit2::UMAG_02297::Tnos	This study
p123	p123_ppit2::UMAG_02297_mCherry_HA::Tnos	This study

## 4.4 Plant material and plant methods

### 4.4.1 Maize varieties

The maize varieties used in this study are listed in Table 4.9. The NAM population inbred parents are described in Yu et al. (2008), McMullen et al. (2009) and Venkatesh et al. (2016).

**Table 4.9: Maize varieties used in this study.**

Maize variety	Broad Group	Collection
Early Golden Bantam	northern flint	Heirloom maize
B73	temperate	NAM population inbred reference parent
CML322	tropical	NAM population inbred parent
NC350	tropical	NAM population inbred parent
Ki3	tropical	NAM population inbred parent
NC358	tropical	NAM population inbred parent
M162W	temperate	NAM population inbred parent



Maize variety	Broad Group	Collection
HP301	northern flint	NAM population inbred parent
CML228	tropical	NAM population inbred parent
Ms71	temperate	NAM population inbred parent
P39	northern flint	NAM population inbred parent
CML52	tropical	NAM population inbred parent
CML69	tropical	NAM population inbred parent
CML333	tropical	NAM population inbred parent
B97	temperate	NAM population inbred parent
M37W	mixed	NAM population inbred parent
CML247	tropical	NAM population inbred parent
Oh7B	temperate	NAM population inbred parent
Ky21	temperate	NAM population inbred parent
Tzi8	tropical	NAM population inbred parent
Ki11	tropical	NAM population inbred parent
CML103	tropical	NAM population inbred parent
Mo18W	mixed	NAM population inbred parent
CML277	tropical	NAM population inbred parent
Il14H	northern flint	NAM population inbred parent
Oh43	temperate	NAM population inbred parent
Tx303	mixed	NAM population inbred parent

#### 4.4.2 Cultivation of maize

Maize was grown in a greenhouse or phytochambers at 28 °C on a long day period (16 h light) with 80% humidity and a 8 h night period at 22 °C in VM soil (Einheitserde®, Sinntal, Germany).

#### 4.4.3 Virulence assay of *U. maydis* on maize

Virulence assays of *U. maydis* on maize were performed and symptoms were classified as described in Redkar and Doehlemann (2016a). The disease index was calculated using the following formula: The number of plants sorted into category 1 (small tumours), category 3 (normal tumours), category 5 (heavy tumours) and category 7 (dead plants) were multiplied by the number of the category (1, 3, 5 or 7), summed and then divided by

the total number of plants:  $\{[(\text{symptom category } X \times \text{number of plants in category } X)^X + (\dots)^{Y-Z}]/\text{total number of plants}\}$ .

## 4.5 Microbiology standard methods

### 4.5.1 Production of competent *E. coli* cells

The production of chemocompetent *E. coli* cells was carried out at 4 °C on ice using ice cold solutions and equipment. *E. coli* cells of a single colony were grown in liquid dYT-medium at 37 °C with shaking at 200 rpm until they reached an OD<sub>600</sub> of approximately 0.6. Cells were then cooled on ice for 30 min and centrifuged for 8 min at 4°C and 1250 ×g. The supernatant was discarded, and the cells were resuspended in 1/3 of the initial culture volume of RF1-solution, followed by incubation at 4 °C for 30 min. The cells were then centrifuged for 8 min at 4 °C and 1250 ×g. The supernatant was again discarded, and the cells were resuspended in 1/20 of the initial culture volume of RF2-solution and incubated at 4 °C for at least 30 min. The cells were finally aliquoted to 50 µl in pre-chilled reaction tubes, shock-frozen with liquid N<sub>2</sub> and stored at -80 °C until further use.

RF1 solution	100 mM RbCl
	50 mM MnCl <sub>2</sub> × 4 H <sub>2</sub> O
	30 mM potassium acetate
	10 mM CaCl <sub>2</sub> × 2 H <sub>2</sub> O
	15% (w/v) Glycerol
	pH 5.8

RF2 solution	10 mM MOPS
	10 mM RbCl
	75 mM CaCl <sub>2</sub> × 2 H <sub>2</sub> O
	15% (w/v) Glycerol
	pH 5.8

### 4.5.2 Heat-shock transformation of *E. coli*

For transformation chemically competent cells of *E. coli* K-12 Top10/DH10 $\beta$  or *E. coli* K-12 DH5 $\alpha$  were used. To 50  $\mu$ l of cells ca. 1-5 ng of plasmid DNA were added and incubated on ice for 15 min. The cells were then heated to 42 °C for 1 min and then directly cooled on ice for 3 min. For regeneration, 200  $\mu$ l dYT liquid medium were added and the cells were incubated for 1 h at 37 °C and 200 rpm. The cells were plated on YT solid plates containing the appropriate antibiotic for selection and incubated at 37 °C overnight.

### 4.5.3 Preparation of *U. maydis* protoplasts

To protoplast *U. maydis*, an overnight culture was diluted to OD<sub>600</sub>=0.2 in 50 ml YEPS<sub>light</sub> and incubated at 28°C until it reached OD<sub>600</sub>=0.6-1.0. The culture was then centrifuged at 2000  $xg$  for 5 min. The pellet was resuspended in 10 ml SCS and again centrifuged at 2000  $xg$  for 5 min. The pellet was then resuspended in 2 ml SCS containing 7 mg/ml Novozyme234 (Novo Nordisk, Copenhagen, Denmark; filtered sterile). The cells were incubated for 10-15 min at room temperature until 30-40% of the cells were protoplasted and the others looked like pinheads. Then, 10 ml ice cold SCS was added and the cells were centrifuged at 4 °C at 1300  $xg$  for 5 min. The pellet was carefully resuspended in 10 ml ice cold SCS and the cells were then centrifuged at 4 °C at 1300  $xg$  for 3 min twice. The pellet was then carefully resuspended in 10 ml ice cold STC and the cells were again centrifuged at 4°C at 1300  $xg$  for 3 min. The pellet was resuspended in 600  $\mu$ l ice cold STC and aliquoted to 100  $\mu$ l in pre-cooled reaction tubes and stored at -80°C.

SCS solution            20 mM Na-Citrate, pH 5.8  
                              1 M Sorbitol  
                              sterile filtered

STC solution            10 mM Tris-HCl, pH 7.5  
                              100 mM CaCl<sub>2</sub>  
                              1 M Sorbitol  
                              sterile filtered

#### 4.5.4 Transformation of *U. maydis*

For transformation, *U. maydis* protoplasts were thawed on ice and 1.5-5 µg linearised (for homologous recombination) or non-linearised plasmid DNA (for CRISPR/Cas9-mediated gene editing) in a maximal volume of 10 µl and 1 µl heparin solution (1 mg/ml) were added. After incubation on ice for 10 min, 500 µl STC/PEG solution were added and the protoplasts were incubated on ice for 15 min. This mixture was then carefully spread on a freshly prepared regeneration agar plate consisting of a 10 ml bottom layer containing 2x selection marker and a 10 ml top layer without selection marker. The plates were incubated for 4-7 days at 28 °C until colonies appeared. Colonies were transferred to PD plates containing the appropriate selection marker. To remove CRISPR/Cas9 plasmids, single colonies were transferred to PD plates without selection marker twice. The resulting colonies were used for DNA extraction (see Chapter 4.6.2) and verified either via sequencing of the target gene (for CRISPR/Cas9) or Southern blot analysis (for homologous recombination, see Chapter 4.6.14).

STC/PEG solution	15 ml STC
	10 g PEG4000
	sterile filtered

#### 4.5.5 Test for filamentous growth of *U. maydis*

To verify filamentous growth of newly generated *U. maydis* strains, the strains were grown in YEPS<sub>light</sub> medium at 28 °C, 200 rpm to an optical density of OD<sub>600</sub>=0.6-1.0. After pelleting the cells at 2000 *xg* for 10 min, the pellet was resuspended in H<sub>2</sub>O<sub>bid</sub> and the OD<sub>600</sub> was set to 1.0. Then, 5 µl of each strain were dropped on PD-charcoal plates to induce filament formation and incubated at 28 °C for 2-3 days.

## 4.6 Molecular biology standard methods

### 4.6.1 Plasmid isolation from *E. coli*

Plasmid isolation from *E. coli* was performed using the NucleoSpin® Plasmid Kit (Macherey-Nagel, Düren, Germany) according to the manufacturer's instructions.

### 4.6.2 Genomic DNA isolation from *U. maydis*

For the isolation of genomic DNA (gDNA) from *U. maydis*, a modified version of the protocol from Hoffman and Winston (1987) was used. For that, 2 ml of a thickly grown *U. maydis* overnight culture were pelleted at 12000  $xg$  for 2 min in a 2 ml reaction tube. After discarding the supernatant, ~ 0.3 g glassbeads (0.4-0.6 mm), 400  $\mu$ l *Ustilago* lysis buffer and 500  $\mu$ l phenol/chloroform were added to the pellet. The reaction tube was then incubated for 20 min on a Vibrax-VXR shaker (IKA, Staufen, Germany) at 2500 rpm for 15-20 min. For separation of the phases, the sample was centrifuged for 15 min at 12000  $xg$ . The upper aqueous phase containing the extracted DNA was transferred to a fresh 1.5 ml reaction tube and precipitated by addition of 1 ml 100% EtOH and centrifugation at 12000  $xg$  for 5 min. The supernatant was discarded, and the resulting pellet was washed with 400  $\mu$ l 70% EtOH for 5 min at 12000  $xg$  and then dried for 10 min at room temperature. The pellet was finally dissolved in 100  $\mu$ l H<sub>2</sub>O<sub>bid</sub> in a Thermomixer (Eppendorf, Hamburg, Germany) at 55 °C, 1200 rpm for 30 min and stored at -20 °C.

<i>Ustilago</i> lysis buffer	50 mM Tris-HCl, pH 7.5
	50 mM Na <sub>2</sub> -EDTA
	1% (w/v) SDS
Phenol / Chloroform	50% (v/v) Phenol (equilibrated in TE buffer)
	50% (v/v) Chloroform

### 4.6.3 Genomic DNA isolation from colonised maize tissue

For isolation of genomic DNA from maize tissue, the tissue was frozen in liquid N<sub>2</sub> and homogenized using a mortar and pestle under constant liquid N<sub>2</sub> cooling. Isolation of genomic DNA then was performed using the MasterPure™ Complete DNA and RNA Purification Kit from Epicentre (Madison, USA) according to manufacturer's instructions.

### 4.6.4 Total RNA isolation from colonised maize tissue

For isolation of total RNA, the maize tissue was frozen in liquid N<sub>2</sub> and homogenised using a mortar and pestle under constant liquid N<sub>2</sub> cooling. TRIzol® reagent (Invitrogen, Carlsbad, USA) was used for extraction of RNA according to the manufacturer's instructions. To approximately 400  $\mu$ l of homogenized tissue 1 ml TRIzol® reagent was immediately added and the sample was mixed. After centrifugation at 12000  $xg$  for 10 min

at 4 °C, the supernatant was transferred to a fresh reaction tube and 200 µl of chloroform were added. The sample was mixed by inversion of the tube and incubated at room temperature for 2-3 min. After centrifugation at 12000 *xg* for 15 min at 4 °C the upper aqueous phase was transferred to a fresh reaction tube containing 500 µl isopropanol and incubated at room temperature for 10 min. For precipitation of RNA, the tube was centrifuged at 12000 *xg* for 10 min at 4 °C and the supernatant was discarded. The resulting pellet was washed with 1 ml 75% EtOH at 7500 *xg* for 5 min and then dried for 5 min at room temperature. The pellet was finally dissolved in 35 µl RNase-free H<sub>2</sub>O at 55 °C for 10 min. RNA concentration was assessed by photometric measurement in a NanoDrop ND\_1000 spectrophotometer (Thermo Fisher Scientific, Waltham, USA).

### 4.6.5 DNase digest after RNA isolation

Digest of contaminating DNA after RNA isolation was performed using the Turbo DNA-Free™ Kit from Ambion Life technologies™ (Carlsbad, USA) according to the manufacturer's instructions. For that, 10 µg of total RNA were treated in a 50 µl reaction containing 5 µl 10X TURBO DNase Buffer and 1 µl TURBO DNase with incubation at 37 °C for 30 min. The DNase was inactivated by adding 5 µl DNase Inactivation Reagent. After incubation for 5 min at room temperature with occasional mixing, the sample was centrifuged at 10000 *xg* for 2 min and 44 µl of the supernatant was transferred to a fresh reaction tube. RNA concentration was assessed by photometric measurement in a NanoDrop ND\_1000 spectrophotometer (Thermo Fisher Scientific, Waltham, USA) and quality was afterwards assessed by loading 1 µl of RNA on a 1% agarose gel (see Chapter 4.6.13).

### 4.6.6 Synthesis of cDNA

Synthesis of cDNA was performed using the Thermo Scientific RevertAid H Minus First Strand cDNA Synthesis Kit (Thermo Fisher Scientific, Waltham, USA) according to manufacturer's instructions. For this, a 6 µl reaction containing 1-5 µg of template RNA and 0.5 µl oligo(dT)<sub>18</sub> primer was set up and incubated at 65 °C for 5 min. Then, 2 µl 5X Reaction Buffer, 0.5 µl RiboLock Rnase inhibitor, 1 µl 10 mM dNTP Mix and 0.5 µl RevertAid H Minus M-MuLV Reverse Transcriptase was added and the sample was incubated at 42 °C for 60 min. The reaction was terminated by heating at 70 °C for 5 min. The cDNA was stored at -80 °C until further use.

### **4.6.7 Quantification of nucleic acids**

Quantification of nucleic acids was performed using a NanoDrop ND\_1000 spectrophotometer (Thermo Fisher Scientific, Waltham, USA) according to manufacturer's instructions in a volume of 1 µl and using the appropriate buffer as a blank control.

### **4.6.8 Polymerase chain reaction (PCR)**

For specific amplification of DNA fragments, polymerase chain reaction (PCR) was performed in T100 Thermal cyclers from Bio-Rad Laboratories GmbH (Hercules; USA). Depending on the purpose, different polymerases were used. For analytic purposes, the GoTaq® Green Master Mix (Promega GmbH, Madison, USA) was used. For the amplification of long fragments or coding sequences for vector construction the Phusion® High Fidelity DNA Polymerase or Q5® High Fidelity DNA Polymerase (New England Biolabs, Ipswich, USA) were used. Reactions were carried out with the supplied buffers and solutions according to the manufacturer's instructions.

### **4.6.9 Quantitative real-time PCR (qRT-PCR)**

As a template for quantitative real-time PCR (qRT-PCR), cDNA (Chapter 4.6.6) synthesized from freshly isolated RNA was used. The qRT-PCR reactions were set up using the GoTaq® qPCR Mastermix (Promega GmbH, Madison, USA) according to the manufacturer's instructions in a total volume of 15 µl. For one reaction, 5 µl of a 1:500 dilution of cDNA was used. All qRT-PCRs were performed in an iCycler system (Bio-Rad, Hercules, USA) with the following program: 95 °C / 2 min-(95 °C / 30 s-62 °C / 30 s-72 °C / 30 s) x 45 cycles.

### **4.6.10 Restriction enzyme digestion of DNA**

Restriction digestion of DNA was performed via type II restriction endonucleases (New England Biolabs, Ipswich, USA). The amount of digested DNA ranged from 1-5 µg. The restriction reaction was set up according to the manufacturer's instructions.

#### 4.6.11 Ligation of DNA fragments

Ligation of DNA fragments was performed using the T4 DNA ligase (Thermo Fisher Scientific, Waltham, USA) according to the manufacturer's instructions.

#### 4.6.12 Gibson assembly cloning

Gibson assembly cloning makes use of homologous recombination of DNA fragments (Gibson et al. 2009). DNA fragments were designed to have 20 nt overlap with the DNA fragments to assemble them with. Gibson assembly was performed using the NEBuilder® HiFi DNA Assembly Master Mix (New England Biolabs, Ipswich, USA) according to the manufacturer's instructions.

#### 4.6.13 Agarose gel electrophoresis

Separation of DNA fragments by size was done by agarose gel electrophoresis. Samples were prepared by adding 1/5 of sample volume of 6x DNA loading dye. Depending on the size of the DNA fragment of interest, the agarose concentration of the gel was 0.8-2% (w/v) with 0.25 µg/ml ethidium bromide in 1x TAE buffer. For size estimation of the separated DNA fragments a DNA marker of defined size was run on each gel. The electrophoresis was run at constant voltage in 1x TAE at 80-150 V for 20-60 min. DNA was then visualised by UV radiation using a gel documentation unit (Peglab/VWR, Radnor, USA).

To prepare DNA from the gel the agarose gel piece containing the fragment of interest was cut out. The DNA was extracted using the NucleoSpin® Gel and PCR Clean-up Kit (Macherey Nagel, Düren, Germany) following the manufacturer's instructions.

50x TAE-buffer	2 M Tris-Base 2 M Acetic acid 50 mM EDTA pH 8.0
6x DNA loading dye	50% Sucrose 0.1% (v/v) Bromophenol blue in TE-Buffer



### 4.6.14 Southern Blot analysis

Specific DNA fragments in complete genomic DNA were detected by Southern Blot as described by Southern (1975). First, the genomic DNA was restricted with an appropriate endonuclease. To increase concentration and purity of the DNA a sodium acetate/ethanol precipitation was performed subsequently: 1/10 volumes of 3 M sodium acetate and 2 volumes of 100% EtOH were added after the restriction to the reaction mixture. The DNA was precipitated and pelleted by incubation at -20 °C for 1 h and centrifugation for 30 min at 4 °C and 12000 *xg*. The pellet was solved in 20 µl 1x DNA loading dye. Then the DNA fragments were separated by gel electrophoresis at 100 V for 2 h using a 0.8% agarose gel. For depurination, the gel was then incubated in depurination solution for 15 min until the marker colour shifted from blue to yellow and subsequently neutralised in transfer buffer for 30 min. By upward blotting using transfer buffer the DNA was transferred over night to an Amersham Hybond-XL membrane (GE Health Care Life Sciences, Freiburg, Germany). After blotting the DNA fragments were fixed to the membrane by UV cross-linking using an ultraviolet cross linker (Amersham Biosciences, Little Chalfont, UK). The membrane was then incubated in 20 ml hybridisation buffer in a hybridisation oven (UVP HB-1000 Hybridizer, Ultra-violet products Ltd., Cambridge, UK) with turning at 65 °C for 2 h. Detection of nucleic acids was done using dioxigenin (DIG)-labelled DNA probes. Probes were synthesized using the PCR DIG Labelling Mix kit (Roche, Mannheim, Germany) following the manufacturer's instructions. DIG-labelled PCR products were added to 20 ml hybridisation buffer and boiled for 10 min for denaturation. The membrane was incubated in probe-containing hybridisation buffer in a hybridisation oven with turning at 65 °C overnight and then washed three times for 15 min with southern wash buffer at 65 °C. The membrane was then incubated in DIG wash buffer for 5 min, then incubated in 50 ml DIG buffer 2 for 30 mins and finally incubated in 20 ml antibody solution for 30 mins, all in a hybridisation oven with turning at room temperature. The membrane was subsequently washed 3 times for 15 min with DIG wash buffer and then equilibrated for 5 min with DIG buffer 3. After that, the membrane was incubated in a cut, small autoclaving bag with 2.5 ml CDP-star solution for 15 min at 37 °C. The membrane was then put in a fresh, small cut autoclave bag and luminescence was detected in a ChemiDoc™MMP (Bio-Rad Laboratories GmbH, Hercules; USA).

Depurination solution                      0.25 M HCl

Transfer buffer                                0.5 M NaOH

1.5 M NaCl

Southern hybridization buffer	0.5 M NaPO <sub>4</sub> , pH 7 7% (w/v) SDS
Southern wash buffer	0.1 M 1M NaPO <sub>4</sub> , pH 7 1% (w/v) SDS
DIG buffer 1	0.1 M maleic acid 0.15 M NaOH set pH to 7.5 with NaOH autoclave
DIG buffer 2	1 g skimmed milk powder 100 ml DIG buffer 1
DIG buffer 3	0.1 M Tris-HCl (pH 9.5) 0.1 M NaCl 0.05 M MgCl <sub>2</sub>
DIG wash buffer	6 ml Tween20 2 L DIG buffer 1
Southern antibody solution	2 µl Anti-Dioxigenin-AP, Fab fragments (Roche, Mannheim, Germany) 20 ml DIG buffer 2
CDP-star solution	200 µl CDP-star solution (Roche, Mannheim, Germany) 20 ml DIG buffer 3

### 4.6.15 Purification of DNA

Nucleic acids were purified using the NucleoSpin® gel and PCR Clean-up kit (Macherey-Nagel, Düren, Germany) according to the manufacturer's instructions.

### 4.6.16 Sequencing of DNA

Sequencing reactions were performed by Eurofins (formerly GATC, Luxembourg, Luxembourg). Prior to sequencing of plasmids or PCR fragments, DNA was purified using Nucleospin® Gel and PCR Clean-up kit (Macherey-Nagel, Düren, Germany) as described in 4.6.1 and 4.6.15. DNA sequencing results were analysed and validated using the program Clone Manager 9 (Sci-Ed, Denver, USA).

### 4.6.17 Sequencing of RNA

Sequencing library preparation was done using the Illumina TruSeq mRNA stranded Kit (Illumina, San Diego, USA) or NEB Next® Ultra™ RNA Library Prep Kit (NEB, Ipswich, USA). Illumina sequencing of mRNA was performed with 150 bp paired-end reads at the Cologne Center for Genomics (CCG, Cologne, Germany) on an Illumina HiSeq 4000 (Illumina, San Diego, USA) and at Novogene (Peking, China) on an Illumina NovaSeq 6000 (Illumina, San Diego, USA). Approximately 60 million 150 bp paired-end reads per *U. maydis*-infected sample and 40 million paired-end reads per mock-treated sample were created.

### 4.6.18 KASP sequencing

From 56,110 single nucleotide polymorphisms (SNPs) identified by Ganai et al. (2011), 111 SNP markers were selected to genotype the individuals of the segregating populations. Selected SNP markers were polymorphic between the two parental inbreds and showed no heterozygosity in the parental inbreds. SNP marker selection was optimized for equal distribution across the physical map. The selected SNP markers were genotyped using competitive allele-specific PCR (KASP) SNP technology by TraitGenetics GmbH (Gatersleben, Germany) on a bulk of 5 F<sub>3</sub> plants per genotype in the respective populations.

## 4.7 Tissue fixation, staining and microscopy

### 4.7.1 WGA-AF488/Propidium iodide co-staining of colonised maize tissue

Visualisation of growth and morphology of *U. maydis* in maize using WGA-AF488 and propidium iodide co-staining was performed as described in Redkar et al. (2018).

### 4.7.2 Fluorescence microscopy

WGA-AF488/propidium iodide stained samples were analysed using a Zeiss Axio Zoom V16 using the GFP filter for WGA-AF488 and the DsRed filter for propidium iodide visualisation. Image processing was done using ImageJ.

### 4.7.3 Confocal laser-scanning microscopy

For analysis of effector secretion, maize leaves infected with *U. maydis* strains expressing mCherry-tagged effectors were analysed with a Leica TCS SP8 Confocal Laser Scanning Microscope. mCherry fluorescence was visualised 2 dpi with an excitation wavelength of 561 nm and detection wavelength of 580-630 nm using a 561 DPSS laser. Plant cell wall auto fluorescence was visualised with an excitation wavelength of 405 nm and a detection wavelength of 435-480 nm using a 405 Diode. Images were processed using the Leica software LAS AFLite.

## 4.8 Bioinformatics

### 4.8.1 RNA-Seq analysis

Illumina reads (see Chapter 4.6.17). were filtered using the Trinity software (v2.9.1) option trimmomatic under the standard settings (Grabherr et al. 2011). The reads were then mapped to the reference genome using Bowtie 2 (v2.3.5.1) with the first 15 nucleotides on the 5'-end of the reads being trimmed (Langmead and Salzberg 2012). As reference genome the *U. maydis* genome assembly (Kämper et al. 2006) and the *Z. mays* B73 version 3 (Schnable et al. 2009) genome assembly combined in one file were used. Reads were counted to the *U. maydis* and *Z. mays* loci using the R package Rsubread (v1.34.7) (Liao et al. 2019). On average, 640 thousand read counts were mapped to the *U. maydis* genome per sample for the data set of different maize lines (1.3% of total read

counts) and 783 thousand read counts for the data set of CML322 infected by SG200 or KO\_UMAG\_02297 (1.8% of total read counts). For maize, approximately 50 million read counts for the *U. maydis* inoculated samples and 43 million read counts for the mock samples were mapped to the genome. Pre-filtering was applied to keep only genes with at least 10 counts in 3 samples (6284 genes for *U. maydis*, 40056 genes for the data set of different maize lines and 30637 genes for the data set of CML322 infected by SG200 or KO\_UMAG\_02297). Counts mapped to *U. maydis* or maize were normalised and differential gene expression was analysed by DESeq2 v1.26.0 (differential expression analysis for sequence count data 2, Love et al. 2014) in R. For *U. maydis*, the design formula was  $\sim$  genotype, for maize, the design formula was  $\sim$ genotype + condition + genotype:condition to identify differences in condition effects (SG200-infected vs Mock) between genotypes. Genes with a  $\log_2$  expression fold change  $>0.5$  or  $<-0.5$  and Benjamini-Hochberg-adjusted p value  $< 0.05$  were considered differentially expressed.

### 4.8.2 WGCNA

To identify co-expressed genes, a weighted gene co-expression network analysis (WGCNA) was done using the WGCNA package (v1.69) (Zhang and Horvath 2005; Langfelder and Horvath 2008) in R. Only genes with at least 10 counts in 50% of the analysed maize samples or in 90% of the analysed *U. maydis* samples were considered. For *U. maydis* 4013 genes and for maize 29729 genes passed this filtering.  $\log_2$ -transformed DESeq2-normalized counts were used as input for the network analysis. The function `blockwiseModules` was used to create a signed network of a Pearson correlated matrix, only positive correlations were considered. For *U. maydis*, all genes were treated in a single block. For maize, the maximum blocksize was set to 15000. The soft power threshold was set to 4 for *U. maydis* and for maize because this was the lowest power needed to reach scale-free topology ( $R^2 = 0.901$  and  $0.871$  respectively). Modules were detected using default settings with a `mergeCutHeight` of 0.15 and a minimal module size of 25 genes. For each module, the expression profile of the module eigengene was calculated, which represents the modules by summary expression profiles of all genes of a given module. For each gene and module eigengene, the Pearson correlation to the disease index of the different maize lines was calculated (= gene significance for the trait).

### 4.8.3 GO enrichment analysis

GO term enrichment analysis (Ashburner et al. 2000; The Gene Ontology Consortium 2017) for *U. maydis* was performed with the Gene Ontology Panther Classification System (Mi et al. 2019) using a p value cut-off of <0.05. For the enrichment analysis of the modules correlated to the disease index, only genes were considered that had a gene significance for disease index > 0.5 or < -0.5 and p value <0.05. For maize, Gene Ontology (GO) terms were annotated to the version 3 protein annotation of maize line B73 using InterProScan (v5.42-78.0; Schnable et al. 2009; Jones et al. 2014; El-Gebali et al. 2019). Significance of GO term enrichments in a subset of genes were calculated for all expressed genes with a Fisher's exact test with the alternative hypothesis being one-sided (greater).

### 4.8.4 Mapping of maize genes to Arabidopsis

For comparison of maize genes to genes previously described to be involved in PTI or ETI in Arabidopsis, mapping of maize gene IDs to Arabidopsis was performed on the Monocots PLAZA 4.0 workbench (<https://bioinformatics.psb.ugent.be/plaza/>; Van Bel et al. 2018) using the PLAZA orthologous genes integrative method with standard settings and a minimum number of required evidence types of three.

### 4.8.5 Intraspecific sequence variation analysis

For comparison of effector amino acid sequences between different *U. maydis* strains, the number of nonsynonymous substitutions per nonsynonymous site (ds) was calculated. From the 5 strains with highest ds with the reference strain 521 the median was calculated. All effectors were then ranked based on their ds from low divergence to high divergence. For this analysis, only genes upregulated *in planta* in the Lanver et al. (2018) data set, with a minimum expression level of 150 tpm, that do not contain a functional domain that is related to sugar metabolism and do not contain multiple transmembrane domains were considered as effectors (214 genes).

### 4.8.6 QTL Mapping

A consensus genetic linkage map was calculated chromosome-wise using the allele frequencies identified by KASP with the R package R/qtl v1.46-2 (Broman et al. 2003). Cross type was set to 2. Markers that had been genotyped in less than 70% of individuals and individuals with less than 80% of markers genotyped were omitted from the analysis. Markers with high levels of segregation distortion were dropped ( $\chi^2$   $p < 10^{-15}$ ). Linked markers localised on different chromosomes were moved to the same chromosome and switched alleles were switched to the correct alleles. To choose marker orders minimising number of obligate crossovers, the ripple function with a window size of 6 was used. For QTL mapping, adjusted entry means of the phenotypic data were estimated as follows: A linear model containing the overall mean, error and a fixed genotype effect was fitted in R. QTL detection was performed using Haley-Knott regression with the R package R/qtl v1.46-2 (Broman et al. 2003). LOD thresholds to detect QTL for each trait were determined by 1000 permutations in the scanone function and the global type I error was set to 5%.

### 4.8.7 Further bioinformatics tools

Clone Manager 9.0 software (Sci-Ed Software, Cary/USA) was used for planning cloning strategies in silico. National Center for Biotechnology Information (NCBI; [www.ncbi.nlm.nih.gov](http://www.ncbi.nlm.nih.gov); Altschul et al. 1997). Maize Genetics and Genomics Database (maizeGDB; <https://www.maizegdb.org/>; Portwood et al. 2019) and the Ensembl Fungi database (<https://fungi.ensembl.org>; Howe et al. 2020) was used to obtain nucleotide sequences of interest. Protein domains were analysed using the SignalP 5.0 online tool (<http://www.cbs.dtu.dk/services/SignalP>; Almagro Armenteros et al. 2019).

### 4.8.8 Data availability

All RNA sequencing data has been submitted to NCBI Genbank and is available under the BioProject ID PRJNA673988.

## 5 Bibliography

- Aichinger C, Hansson K, Eichhorn H, Lessing F, Mannhaupt G, Mewes W, Kahmann R (2003) Identification of plant-regulated genes in *Ustilago maydis* by enhancer-trapping mutagenesis. *Mol Genet Genomics* 270:303–314. doi: 10.1007/s00438-003-0926-z
- Albert M (2013) Peptides as triggers of plant defence. *J Exp Bot* 64:5269–5279. doi: 10.1093/jxb/ert275
- Alexandratos N, Bruinsma J (2012) World agriculture towards 2015/2030: the 2012 revision. ESA Working paper (Vol. 12 No. 3).
- Almagro Armenteros JJ, Tsirigos KD, Sønderby CK, Petersen TN, Winther O, Brunak S, von Heijne G, Nielsen H (2019) SignalP 5.0 improves signal peptide predictions using deep neural networks. *Nat Biotechnol* 37:420–423. doi: 10.1038/s41587-019-0036-z
- Altschul S (1997) Gapped BLAST and PSI-BLAST: a new generation of protein database search programs. *Nucleic Acids Res* 25:3389–3402. doi: 10.1093/nar/25.17.3389
- Alves AA, Guimarães LM da S, Chaves AR de M, DaMatta FM, Alfenas AC (2011) Leaf gas exchange and chlorophyll a fluorescence of *Eucalyptus urophylla* in response to *Puccinia psidii* infection. *Acta Physiol Plant* 33:1831–1839. doi: 10.1007/s11738-011-0722-z
- Apel K, Hirt H (2004) Reactive oxygen species: metabolism, oxidative stress, and signal transduction. *Annu Rev Plant Biol* 55:373–399. doi: 10.1146/annurev.arplant.55.031903.141701
- Armstrong MR, Whisson SC, Pritchard L, Bos JIB, Venter E, Avrova AO, Rehmany AP, Bohme U, Brooks K, Cherevach I, Hamlin N, White B, Fraser A, Lord A, Quail MA, Churcher C, Hall N, Berriman M, Huang S, Kamoun S, Beynon JL, Birch PRJ (2005) An ancestral oomycete locus contains late blight avirulence gene *Avr3a*, encoding a protein that is recognized in the host cytoplasm. *Proc Natl Acad Sci* 102:7766–7771. doi: 10.1073/pnas.0500113102
- Ashburner M, Ball CA, Blake JA, Botstein D, Butler H, Cherry JM, Davis AP, Dolinski K, Dwight SS, Eppig JT, Harris MA, Hill DP, Issel-Tarver L, Kasarskis A, Lewis S, Matese JC, Richardson JE, Ringwald M, Rubin GM, Sherlock G (2000) Gene ontology: tool for the unification of biology. The Gene Ontology Consortium. *Nat Genet* 25:25–29. doi: 10.1038/75556
- Bacete L, Mélida H, López G, Dabos P, Tremousaygue D, Denancé N, Miedes E, Bulone V, Goffner D, Molina A (2020) *Arabidopsis* response reGULATOR 6 (ARR6) modulates plant cell-wall composition and disease resistance. *Mol Plant-Microbe Interact* 33:767–780. doi: 10.1094/MPMI-12-19-0341-R
- Banuett F, Herskowitz I (1996) Discrete developmental stages during teliospore formation in the corn smut fungus, *Ustilago maydis*. *Development* 122:2965–76.
- Bao Z, Yang H, Hua J (2013) Perturbation of cell cycle regulation triggers plant immune response via activation of disease resistance genes. *Proc Natl Acad Sci* 110:2407–2412. doi: 10.1073/pnas.1217024110



## 5. Bibliography

---

- Barbacci A, Navaud O, Mbengue M, Barascud M, Godiard L, Khafif M, Lacaze A, Raffaele S (2020) Rapid identification of an *Arabidopsis* NLR gene as a candidate conferring susceptibility to *Sclerotinia sclerotiorum* using time-resolved automated phenotyping. *Plant J* 103:903–917. doi: 10.1111/tpj.14747
- Bari R, Jones JDG (2009) Role of plant hormones in plant defence responses. *Plant Mol Biol* 69:473–488. doi: 10.1007/s11103-008-9435-0
- Bartoli C, Roux F (2017) Genome-Wide Association Studies In Plant Pathosystems: Toward an Ecological Genomics Approach. *Front Plant Sci*. doi: 10.3389/fpls.2017.00763
- Basse CW, Steinberg G (2004) *Ustilago maydis*, model system for analysis of the molecular basis of fungal pathogenicity. *Mol Plant Pathol* 5:83–92. doi: 10.1111/j.1364-3703.2004.00210.x
- Bauer R, Oberwinkler F, Vánky K (1997) Ultrastructural markers and systematics in smut fungi and allied taxa. *Can J Bot* 75:1273–1314. doi: 10.1139/b97-842
- Baumgarten AM, Suresh J, May G, Phillips RL (2007) Mapping QTLs contributing to *Ustilago maydis* resistance in specific plant tissues of maize. *Theor Appl Genet* 114:1229–1238. doi: 10.1007/s00122-007-0513-5
- Begerow D, Stoll M, Bauer R (2006) A phylogenetic hypothesis of Ustilaginomycotina based on multiple gene analyses and morphological data. *Mycologia* 98:906–916. doi: 10.3852/mycologia.98.6.906
- Birren B, Fink G, Lander E (2002) Fungal Genome Initiative: White Paper developed by the Fungal Research Community.
- Bölker M, Urban M, Kahmann R (1992) The a mating type locus of *U. maydis* specifies cell signaling components. *Cell* 68:441–450. doi: [https://doi.org/10.1016/0092-8674\(92\)90182-C](https://doi.org/10.1016/0092-8674(92)90182-C)
- Boller T, Felix G (2009) A renaissance of elicitors: perception of microbe-associated molecular patterns and danger signals by pattern-recognition receptors. *Annu Rev Plant Biol* 60:379–406. doi: 10.1146/annurev.arplant.57.032905.105346
- Bolouri Moghaddam MR, Van den Ende W (2013) Sweet immunity in the plant circadian regulatory network. *J Exp Bot* 64:1439–1449. doi: 10.1093/jxb/ert046
- Brefort T, Doehlemann G, Mendoza-Mendoza A, Reissmann S, Djamei A, Kallmann R, Kahmann R (2009) *Ustilago maydis* as a pathogen. *Annu Rev Phytopathol* 47:423–445. doi: 10.1146/annurev-phyto-080508-081923
- Broman KW, Wu H, Sen S, Churchill GA (2003) R/qtl: QTL mapping in experimental crosses. *Bioinformatics* 19:889–890. doi: 10.1093/bioinformatics/btg112
- Brown JK, Tellier A (2011) Plant-parasite coevolution: bridging the gap between genetics and ecology. *Annu Rev Phytopathol* 49:345–367. doi: 10.1146/annurev-phyto-072910-095301
- Bubeck DM, Goodman MM, Beavis WD, Grant D (1993) Quantitative Trait Loci Controlling Resistance to Gray Leaf Spot in Maize. *Crop Sci* 33:838–847. doi: 10.2135/cropsci1993.0011183X003300040041x

- Cesari S (2018) Multiple strategies for pathogen perception by plant immune receptors. *New Phytol* 219:17–24. doi: 10.1111/nph.14877
- Cesari S, Bernoux M, Moncuquet P, Kroj T, Dodds PN (2014) A novel conserved mechanism for plant NLR protein pairs: the ‘‘integrated decoy’’ hypothesis. *Front Plant Sci*. doi: 10.3389/fpls.2014.00606
- Christensen JJ (1963) Corn smut caused by *Ustilago maydis*. American Phytopathological Society, Worcester, Massachusetts
- Chung K-M, Igari K, Uchida N, Tasaka M (2008) New perspectives on plant defense responses through modulation of developmental pathways. *Mol Cells* 26:107–12.
- Collemare J, O’Connell R, Lebrun M (2019) Nonproteinaceous effectors: the terra incognita of plant–fungal interactions. *New Phytol* 223:590–596. doi: 10.1111/nph.15785
- Collins A, Milbourne D, Ramsay L, Meyer R, Chatot-Balandras C, Oberhagemann P, De Jong W, Gebhardt C, Bonnel E, Waugh R (1999) QTL for field resistance to late blight in potato are strongly correlated with maturity and vigour. *Mol Breed* 5:387–398. doi: 10.1023/A:1009601427062
- Conrath U, Beckers GJM, Langenbach CJG, Jaskiewicz MR (2015) Priming for Enhanced Defense. *Annu Rev Phytopathol* 53:97–119. doi: 10.1146/annurev-phyto-080614-120132
- Cook DE, Lee TG, Guo X, Melito S, Wang K, Bayless AM, Wang J, Hughes TJ, Willis DK, Clemente TE, Diers BW, Jiang J, Hudson ME, Bent AF (2012) Copy Number Variation of Multiple Genes at *Rhg1* Mediates Nematode Resistance in Soybean. *Science* (80- ) 338:1206–1209. doi: 10.1126/science.1228746
- Cook DE, Mesarich CH, Thomma BPHJ (2015) Understanding Plant Immunity as a Surveillance System to Detect Invasion. *Annu Rev Phytopathol* 53:541–563. doi: 10.1146/annurev-phyto-080614-120114
- Corwin JA, Kliebenstein DJ (2017) Quantitative resistance: More than just perception of a pathogen. *Plant Cell* 29:655–665. doi: 10.1105/tpc.16.00915
- Couto D, Zipfel C (2016) Regulation of pattern recognition receptor signalling in plants. *Nat Rev Immunol* 16:537–552. doi: 10.1038/nri.2016.77
- Cui F, Wu S, Sun W, Coaker G, Kunkel B, He P, Shan L (2013) The *Pseudomonas syringae* type III effector *AvrRpt2* promotes pathogen virulence via stimulating arabidopsis auxin/indole acetic acid protein turnover. *Plant Physiol*. doi: 10.1104/pp.113.219659
- Cui H, Tsuda K, Parker JE (2015) Effector-Triggered Immunity: From Pathogen Perception to Robust Defense. *Annu Rev Plant Biol* 66:487–511. doi: 10.1146/annurev-arplant-050213-040012
- Dangl JL, Horvath DM, Staskawicz BJ (2013) Pivoting the Plant Immune System from Dissection to Deployment. *Science* (80- ) 341:746–751. doi: 10.1126/science.1236011

## 5. Bibliography

---

- Dangl JL, Jones JDG (2001) Plant pathogens and integrated defence responses to infection. *Nature* 411:826–833. doi: 10.1038/35081161
- Daverdin G, Rouxel T, Gout L, Aubertot J-N, Fudal I, Meyer M, Parlange F, Carpezat J, Balesdent M-H (2012) Genome Structure and Reproductive Behaviour Influence the Evolutionary Potential of a Fungal Phytopathogen. *PLoS Pathog* 8:e1003020. doi: 10.1371/journal.ppat.1003020
- de Jonge R, Bolton MD, Thomma BPHJ (2011) How filamentous pathogens co-opt plants: The ins and outs of fungal effectors. *Curr Opin Plant Biol* 14:400–406. doi: 10.1016/j.pbi.2011.03.005
- de Jonge R, Thomma BPHJ (2009) Fungal LysM effectors: extinguishers of host immunity? *Trends Microbiol* 17:151–7. doi: 10.1016/j.tim.2009.01.002
- de Jonge R, van Esse HP, Kombrink A, Shinya T, Desaki Y, Bours R, van der Krol S, Shibuya N, Joosten MHAJ, Thomma BPHJ (2010) Conserved fungal LysM effector Ecp6 prevents chitin-triggered immunity in plants. *Science* 329:953–955.
- Dean R, Van Kan JAL, Pretorius ZA, Hammond-Kosack KE, Di Pietro A, Spanu PD, Rudd JJ, Dickman M, Kahmann R, Ellis J, Foster GD (2012) The Top 10 fungal pathogens in molecular plant pathology. *Mol Plant Pathol* 13:414–430. doi: 10.1111/j.1364-3703.2011.00783.x
- Delplace F, Huard-Chauveau C, Dubiella U, Khafif M, Alvarez E, Langin G, Roux F, Peyraud R, Roby D (2020) Robustness of plant quantitative disease resistance is provided by a decentralized immune network. *Proc Natl Acad Sci* 117:18099–18109. doi: 10.1073/pnas.2000078117
- Denby KJ, Kumar P, Kliebenstein DJ (2004) Identification of *Botrytis cinerea* susceptibility loci in *Arabidopsis thaliana*. *Plant J* 38:473–486. doi: 10.1111/j.0960-7412.2004.02059.x
- Depotter JRL, Doehlemann G (2020) Target the core: durable plant resistance against filamentous plant pathogens through effector recognition. *Pest Manag Sci* 76:426–431. doi: 10.1002/ps.5677
- Develey-Rivière M-P, Galiana E (2007) Resistance to pathogens and host developmental stage: a multifaceted relationship within the plant kingdom. *New Phytol* 175:405–416. doi: 10.1111/j.1469-8137.2007.02130.x
- Ding JQ, Wang XM, Chander S, Li JS (2008) Identification of QTL for maize resistance to common smut by using recombinant inbred lines developed from the Chinese hybrid Yuyu22. *J Appl Genet* 49:147–154. doi: 10.1007/BF03195608
- Djamei A, Schipper K, Rabe F, Ghosh A, Vincon V, Kahnt J, Osorio S, Tohge T, Fernie AR, Feussner I, Feussner K, Meinicke P, Stierhof Y-D, Schwarz H, Macek B, Mann M, Kahmann R (2011) Metabolic priming by a secreted fungal effector. *Nature* 478:395–398. doi: 10.1038/nature10454
- Dodds PN, Rafiqi M, Gan PHP, Hardham AR, Jones DA, Ellis JG (2009) Effectors of biotrophic fungi and oomycetes: pathogenicity factors and triggers of host resistance. *New Phytol* 183:993–1000. doi: 10.1111/j.1469-8137.2009.02922.x
- Dodds PN, Rathjen JP (2010) Plant immunity: towards an integrated view of plant–pathogen interactions. *Nat Rev Genet* 11:539–548. doi: 10.1038/nrg2812

- Doehlemann G, Hemetsberger C (2013) Apoplastic immunity and its suppression by filamentous plant pathogens. *New Phytol* 198:1001–1016. doi: 10.1111/nph.12277
- Doehlemann G, Reissmann S, Aßmann D, Fleckenstein M, Kahmann R (2011) Two linked genes encoding a secreted effector and a membrane protein are essential for *Ustilago maydis*-induced tumour formation. *Mol Microbiol* 81:751–766. doi: 10.1111/j.1365-2958.2011.07728.x
- Doehlemann G, van der Linde K, Aßmann D, Schwammbach D, Hof A, Mohanty A, Jackson D, Kahmann R (2009) Pep1, a Secreted Effector Protein of *Ustilago maydis*, Is Required for Successful Invasion of Plant Cells. *PLoS Pathog* 5:e1000290. doi: 10.1371/journal.ppat.1000290
- Doehlemann G, Wahl R, Horst RJ, Voll LM, Usadel B, Poree F, Stitt M, Pons-Kühnemann J, Sonnewald U, Kahmann R, Kämper J (2008a) Reprogramming a maize plant: Transcriptional and metabolic changes induced by the fungal biotroph *Ustilago maydis*. *Plant J* 56:181–195. doi: 10.1111/j.1365-313X.2008.03590.x
- Doehlemann G, Wahl R, Vranes M, de Vries RP, Kämper J, Kahmann R (2008b) Establishment of compatibility in the *Ustilago maydis*/maize pathosystem. *J Plant Physiol* 165:29–40. doi: 10.1016/j.jplph.2007.05.016
- Dong S, Stam R, Cano LM, Song J, Sklenar J, Yoshida K, Bozkurt TO, Oliva R, Liu Z, Tian M, Win J, Banfield MJ, Jones AME, van der Hoorn RAL, Kamoun S (2014) Effector Specialization in a Lineage of the Irish Potato Famine Pathogen. *Science* (80- ) 343:552–555. doi: 10.1126/science.1246300
- Dong X, Jiang Z, Peng YL, Zhang Z (2015) Revealing shared and distinct gene network organization in arabidopsis immune responses by integrative analysis. *Plant Physiol*. doi: 10.1104/pp.114.254292
- Dutheil JY, Mannhaupt G, Schweizer G, Sieber CMK, Münsterkötter M, Güldener U, Schirawski J, Kahmann R (2016) A tale of genome compartmentalization: The evolution of virulence clusters in smut fungi. *Genome Biol Evol* 8:681–704. doi: 10.1093/gbe/evw026
- El-Gebali S, Mistry J, Bateman A, Eddy SR, Luciani A, Potter SC, Qureshi M, Richardson LJ, Salazar GA, Smart A, Sonnhammer ELL, Hirsh L, Paladin L, Piovesan D, Tosatto SCE, Finn RD (2019) The Pfam protein families database in 2019. *Nucleic Acids Res* 47:D427–D432. doi: 10.1093/nar/gky995
- Evangelisti E, Govetto B, Minet-Kebdani N, Kuhn M-L, Attard A, Ponchet M, Panabières F, Gourgues M (2013) The *Phytophthora parasitica* RXLR effector Penetration-Specific Effector 1 favours *Arabidopsis thaliana* infection by interfering with auxin physiology. *New Phytol* 199:476–489. doi: 10.1111/nph.12270
- Feehan JM, Castel B, Bentham AR, Jones JD (2020) Plant NLRs get by with a little help from their friends. *Curr Opin Plant Biol* 56:99–108. doi: 10.1016/j.pbi.2020.04.006
- Fisher MC, Henk D a, Briggs CJ, Brownstein JS, Madoff LC, McCraw SL, Gurr SJ (2012) Emerging fungal threats to animal, plant and ecosystem health. *Nature* 484:186–94. doi: 10.1038/nature10947

## 5. Bibliography

---

- Forbes GA, Morales JG, Restrepo S, Pérez W, Gamboa S, Ruiz R, Cedeño L, Fermin G, Andreu AB, Acuña I, Oliva R (2013) *Phytophthora infestans* and *Phytophthora andina* on Solanaceous hosts in South America. In: *Phytophthora: a global perspective*. CABI, Wallingford, pp 48–58
- Fu J, Wang S (2011) Insights into Auxin Signaling in Plant-Pathogen Interactions. *Front Plant Sci*. doi: 10.3389/fpls.2011.00074
- Fu M, Crous PW, Bai Q, Zhang PF, Xiang J, Guo YS, Zhao FF, Yang MM, Hong N, Xu WX, Wang GP (2019) *Colletotrichum* species associated with anthracnose of *Pyrus* spp. in China. *Persoonia - Mol Phylogeny Evol Fungi* 42:1–35. doi: 10.3767/persoonia.2019.42.01
- Fu ZQ, Dong X (2013) Systemic Acquired Resistance: Turning Local Infection into Global Defense. *Annu Rev Plant Biol* 64:839–863. doi: 10.1146/annurev-arplant-042811-105606
- Fukuoka S, Saka N, Koga H, Ono K, Shimizu T, Ebana K, Hayashi N, Takahashi A, Hirochika H, Okuno K, Yano M (2009) Loss of Function of a Proline-Containing Protein Confers Durable Disease Resistance in Rice. *Science* (80- ) 325:998–1001. doi: 10.1126/science.1175550
- Galicia-García PR, Silva-Rojas HV, Mendoza-Onofre LE, Zavaleta-Mancera HA, Córdova-Téllez L, Espinosa-Calderón A (2016) Selection of aggressive pathogenic and solopathogenic strains of *Ustilago maydis* to improve Huitlacoche production. *Acta Bot Brasilica* 30:683–692. doi: 10.1590/0102-33062016abb0097
- Gamalero E, Glick BR (2012) Ethylene and Abiotic Stress Tolerance in Plants. In: *Environmental Adaptations and Stress Tolerance of Plants in the Era of Climate Change*. Springer New York, New York, NY, pp 395–412
- Gan P, Ikeda K, Irieda H, Narusaka M, O'Connell RJ, Narusaka Y, Takano Y, Kubo Y, Shirasu K (2013) Comparative genomic and transcriptomic analyses reveal the hemibiotrophic stage shift of *Colletotrichum* fungi. *New Phytol* 197:1236–1249. doi: 10.1111/nph.12085
- Ganal MW, Durstewitz G, Polley A, Bérard A, Buckler ES, Charcosset A, Clarke JD, Graner E-M, Hansen M, Joets J, Le Paslier M-C, McMullen MD, Montalent P, Rose M, Schön C-C, Sun Q, Walter H, Martin OC, Falque M (2011) A Large Maize (*Zea mays* L.) SNP Genotyping Array: Development and Germplasm Genotyping, and Genetic Mapping to Compare with the B73 Reference Genome. *PLoS One* 6:e28334. doi: 10.1371/journal.pone.0028334
- Gao L, Kelliher T, Nguyen L, Walbot V (2013) *Ustilago maydis* reprograms cell proliferation in maize anthers. *Plant J* 75:903–914. doi: 10.1111/tpj.12270
- Gao X, Starr J, Göbel C, Engelberth J, Feussner I, Tumlinson J, Kolomiets M (2008) Maize 9-Lipoxygenase ZmLOX3 Controls Development, Root-Specific Expression of Defense Genes, and Resistance to Root-Knot Nematodes. *Mol Plant-Microbe Interact* 21:98–109. doi: 10.1094/MPMI-21-1-0098
- Gebhardt C, Valkonen JPT (2001) Organization of genes controlling disease resistance in the potato genome. *Annu Rev Phytopathol* 39:79–102. doi: 10.1146/annurev.phyto.39.1.79

- Gianinazzi-Pearson V, Smith Se, Gianinazzi S, Smith Fa (1991) Enzymatic studies on the metabolism of vesicular-arbuscular mycorrhizas. V. Is H<sup>+</sup>-ATPase a component of ATP-hydrolysing enzyme activities in plant-fungus interfaces? *New Phytol* 117:61–74. doi: 10.1111/j.1469-8137.1991.tb00945.x
- Gibson DG, Young L, Chuang RY, Venter JC, Hutchison CA, Smith HO (2009) Enzymatic assembly of DNA molecules up to several hundred kilobases. *Nat Methods* 6:343–345. doi: 10.1038/nmeth.1318
- Giménez-Ibáñez S (2020) Designing disease-resistant crops: From basic knowledge to biotechnology. *Mètode Rev difusió la Investig.* doi: 10.7203/metode.11.15496
- Giraldo MC, Valent B (2013) Filamentous plant pathogen effectors in action. *Nat Rev Microbiol* 11:800–14. doi: 10.1038/nrmicro3119
- Glazebrook J (2005) Contrasting Mechanisms of Defense Against Biotrophic and Necrotrophic Pathogens. *Annu Rev Phytopathol* 43:205–227. doi: 10.1146/annurev.phyto.43.040204.135923
- Göhre V, Robatzek S (2008) Breaking the barriers: microbial effector molecules subvert plant immunity. *Annu Rev Phytopathol* 46:189–215. doi: 10.1146/annurev.phyto.46.120407.110050
- Gomez LD (2004) Regulation of calcium signalling and gene expression by glutathione. *J Exp Bot* 55:1851–1859. doi: 10.1093/jxb/erh202
- Grabherr MG., Haas BJ, Yassour M, Levin JZ, Thompson DA, Amit I, Adiconis X, Fan L, Raychowdhury R, Zeng Q, Chen Z, Mauceli E, Hacohen N, Gnirke A, Rhind N, Di Palma F, Birren BW, Nusbaum C, Lindblad-Toh K, Friedman N, Regev A (2011) Full-length transcriptome assembly from RNA-Seq data without a reference genome. *Nat Biotechnol* 29:644–652. doi: 10.1038/nbt.1883
- Grant SG, Jessee J, Bloom FR, Hanahan D (1990) Differential plasmid rescue from transgenic mouse DNAs into *Escherichia coli* methylation-restriction mutants. *Proc Natl Acad Sci U S A* 87:4645–4649. doi: 10.1073/pnas.87.12.4645
- Grunewald W, Cannoot B, Friml J, Gheysen G (2009) Parasitic Nematodes Modulate PIN-Mediated Auxin Transport to Facilitate Infection. *PLoS Pathog* 5:e1000266. doi: 10.1371/journal.ppat.1000266
- Hacquard S, Kracher B, Maekawa T, Vernaldi S, Schulze-Lefert P, Ver Loren van Themaat E, Van Themaat EVL (2013) Mosaic genome structure of the barley powdery mildew pathogen and conservation of transcriptional programs in divergent hosts. *Proc Natl Acad Sci U S A* 110:E2219-28. doi: 10.1073/pnas.1306807110
- Han X, Altegoer F, Steinchen W, Binnebesel L, Schuhmacher J, Glatter T, Giammarinaro PI, Djamei A, Rensing SA, Reissmann S, Kahmann R, Bange G (2019) A kiwellin disarms the metabolic activity of a secreted fungal virulence factor. *Nature* 565:650–653. doi: 10.1038/s41586-018-0857-9
- Hanahan D (1983) Studies on transformation of *Escherichia coli* with plasmids. *J Mol Biol* 166:557–580. doi: 10.1016/s0022-2836(83)80284-8

## 5. Bibliography

---

- Hatsugai N, Igarashi D, Mase K, Lu Y, Tsuda Y, Chakravarthy S, Wei H, Foley JW, Collmer A, Glazebrook J, Katagiri F (2017) A plant effector-triggered immunity signaling sector is inhibited by pattern-triggered immunity. *EMBO J* 36:2758–2769. doi: 10.15252/emj.201796529
- Hazen SP, Hawley RM, Davis GL, Henrissat B, Walton JD (2003) Quantitative Trait Loci and Comparative Genomics of Cereal Cell Wall Composition. *Plant Physiol* 132:263–271. doi: 10.1104/pp.103.020016
- Heath MC (2000) Hypersensitive response-related death. *Plant Mol Biol* 44:321–34. doi: 10.1023/a:1026592509060
- Heigwer F, Kerr G, Boutros M (2014) E-CRISP: Fast CRISPR target site identification. *Nat Methods* 11:122–123. doi: 10.1038/nmeth.2812
- Hemetsberger C, Herrberger C, Zechmann B, Hillmer M, Doehlemann G (2012) The *Ustilago maydis* effector Pep1 suppresses plant immunity by inhibition of host peroxidase activity. *PLoS Pathog* 8:e1002684. doi: 10.1371/journal.ppat.1002684
- Hemetsberger C, Mueller AN, Matei A, Herrberger C, Hensel G, Kumlehn J, Mishra B, Sharma R, Thines M, Hüchelhoven R, Doehlemann G (2015) The fungal core effector Pep1 is conserved across smuts of dicots and monocots. *New Phytol* 206:1116–1126. doi: 10.1111/nph.13304
- Hoffman CS, Winston F (1987) A ten-minute DNA preparation from yeast efficiently releases autonomous plasmids for transformation of *Escherichia coli*. *Gene* 57:267–272. doi: 10.1016/0378-1119(87)90131-4
- Hogenhout SA, Van der Hoorn RAL, Terauchi R, Kamoun S (2009) Emerging concepts in effector biology of plant-associated organisms. *Mol Plant Microbe Interact* 22:115–122. doi: 10.1094/MPMI-22-2-0115
- Hoover MM (1932) Inheritance Studies of the Reaction to Selfed Lines of Maize to Smut (*Ustilago Zeae* ).
- Horbach R, Navarro-Quesada AR, Knogge W, Deising HB (2011) When and how to kill a plant cell: Infection strategies of plant pathogenic fungi. *J Plant Physiol* 168:51–62. doi: 10.1016/j.jplph.2010.06.014
- Horst RJ, Doehlemann G, Wahl R, Hofmann J, Schmiedl A, Kahmann R, Kämper J, Sonnewald U, Voll LM (2010) *Ustilago maydis* Infection Strongly Alters Organic Nitrogen Allocation in Maize and Stimulates Productivity of Systemic Source Leaves. *Plant Physiol* 152:293–308. doi: 10.1104/pp.109.147702
- Horst RJ, Engelsdorf T, Sonnewald U, Voll LM (2008) Infection of maize leaves with *Ustilago maydis* prevents establishment of C4 photosynthesis. *J Plant Physiol*. doi: 10.1016/j.jplph.2007.05.008
- Horst RJ, Zeh C, Saur A, Sonnewald S, Sonnewald U, Voll LM (2012) The *Ustilago maydis* Nit2 Homolog Regulates Nitrogen Utilization and Is Required for Efficient Induction of Filamentous Growth. *Eukaryot Cell* 11:368–380. doi: 10.1128/EC.05191-11

- Howe KL, Contreras-Moreira B, De Silva N, Maslen G, Akanni W, Allen J, Alvarez-Jarreta J, Barba M, Bolser DM, Cambell L, Carbajo M, Chakiachvili M, Christensen M, Cummins C, Cuzick A, Davis P, Fexova S, Gall A, George N, Gil L, Gupta P, Hammond-Kosack KE, Haskell E, Hunt SE, Jaiswal P, Janacek SH, Kersey PJ, Langridge N, Maheswari U, Maurel T, McDowall MD, Moore B, Muffato M, Naamati G, Naithani S, Olson A, Papatheodorou I, Patricio M, Paulini M, Pedro H, Perry E, Preece J, Rosello M, Russell M, Sitnik V, Staines DM, Stein J, Tello-Ruiz MK, Trevanion SJ, Urban M, Wei S, Ware D, Williams G, Yates AD, Flicek P (2020) Ensembl Genomes 2020—enabling non-vertebrate genomic research. *Nucleic Acids Res* 48:D689–D695. doi: 10.1093/nar/gkz890
- Hu GG, Linning R, Bakkeren G (2002) Sporidial mating and infection process of the smut fungus, *Ustilago hordei*, in susceptible barley. *Can J Bot* 80:1103–1114. doi: 10.1139/b02-098
- Hurni S, Scheuermann D, Krattinger SG, Kessel B, Wicker T, Herren G, Fitze MN, Breen J, Presterl T, Ouzunova M, Keller B (2015) The maize disease resistance gene *Htn1* against northern corn leaf blight encodes a wall-associated receptor-like kinase. *Proc Natl Acad Sci* 112:8780–8785. doi: 10.1073/pnas.1502522112
- Immer F (1927) The Inheritance of Reaction to *Ustilago Zeae* in Maize.
- Jacob F, Vernaldi S, Maekawa T (2013) Evolution and Conservation of Plant NLR Functions. *Front Immunol*. doi: 10.3389/fimmu.2013.00297
- Jiang S, Yao J, Ma K-W, Zhou H, Song J, He SY, Ma W (2013) Bacterial effector activates jasmonate signaling by directly targeting JAZ transcriptional repressors. *PLoS Pathog* 9:e1003715. doi: 10.1371/journal.ppat.1003715
- Jones JDG, Dangl JL (2006) The plant immune system. *Nature* 444:323–329. doi: 10.1038/nature05286
- Jones JDGG, Vance RE, Dangl JL (2016) Intracellular innate immune surveillance devices in plants and animals. *Science* (80- ) 354:aaf6395–aaf6395. doi: 10.1126/science.aaf6395
- Jones P, Binns D, Chang HY, Fraser M, Li W, McAnulla C, McWilliam H, Maslen J, Mitchell A, Nuka G, Pesseat S, Quinn AF, Sangrador-Vegas A, Scheremetjew M, Yong SY, Lopez R, Hunter S (2014) InterProScan 5: genome-scale protein function classification. *Bioinformatics* 30:1236–1240. doi: 10.1093/bioinformatics/btu031
- Jubault M, Lariagon C, Taconnat L, Renou J-P, Gravot A, Delourme R, Manzanares-Dauleux MJ (2013) Partial resistance to clubroot in *Arabidopsis* is based on changes in the host primary metabolism and targeted cell division and expansion capacity. *Funct Integr Genomics* 13:191–205. doi: 10.1007/s10142-013-0312-9
- Kämper J (2004) A PCR-based system for highly efficient generation of gene replacement mutants in *Ustilago maydis*. *Mol Genet Genomics* 271:103–110. doi: 10.1007/s00438-003-0962-8



## 5. Bibliography

---

- Kämper J, Kahmann R, Bölker M, Ma L-J, Brefort T, Saville BJ, Banuett F, Kronstad JW, Gold SE, Müller O, Perlin MH, Wösten H a B, de Vries R, Ruiz-Herrera J, Reynaga-Peña CG, Snetselaar K, McCann M, Pérez-Martín J, Feldbrügge M, Basse CW, Steinberg G, Ibeas JI, Holloman W, Guzman P, Farman M, Stajich JE, Sentandreu R, González-Prieto JM, Kennell JC, Molina L, Schirawski J, Mendoza-Mendoza A, Greilinger D, Münch K, Rössel N, Scherer M, Vranes M, Ladendorf O, Vincon V, Fuchs U, Sandrock B, Meng S, Ho ECH, Cahill MJ, Boyce KJ, Klose J, Klosterman SJ, Deelstra HJ, Ortiz-Castellanos L, Li W, Sanchez-Alonso P, Schreier PH, Häuser-Hahn I, Vaupel M, Koopmann E, Friedrich G, Voss H, Schlüter T, Margolis J, Platt D, Swimmer C, Gnirke A, Chen F, Vysotskaia V, Mannhaupt G, Güldener U, Münsterkötter M, Haase D, Oesterheld M, Mewes H-W, Mauceli EW, DeCaprio D, Wade CM, Butler J, Young S, Jaffe DB, Calvo S, Nusbaum C, Galagan J, Birren BW (2006) Insights from the genome of the biotrophic fungal plant pathogen *Ustilago maydis*. *Nature* 444:97–101. doi: 10.1038/nature05248
- Kanja C, Hammond-Kosack KE (2020) Proteinaceous effector discovery and characterization in filamentous plant pathogens. *Mol Plant Pathol* 21:1353–1376. doi: 10.1111/mpp.12980
- Kanyuka K, Rudd JJ (2019) Cell surface immune receptors: the guardians of the plant's extracellular spaces. *Curr Opin Plant Biol* 50:1–8. doi: 10.1016/j.pbi.2019.02.005
- Kazan K, Lyons R (2014) Intervention of Phytohormone Pathways by Pathogen Effectors. *Plant Cell* 26:2285–2309. doi: 10.1105/tpc.114.125419
- Kazan K, Manners JM (2009) Linking development to defense: auxin in plant–pathogen interactions. *Trends Plant Sci* 14:373–382. doi: 10.1016/j.tplants.2009.04.005
- Kebede AZ, Johnston A, Schneiderman D, Bosnich W, Harris LJ (2018) Transcriptome profiling of two maize inbreds with distinct responses to *Gibberella ear rot* disease to identify candidate resistance genes. *BMC Genomics* 19:131. doi: 10.1186/s12864-018-4513-4
- Kellner R, Bhattacharyya A, Poppe S, Hsu TY, Brem RB, Stukenbrock EH (2014) Expression Profiling of the Wheat Pathogen *Zymoseptoria tritici* Reveals Genomic Patterns of Transcription and Host-Specific Regulatory Programs. *Genome Biol Evol* 6:1353–1365. doi: 10.1093/gbe/evu101
- Kirsten S, Navarro-Quezada A, Penselin D, Wenzel C, Matern A, Leitner A, Baum T, Seiffert U, Knogge W (2012) Necrosis-inducing proteins of *rhynchosporium commune*, effectors in quantitative disease resistance. *Mol Plant-Microbe Interact* 25:1314–1325. doi: 10.1094/MPMI-03-12-0065-R
- Kostandi SF, Geisler G (1989) Maize Smut Induced by *Ustilago maydis* (D. C.) Corda – Reaction of Maize Hybrids and Lines to Smut Disease. *J Agron Crop Sci* 162:149–156. doi: 10.1111/j.1439-037X.1989.tb00702.x
- Krattinger SG, Lagudah ES, Spielmeier W, Singh RP, Huerta-Espino J, McFadden H, Bossolini E, Selter LL, Keller B (2009) A Putative ABC Transporter Confers Durable Resistance to Multiple Fungal Pathogens in Wheat. *Science* (80- ) 323:1360–1363. doi: 10.1126/science.1166453
- Kretschmer M, Croll D, Kronstad JW (2017a) Chloroplast-associated metabolic functions influence the susceptibility of maize to *Ustilago maydis*. *Mol Plant Pathol* 18:1210–1221. doi: 10.1111/mpp.12485

- Kretschmer M, Croll D, Kronstad JW (2017b) Maize susceptibility to *Ustilago maydis* is influenced by genetic and chemical perturbation of carbohydrate allocation. *Mol Plant Pathol* 18:1222–1237. doi: 10.1111/mpp.12486
- Langfelder P, Horvath S (2008) WGCNA: an R package for weighted correlation network analysis. *BMC Bioinformatics* 9:559. doi: 10.1186/1471-2105-9-559
- Langmead B, Salzberg SL (2012) Fast gapped-read alignment with Bowtie 2. *Nat Methods* 9:357–359. doi: 10.1038/nmeth.1923
- Lanver D, Müller AN, Happel P, Schweizer G, Haas FB, Franitza M, Pellegrin C, Reissmann S, Altmüller J, Rensing SA, Kahmann R (2018) The Biotrophic Development of *Ustilago maydis* Studied by RNA-Seq Analysis. *Plant Cell* 30:300–323. doi: 10.1105/tpc.17.00764
- Lanver D, Tollot M, Schweizer G, Lo Presti L, Reissmann S, Ma LS, Schuster M, Tanaka S, Liang L, Ludwig N, Kahmann R (2017) *Ustilago maydis* effectors and their impact on virulence. *Nat Rev Microbiol* 15:409–421. doi: 10.1038/nrmicro.2017.33
- Lee J, Eschen-Lippold L, Lassowskat I, Böttcher C, Scheel D (2015) Cellular reprogramming through mitogen-activated protein kinases. *Front Plant Sci*. doi: 10.3389/fpls.2015.00940
- Liao Y, Smyth GK, Shi W (2019) The R package Rsubread is easier, faster, cheaper and better for alignment and quantification of RNA sequencing reads. *Nucleic Acids Res* 47:e47–e47. doi: 10.1093/nar/gkz114
- Lim GTT, Wang G-P, Hemming MN, Basuki S, McGrath DJ, Carroll BJ, Jones DA (2006) Mapping the I-3 gene for resistance to *Fusarium* wilt in tomato: application of an I-3 marker in tomato improvement and progress towards the cloning of I-3. *Australas Plant Pathol* 35:671. doi: 10.1071/AP06073
- Linning R, Lin D, Lee N, Abdennadher M, Gaudet D, Thomas P, Mills D, Kronstad JW, Bakkeren G (2004) Marker-Based Cloning of the Region Containing the *UhAvr1* Avirulence Gene from the Basidiomycete Barley Pathogen *Ustilago hordei*. *Genetics*. doi: 10.1534/genetics.166.1.99
- Liu T, Song T, Zhang X, Yuan H, Su L, Li W, Xu J, Liu S, Chen L, Chen T, Zhang M, Gu L, Zhang B, Dou D (2014) Unconventionally secreted effectors of two filamentous pathogens target plant salicylate biosynthesis. *Nat Commun*. doi: 10.1038/ncomms5686
- Lo Presti L, Kahmann R (2017) How filamentous plant pathogen effectors are translocated to host cells. *Curr Opin Plant Biol* 38:19–24. doi: 10.1016/j.pbi.2017.04.005
- Lo Presti L, Lanver D, Schweizer G, Tanaka S, Liang L, Tollot M, Zuccaro A, Reissmann S, Kahmann R (2015) Fungal Effectors and Plant Susceptibility. *Annu Rev Plant Biol* 66:513–545. doi: 10.1146/annurev-arplant-043014-114623
- Love MI, Huber W, Anders S (2014) Moderated estimation of fold change and dispersion for RNA-seq data with DESeq2. *Genome Biol* 15:1–21. doi: 10.1186/s13059-014-0550-8

## 5. Bibliography

---

- Loyall L, Uchida K, Braun S, Furuya M, Frohnmeyer H (2000) Glutathione and a UV Light-Induced Glutathione S-Transferase Are Involved in Signaling to Chalcone Synthase in Cell Cultures. *Plant Cell* 12:1939. doi: 10.2307/3871204
- Lübberstedt T, Klein D, Melchinger AE (1998a) Comparative QTL mapping of resistance to *Ustilago maydis* across four populations of European flint-maize. *Theor Appl Genet* 97:1321–1330. doi: 10.1007/s001220051025
- Lübberstedt T, Klein D, Melchinger AE (1998b) Comparative Quantitative Trait Loci Mapping of Partial Resistance to *Puccinia sorghi* Across Four Populations of European Flint Maize. *Phytopathology*® 88:1324–1329. doi: 10.1094/PHYTO.1998.88.12.1324
- Ma L-S, Wang L, Trippel C, Mendoza-Mendoza A, Ullmann S, Moretti M, Carsten A, Kahnt J, Reissmann S, Zechmann B, Bange G, Kahmann R (2018) The *Ustilago maydis* repetitive effector Rsp3 blocks the antifungal activity of mannose-binding maize proteins. *Nat Commun* 9:1711. doi: 10.1038/s41467-018-04149-0
- Martínez-Espinoza AD, García-Pedrajas MD, Gold SE (2002) The Ustilaginales as plant pests and model systems. *Fungal Genet Biol* 35:1–20. doi: 10.1006/fgbi.2001.1301
- Matei A, Doehlemann G (2016) Cell biology of corn smut disease — *Ustilago maydis* as a model for biotrophic interactions. *Curr Opin Microbiol* 34:60–66. doi: 10.1016/j.mib.2016.07.020
- Matei A, Ernst C, Günl M, Thiele B, Altmüller J, Walbot V, Usadel B, Doehlemann G (2018) How to make a tumour: cell type specific dissection of *Ustilago maydis*-induced tumour development in maize leaves. *New Phytol* 217:1681–1695. doi: 10.1111/nph.14960
- McHale L, Tan X, Koehl P, Michelmore RW (2006) Plant NBS-LRR proteins: adaptable guards. *Genome Biol* 7:212. doi: 10.1186/gb-2006-7-4-212
- McMullen MD, Kresovich S, Villeda HS, Bradbury P, Li H, Sun Q, Flint-Garcia S, Thornsberry J, Acharya C, Bottoms C, Brown P, Browne C, Eller M, Guill K, Harjes C, Kroon D, Lepak N, Mitchell SE, Peterson B, Pressoir G, Romero S, Rosas MO, Salvo S, Yates H, Hanson M, Jones E, Smith S, Glaubitz JC, Goodman M, Ware D, Holland JB, Buckler ES (2009) Genetic Properties of the Maize Nested Association Mapping Population. *Science* (80- ) 325:737–740. doi: 10.1126/science.1174320
- Meihls LN, Handrick V, Glauser G, Barbier H, Kaur H, Haribal MM, Lipka AE, Gershenzon J, Buckler ES, Erb M, Köllner TG, Jander G (2013) Natural Variation in Maize Aphid Resistance Is Associated with 2,4-Dihydroxy-7-Methoxy-1,4-Benzoxazin-3-One Glucoside Methyltransferase Activity. *Plant Cell* 25:1–16. doi: 10.1105/tpc.113.112409
- Mendoza-Mendoza A, Berndt P, Djamei A, Weise C, Linne U, Marahiel M, Vraneš M, Kämper J, Kahmann R (2009) Physical-chemical plant-derived signals induce differentiation in *Ustilago maydis*. *Mol Microbiol* 71:895–911. doi: 10.1111/j.1365-2958.2008.06567.x
- Mentlak TA, Kombrink A, Shinya T, Ryder LS, Otomo I, Saitoh H, Terauchi R, Nishizawa Y, Shibuya N, Thomma BPHJ, Talbot NJ (2012) Effector-mediated suppression of chitin-triggered immunity by *magnaporthe oryzae* is necessary for rice blast disease. *Plant Cell* 24:322–335. doi: 10.1105/tpc.111.092957

- Mi H, Muruganujan A, Ebert D, Huang X, Thomas PD (2019) PANTHER version 14: more genomes, a new PANTHER GO-slim and improvements in enrichment analysis tools. *Nucleic Acids Res* 47:D419–D426. doi: 10.1093/nar/gky1038
- Mine A, Seyfferth C, Kracher B, Berens ML, Becker D, Tsuda K (2018) The Defense Phytohormone Signaling Network Enables Rapid, High-Amplitude Transcriptional Reprogramming during Effector-Triggered Immunity. *Plant Cell* 30:1199–1219. doi: 10.1105/tpc.17.00970
- Misas Villamil JC, Mueller AN, Demir F, Meyer U, Ökmen B, Schulze Hüynck J, Breuer M, Dauben H, Win J, Huesgen PF, Doehlemann G (2019) A fungal substrate mimicking molecule suppresses plant immunity via an inter-kingdom conserved motif. *Nat Commun* 10:1576. doi: 10.1038/s41467-019-09472-8
- Monaghan J, Zipfel C (2012) Plant pattern recognition receptor complexes at the plasma membrane. *Curr Opin Plant Biol* 15:349–357. doi: 10.1016/j.pbi.2012.05.006
- Monteiro F, Nishimura MT (2018) Structural, Functional, and Genomic Diversity of Plant NLR Proteins: An Evolved Resource for Rational Engineering of Plant Immunity. *Annu Rev Phytopathol* 56:243–267. doi: 10.1146/annurev-phyto-080417-045817
- Morales JG, Gaviria AE, Gilchrist E (2020) Allelic variation and selection in effector genes of *Phytophthora infestans* (Mont.) de Bary. *Pathogens* 9:1–18. doi: 10.3390/pathogens9070551
- Mueller AN, Ziemann S, Treitschke S, Aßmann D, Doehlemann G (2013) Compatibility in the *Ustilago maydis*–Maize Interaction Requires Inhibition of Host Cysteine Proteases by the Fungal Effector Pit2. *PLoS Pathog* 9:e1003177. doi: 10.1371/journal.ppat.1003177
- Mukhi N, Gorenkin D, Banfield MJ (2020) Exploring folds, evolution and host interactions: understanding effector structure/function in disease and immunity. *New Phytol* 227:326–333. doi: 10.1111/nph.16563
- Müller DB, Vogel C, Bai Y, Vorholt JA (2016) The Plant Microbiota: Systems-Level Insights and Perspectives. *Annu Rev Genet* 50:211–234. doi: 10.1146/annurev-genet-120215-034952
- Muthamilarasan M, Prasad M (2013) Plant innate immunity: An updated insight into defense mechanism. *J Biosci* 38:433–449. doi: 10.1007/s12038-013-9302-2
- Mutka AM, Fawley S, Tsao T, Kunkel BN (2013) Auxin promotes susceptibility to *Pseudomonas syringae* via a mechanism independent of suppression of salicylic acid-mediated defenses. *Plant J* 74:746–754. doi: 10.1111/tpj.12157
- Navarro L, Bari R, Achard P, Lisón P, Nemri A, Harberd NP, Jones JDG (2008) DELLAs Control Plant Immune Responses by Modulating the Balance of Jasmonic Acid and Salicylic Acid Signaling. *Curr Biol* 18:650–655. doi: <http://dx.doi.org/10.1016/j.cub.2008.03.060>
- Navarro L, Dunoyer P, Jay F, Arnold B, Dharmasiri N, Estelle M, Voinnet O, Jones JDG (2006) A Plant miRNA Contributes to Antibacterial Resistance by Repressing Auxin Signaling. *Science* (80-) 312:436–439. doi: 10.1126/science.1126088

## 5. Bibliography

---

- Navarro L, Zipfel C, Rowland O, Keller I, Robatzek S, Boller T, Jones JDG (2004) The Transcriptional Innate Immune Response to flg22. Interplay and Overlap with Avr Gene-Dependent Defense Responses and Bacterial Pathogenesis. *Plant Physiol* 135:1113–1128. doi: 10.1104/pp.103.036749
- Ng JLP, Perrine-Walker F, Wasson AP, Mathesius U (2015) The control of auxin transport in parasitic and symbiotic root–microbe interactions. *Plants* 4:606–643. doi: 10.3390/plants4030606
- Niks RE, Qi X, Marcel TC (2015) Quantitative Resistance to Biotrophic Filamentous Plant Pathogens: Concepts, Misconceptions, and Mechanisms. *Annu Rev Phytopathol* 53:445–470. doi: 10.1146/annurev-phyto-080614-115928
- Oerke E-C (2006) Crop losses to pests. *J Agric Sci* 144:31. doi: 10.1017/S0021859605005708
- Oerke EC, Dehne HW (2004) Safeguarding production - Losses in major crops and the role of crop protection. *Crop Prot* 23:275–285. doi: 10.1016/j.cropro.2003.10.001
- Ökmen B, Doehlemann G (2014) Inside plant: biotrophic strategies to modulate host immunity and metabolism. *Curr Opin Plant Biol* 20:19–25. doi: 10.1016/j.pbi.2014.03.011
- Ökmen B, Kemmerich B, Hilbig D, Wemhöner R, Aschenbroich J, Perrar A, Huesgen PF, Schipper K, Doehlemann G (2018) Dual function of a secreted fungalysin metalloprotease in *Ustilago maydis*. *New Phytol* 220:249–261. doi: 10.1111/nph.15265
- Orbach MJ, Farrall L, Sweigard JA, Chumley FG, Valent B (2000) A telomeric avirulence gene determines efficacy for the rice blast resistance gene Pi-ta. *Plant Cell* 12:2019–32. doi: 10.1105/tpc.12.11.2019
- Ospina-Giraldo MD, Mullins E, Kang S (2003) Loss of function of the *Fusarium oxysporum* SNF1 gene reduces virulence on cabbage and *Arabidopsis*. *Curr Genet* 44:49–57. doi: 10.1007/s00294-003-0419-y
- Palmgren MG (1990) An H<sup>+</sup>-ATPase Assay: Proton Pumping and ATPase Activity Determined Simultaneously in the Same Sample. *Plant Physiol* 94:882–886. doi: 10.1104/pp.94.3.882
- Pan Y, Liu Z, Rocheleau H, Fauteux F, Wang Y, McCartney C, Ouellet T (2018) Transcriptome dynamics associated with resistance and susceptibility against fusarium head blight in four wheat genotypes. *BMC Genomics* 19:642. doi: 10.1186/s12864-018-5012-3
- Parisy V, Poinssot B, Owsianowski L, Buchala A, Glazebrook J, Mauch F (2006) Identification of PAD2 as a  $\gamma$ -glutamylcysteine synthetase highlights the importance of glutathione in disease resistance of *Arabidopsis*. *Plant J* 49:159–172. doi: 10.1111/j.1365-313X.2006.02938.x
- Parlevliet JE (2002) Durability of resistance against fungal, bacterial and viral pathogens; present situation. *Euphytica* 124:147–156. doi: 10.1023/A:1015601731446

- Pathi KM, Rink P, Budhagatapalli N, Betz R, Saado I, Hiekel S, Becker M, Djamei A, Kumlehn J (2020) Engineering Smut Resistance in Maize by Site-Directed Mutagenesis of LIPOXYGENASE 3. *Front Plant Sci* 11:1–13. doi: 10.3389/fpls.2020.543895
- Patten CL, Blakney AJC, Coulson TJD (2013) Activity, distribution and function of indole-3-acetic acid biosynthetic pathways in bacteria. *Crit Rev Microbiol* 39:395–415. doi: 10.3109/1040841X.2012.716819
- Perchepied L, Balagué C, Riou C, Claudel-Renard C, Rivière N, Grezes-Besset B, Roby D (2010) Nitric Oxide Participates in the Complex Interplay of Defense-Related Signaling Pathways Controlling Disease Resistance to *Sclerotinia sclerotiorum* in *Arabidopsis thaliana*. *Mol Plant-Microbe Interact* 23:846–860. doi: 10.1094/MPMI-23-7-0846
- Petrasch S, Knapp SJ, van Kan JAL, Blanco-Ulate B (2019) Grey mould of strawberry, a devastating disease caused by the ubiquitous necrotrophic fungal pathogen *Botrytis cinerea*. *Mol Plant Pathol* 20:877–892. doi: 10.1111/mpp.12794
- Petre B, Kamoun S (2014) How Do Filamentous Pathogens Deliver Effector Proteins into Plant Cells? *PLoS Biol* 12:e1001801. doi: 10.1371/journal.pbio.1001801
- Plett JM, Daguerre Y, Wittulsky S, Vayssieres A, Deveau A, Melton SJ, Kohler A, Morrell-Falvey JL, Brun A, Veneault-Fourrey C, Martin F (2014) Effector MiSSP7 of the mutualistic fungus *Laccaria bicolor* stabilizes the *Populus* JAZ6 protein and represses jasmonic acid (JA) responsive genes. *Proc Natl Acad Sci U S A* 111:8299–8304. doi: 10.1073/pnas.1322671111
- Plissonneau C, Hartmann FE, Croll D (2018) Pangenome analyses of the wheat pathogen *Zymoseptoria tritici* reveal the structural basis of a highly plastic eukaryotic genome. *BMC Biol* 16:5. doi: 10.1186/s12915-017-0457-4
- Poland JA, Balint-Kurti PJ, Wisser RJ, Pratt RC, Nelson RJ (2009) Shades of gray: the world of quantitative disease resistance. *Trends Plant Sci* 14:21–29. doi: 10.1016/j.tplants.2008.10.006
- Poland JA, Bradbury PJ, Buckler ES, Nelson RJ (2011) Genome-wide nested association mapping of quantitative resistance to northern leaf blight in maize. *Proc Natl Acad Sci* 108:6893–6898. doi: 10.1073/pnas.1010894108
- Portwood JL, Woodhouse MR, Cannon EK, Gardiner JM, Harper LC, Schaeffer ML, Walsh JR, Sen TZ, Cho KT, Schott DA, Braun BL, Dietze M, Dunfee B, Elisk CG, Manchanda N, Coe E, Sachs M, Stinard P, Tolbert J, Zimmerman S, Andorf CM (2019) MaizeGDB 2018: the maize multi-genome genetics and genomics database. *Nucleic Acids Res* 47:D1146–D1154. doi: 10.1093/nar/gky1046
- Qi X, Niks RE, Stam P, Lindhout P (1998) Identification of QTLs for partial resistance to leaf rust (*Puccinia hordei*) in barley. *Theor Appl Genet* 96:1205–1215. doi: 10.1007/s001220050858
- Ramonell K, Berrocal-Lobo M, Koh S, Wan J, Edwards H, Stacey G, Somerville S (2005) Loss-of-Function Mutations in Chitin Responsive Genes Show Increased Susceptibility to the Powdery Mildew Pathogen *Erysiphe cichoracearum*. *Plant Physiol* 138:1027–1036. doi: 10.1104/pp.105.060947

## 5. Bibliography

---

- Rao M V, Lee H, Creelman RA, Mullet JE, Davis KR (2000) Jasmonic acid signaling modulates ozone-induced hypersensitive cell death. *Plant Cell* 12:1633–1646. doi: 10.1105/tpc.12.9.1633
- Rasman S, Agrawal AA (2011) Latitudinal patterns in plant defense: evolution of cardenolides, their toxicity and induction following herbivory. *Ecol Lett* 476–483. doi: 10.1111/j.1461-0248.2011.01609.x
- Redkar A, Doehlemann G (2016) *Ustilago maydis* Virulence Assays in Maize. *Bio-protocol* 6:e1760. doi: 10.21769/BioProtoc.1760
- Redkar A, Hoser R, Schilling L, Zechmann B, Krzymowska M, Walbot V, Doehlemann G (2015) A Secreted Effector Protein of *Ustilago maydis* Guides Maize Leaf Cells to Form Tumors. *Plant Cell* 27:1332–1351. doi: 10.1105/tpc.114.131086
- Redkar A, Jaeger E, Doehlemann G (2018) Visualization of Growth and Morphology of Fungal Hyphae in planta Using WGA-AF488 and Propidium Iodide Co-staining. *Bio-protocol* 8:e2942. doi: 10.21769/BioProtoc.2942
- Ren H, Gray WM (2015) SAUR Proteins as Effectors of Hormonal and Environmental Signals in Plant Growth. *Mol Plant* 8:1153–1164. doi: 10.1016/j.molp.2015.05.003
- Roitsch T, Balibrea ME, Hofmann M, Proels R, Sinha AK (2003) Extracellular invertase: key metabolic enzyme and PR protein. *J Exp Bot* 54:513–524. doi: 10.1093/jxb/erg050
- Rose JKC, Ham K-S, Darvill AG, Albersheim P (2002) Molecular cloning and characterization of glucanase inhibitor proteins: coevolution of a counterdefense mechanism by plant pathogens. *Plant Cell* 14:1329–45. doi: 10.1105/tpc.002253
- Roux F, Voisin D, Badet T, Balagué C, Barlet X, Huard-Chauveau C, Roby D, Raffaele S (2014) Resistance to phytopathogens e tutti quanti: Placing plant quantitative disease resistance on the map. *Mol Plant Pathol* 15:427–432. doi: 10.1111/mpp.12138
- Sambrook J, Fritsch EF, Maniatis T (1989) *Molecular Cloning: A Laboratory Manual*. Cold Spring Harbor laboratory press.
- Sánchez-Rangel D, Sánchez-Nieto S, Plasencia J (2012) Fumonisin B1, a toxin produced by *Fusarium verticillioides*, modulates maize  $\beta$ -1,3-glucanase activities involved in defense response. *Planta* 235:965–78. doi: 10.1007/s00425-011-1555-0
- Sánchez-Vallet A, Fouché S, Fudal I, Hartmann FE, Soyer JL, Tellier A, Croll D (2018) The Genome Biology of Effector Gene Evolution in Filamentous Plant Pathogens. *Annu Rev Phytopathol* 56:21–40. doi: 10.1146/annurev-phyto-080516-035303
- Sánchez-Vallet A, Saleem-Batcha R, Kombrink A, Hansen G, Valkenburg D-J, Thomma BPHJ, Mesters JR (2013) Fungal effector Ecp6 outcompetes host immune receptor for chitin binding through intrachain LysM dimerization. *Elife* 2:e00790. doi: 10.7554/eLife.00790
- Santiago R, Barros-Rios J, Malvar RA (2013) Impact of cell wall composition on maize resistance to pests and diseases. *Int J Mol Sci* 14:6960–6980. doi: 10.3390/ijms14046960

- Schemske DW, Mittelbach GG, Cornell H V., Sobel JM, Roy K (2009) Is There a Latitudinal Gradient in the Importance of Biotic Interactions? *Annu Rev Ecol Evol Syst* 40:245–269. doi: 10.1146/annurev.ecolsys.39.110707.173430
- Schilling L, Matei A, Redkar A, Walbot V, Doehlemann G (2014) Virulence of the maize smut *Ustilago maydis* is shaped by organ-specific effectors. *Mol Plant Pathol* 15:780–789. doi: 10.1111/mpp.12133
- Schirawski J, Mannhaupt G, Münch K, Brefort T, Schipper K, Doehlemann G, Di Stasio M, Rössel N, Mendoza-Mendoza A, Pester D, Müller O, Winterberg B, Meyer E, Ghareeb H, Wollenberg T, Münsterkötter M, Wong P, Walter M, Stukenbrock E, Guldener U, Kahmann R (2010) Pathogenicity Determinants in Smut Fungi Revealed by Genome Comparison. *Science* (80- ) 330:1546–1548. doi: 10.1126/science.1195330
- Schnable PS, Ware D, Fulton RS, Stein JC, Wei F, Pasternak S, Liang C, Zhang J, Fulton L, Graves TA, Minx P, Reily AD, Courtney L, Kruchowski SS, Tomlinson C, Strong C, Delehaunty K, Fronick C, Courtney B, Rock SM, Belter E, Du F, Kim K, Abbott RM, Cotton M, Levy A, Marchetto P, Ochoa K, Jackson SM, Gillam B, Chen W, Yan L, Higginbotham J, Cardenas M, Waligorski J, Applebaum E, Phelps L, Falcone J, Kanchi K, Thane T, Scimone A, Thane N, Henke J, Wang T, Ruppert J, Shah N, Rotter K, Hodges J, Ingenthron E, Cordes M, Kohlberg S, Sgro J, Delgado B, Mead K, Chinwalla A, Leonard S, Crouse K, Collura K, Kudrna D, Currie J, He R, Angelova A, Rajasekar S, Mueller T, Lomeli R, Scara G, Ko A, Delaney K, Wissotski M, Lopez G, Campos D, Braidotti M, Ashley E, Golser W, Kim H, Lee S, Lin J, Dujmic Z, Kim W, Talag J, Zuccolo A, Fan C, Sebastian A, Kramer M, Spiegel L, Nascimento L, Zutavern T, Miller B, Ambroise C, Muller S, Spooner W, Narechania A, Ren L, Wei S, Kumari S, Faga B, Levy MJ, McMahan L, Van Buren P, Vaughn MW, Ying K, Yeh C-T, Emrich SJ, Jia Y, Kalyanaraman A, Hsia A-P, Barbazuk WB, Baucom RS, Brutnell TP, Carpita NC, Chaparro C, Chia J-M, Deragon J-M, Estill JC, Fu Y, Jeddelloh JA, Han Y, Lee H, Li P, Lisch DR, Liu S, Liu Z, Nagel DH, McCann MC, SanMiguel P, Myers AM, Nettleton D, Nguyen J, Penning BW, Ponnala L, Schneider KL, Schwartz DC, Sharma A, Soderlund C, Springer NM, Sun Q, Wang H, Waterman M, Westerman R, Wolfgruber TK, Yang L, Yu Y, Zhang L, Zhou S, Zhu Q, Bennetzen JL, Dawe RK, Jiang J, Jiang N, Presting GG, Wessler SR, Aluru S, Martienssen RA, Clifton SW, McCombie WR, Wing RA, Wilson RK (2009) The B73 Maize Genome: Complexity, Diversity, and Dynamics. *Science* (80- ) 326:1112–1115. doi: 10.1126/science.1178534
- Schuler D, Wahl R, Wippel K, Vranes M, Münsterkötter M, Sauer N, Kämper J (2015) Hxt1, a monosaccharide transporter and sensor required for virulence of the maize pathogen *Ustilago maydis*. *New Phytol* 206:1086–1100. doi: 10.1111/nph.13314
- Schulz B, Banuett F, Dahl M, Schlesinger R, Schäfer W, Martin T, Herskowitz I, Kahmann R (1990) The b alleles of *U. maydis*, whose combinations program pathogenic development, code for polypeptides containing a homeodomain-related motif. *Cell* 60:295–306. doi: 10.1016/0092-8674(90)90744-Y
- Schuster M, Schweizer G, Kahmann R (2018) Comparative analyses of secreted proteins in plant pathogenic smut fungi and related basidiomycetes. *Fungal Genet Biol* 112:21–30. doi: 10.1016/j.fgb.2016.12.003



## 5. Bibliography

---

- Schuster M, Schweizer G, Reissmann S, Kahmann R (2016) Genome editing in *Ustilago maydis* using the CRISPR-Cas system. *Fungal Genet Biol* 89:3–9. doi: 10.1016/j.fgb.2015.09.001
- Senda K, Ogawa K (2004) Induction of PR-1 Accumulation Accompanied by Runaway Cell Death in the *Isd1* Mutant of *Arabidopsis* is Dependent on Glutathione Levels but Independent of the Redox State of Glutathione. *Plant Cell Physiol* 45:1578–1585. doi: 10.1093/pcp/pch179
- Seybold H, Trempel F, Ranf S, Scheel D, Romeis T, Lee J (2014) Ca<sup>2+</sup> signalling in plant immune response: from pattern recognition receptors to Ca<sup>2+</sup> decoding mechanisms. *New Phytol* 204:782–790. doi: 10.1111/nph.13031
- Skibbe DS, Doehlemann G, Fernandes J, Walbot V (2010) Maize Tumors Caused by *Ustilago maydis* Require Organ-Specific Genes in Host and Pathogen. *Science* (80- ) 328:89–92. doi: 10.1126/science.1185775
- Snetselaar KM, Mims CW (1992) Sporidial Fusion and Infection of Maize Seedlings by the Smut Fungus *Ustilago maydis*. *Mycologia* 84:193. doi: 10.2307/3760250
- Snetselaar KM, Mims CW (1994) Light and electron microscopy of *Ustilago maydis* hyphae in maize. *Mycol Res*. doi: 10.1016/S0953-7562(09)80463-2
- Sondergaard TE, Schulz A, Palmgren MG (2004) Energization of Transport Processes in Plants. Roles of the Plasma Membrane H<sup>+</sup>-ATPase. *Plant Physiol* 136:2475–2482. doi: 10.1104/pp.104.048231
- Song J, Win J, Tian M, Schornack S, Kaschani F, Ilyas M, van der Hoorn RALL, Kamoun S (2009) Apoplastic effectors secreted by two unrelated eukaryotic plant pathogens target the tomato defense protease Rcr3. *Proc Natl Acad Sci U S A* 106:1654–1659. doi: 10.1073/pnas.0809201106
- Southern EM (1975) Detection of specific sequences among DNA fragments separated by gel electrophoresis. In: *Biotechnology*. Reading, Massachusetts, pp 122–139
- Spellig T, Regenfelder E, Reichmann M, Schauwecker F, Bohlmann R, Urban M, Bölker M, Kämper J, Kahmann R (1994) Control of mating and development in *Ustilago maydis*. *Antonie Van Leeuwenhoek* 65:191–197. doi: 10.1007/BF00871946
- Sperschneider J, Dodds PN, Gardiner DM, Singh KB, Taylor JM (2018) Improved prediction of fungal effector proteins from secretomes with EffectorP 2.0. *Mol Plant Pathol* 19:2094–2110. doi: 10.1111/mpp.12682
- St.Clair DA (2010) Quantitative Disease Resistance and Quantitative Resistance Loci in Breeding. *Annu Rev Phytopathol* 48:247–268. doi: 10.1146/annurev-phyto-080508-081904
- Stasko AK, Batnini A, Bolanos-Carriel C, Lin JE, Lin Y, Blakeslee JJ, Dorrance AE (2020) Auxin Profiling and GmPIN Expression in *Phytophthora sojae* –Soybean Root Interactions. *Phytopathology*® PHYTO-02-20-004. doi: 10.1094/PHYTO-02-20-0046-R

- Steffenson BJ, Hayes PM, Kleinhofs A (1996) Genetics of seedling and adult plant resistance to net blotch (*Pyrenophora teres* f. *teres*) and spot blotch (*Cochliobolus sativus*) in barley. *Theor Appl Genet* 92:552–558. doi: 10.1007/BF00224557
- Stergiopoulos I, Cordovez V, Okmen B, Beenen HG, Kema GHJ, de Wit PJGM (2014) Positive selection and intragenic recombination contribute to high allelic diversity in effector genes of *Mycosphaerella fijiensis*, causal agent of the black leaf streak disease of banana. *Mol Plant Pathol* 15:447–460. doi: 10.1111/mpp.12104
- Stergiopoulos I, de Wit PJGM (2009) Fungal effector proteins. *Annu Rev Phytopathol* 47:233–263. doi: 10.1146/annurev.phyto.112408.132637
- Stirnberg A, Djamei A (2016) Characterization of ApB73, a virulence factor important for colonization of *Zea mays* by the smut *Ustilago maydis*. *Mol Plant Pathol* 17:1467–1479. doi: 10.1111/mpp.12442
- Talukder ZI, Tharreau D, Price AH (2004) Quantitative trait loci analysis suggests that partial resistance to rice blast is mostly determined by race-specific interactions. *New Phytol* 162:197–209. doi: 10.1111/j.1469-8137.2004.01010.x
- Tamaoki M (2008) The role of phytohormone signaling in ozone-induced cell death in plants. *Plant Signal Behav* 3:166–174. doi: 10.4161/psb.3.3.5538
- Tanaka S, Brefort T, Neidig N, Djamei A, Kahnt J, Vermerris W, Koenig S, Feussner K, Feussner I, Kahmann R (2014) A secreted *Ustilago maydis* effector promotes virulence by targeting anthocyanin biosynthesis in maize. *Elife* 3:e01355. doi: 10.7554/eLife.01355.001
- Tang D, Wang G, Zhou J-M (2017) Receptor Kinases in Plant-Pathogen Interactions: More Than Pattern Recognition. *Plant Cell* 29:618–637. doi: 10.1105/tpc.16.00891
- Tapke VFF (1937) New physiologic races of *Ustilago hordei*. *J Agric Res* 55:663–692.
- The Gene Ontology Consortium (2017) Expansion of the Gene Ontology knowledgebase and resources. *Nucleic Acids Res* 45:D331–D338. doi: 10.1093/nar/gkw1108
- Thomma BPHJ, Nürnberger T, Joosten MHAJ (2011) Of PAMPs and Effectors: The Blurred PTI-ETI Dichotomy. *Plant Cell* 23:4–15. doi: 10.1105/tpc.110.082602
- Thompson DL, Bergquist RR (1984) Inheritance of Mature Plant Resistance to *Helminthosporium maydis* Race 0 in Maize 1. *Crop Sci* 24:807–811. doi: 10.2135/cropsci1984.0011183X002400040042x
- Tian M, Win J, Song J, van der Hoorn R, van der Knaap E, Kamoun S (2007) A *Phytophthora infestans* Cystatin-Like Protein Targets a Novel Tomato Papain-Like Apoplastic Protease. *Plant Physiol* 143:364–377. doi: 10.1104/pp.106.090050
- Tonukari NJ, Scott-Craig JS, Waltonb JD (2000) The *Cochliobolus carbonum* SNF1 Gene Is Required for Cell Wall-Degrading Enzyme Expression and Virulence on Maize. *Plant Cell* 12:237–247. doi: 10.1105/tpc.12.2.237
- Toruño TY, Stergiopoulos I, Coaker G (2016) Plant-Pathogen Effectors: Cellular Probes Interfering with Plant Defenses in Spatial and Temporal Manners. *Annu Rev Phytopathol* 54:419–441. doi: 10.1146/annurev-phyto-080615-100204

## 5. Bibliography

---

- Turian G, Hamilton RH (1960) Chemical detection of 3-indolylacetic acid in *Ustilago zeae* tumors. *Biochim Biophys Acta* 41:148–150. doi: 10.1016/0006-3002(60)90381-4
- Turner RS (2005) After the famine: Plant pathology, *Phytophthora infestans*, and the late blight of potatoes, 1845—1960. *Hist Stud Phys Biol Sci* 35:341–370. doi: 10.1525/hsp.2005.35.2.341
- Utz HF, Melchinger AE, Ooijen JW van, Jansen J (1994) Comparison of different approaches to interval mapping of quantitative trait loci. *Biometrics plant Breed Appl Mol markers* 195–204.
- Van Bel M, Diels T, Vancaester E, Kreft L, Botzki A, Van de Peer Y, Coppens F, Vandepoele K (2018) PLAZA 4.0: an integrative resource for functional, evolutionary and comparative plant genomics. *Nucleic Acids Res* 46:D1190–D1196. doi: 10.1093/nar/gkx1002
- van den Burg HA, Harrison SJ, Joosten MHAJ, Vervoort J, de Wit PJGM (2006) *Cladosporium fulvum* Avr4 protects fungal cell walls against hydrolysis by plant chitinases accumulating during infection. *Mol Plant Microbe Interact* 19:1420–30. doi: 10.1094/MPMI-19-1420
- van der Burgh AM, Joosten MHAJ (2019) Plant Immunity: Thinking Outside and Inside the Box. *Trends Plant Sci* 24:587–601. doi: 10.1016/j.tplants.2019.04.009
- van Esse HP, Bolton MD, Stergiopoulos I, de Wit PJGM, Thomma BPHJ (2007) The chitin-binding *Cladosporium fulvum* effector protein Avr4 is a virulence factor. *Mol Plant Microbe Interact* 20:1092–101. doi: 10.1094/MPMI-20-9-1092
- Venkatesh T V., Chassy AW, Fiehn O, Flint-Garcia S, Zeng Q, Skogerson K, Harrigan GG (2016) Metabolomic Assessment of Key Maize Resources: GC-MS and NMR Profiling of Grain from B73 Hybrids of the Nested Association Mapping (NAM) Founders and of Geographically Diverse Landraces. *J Agric Food Chem* 64:2162–2172. doi: 10.1021/acs.jafc.5b04901
- Villajuana-Bonequi M, Matei A, Ernst C, Hallab A, Usadel B, Doehlemann G (2019) Cell type specific transcriptional reprogramming of maize leaves during *Ustilago maydis* induced tumor formation. *Sci Rep* 9:1–15. doi: 10.1038/s41598-019-46734-3
- Vogel JP, Raab TK, Schiff C, Somerville SC (2002) PMR6 , a Pectate Lyase–Like Gene Required for Powdery Mildew Susceptibility in *Arabidopsis*. *Plant Cell* 14:2095–2106. doi: 10.1105/tpc.003509
- Vorwerk S, Somerville S, Somerville C (2004) The role of plant cell wall polysaccharide composition in disease resistance. *Trends Plant Sci* 9:203–209. doi: 10.1016/j.tplants.2004.02.005
- Wahl R, Wippel K, Goos S, Kämper J, Sauer N (2010) A Novel High-Affinity Sucrose Transporter Is Required for Virulence of the Plant Pathogen *Ustilago maydis*. *PLoS Biol* 8:e1000303. doi: 10.1371/journal.pbio.1000303
- Walbot V, Skibbe DS (2010) Maize host requirements for *Ustilago maydis* tumor induction. *Sex Plant Reprod* 23:1–13. doi: 10.1007/s00497-009-0109-0

- Wan J, Zhang X-C, Neece D, Ramonell KM, Clough S, Kim S, Stacey MG, Stacey G (2008) A LysM Receptor-Like Kinase Plays a Critical Role in Chitin Signaling and Fungal Resistance in Arabidopsis. *Plant Cell* 20:471–481. doi: 10.1105/tpc.107.056754
- Wang D, Pajerowska-Mukhtar K, Culler AH, Dong X (2007) Salicylic Acid Inhibits Pathogen Growth in Plants through Repression of the Auxin Signaling Pathway. *Curr Biol* 17:1784–1790. doi: 10.1016/j.cub.2007.09.025
- Wang E, Yu N, Bano SA, Liu C, Miller AJ, Cousins D, Zhang X, Ratet P, Tadege M, Mysore KS, Downie JA, Murray JD, Oldroyd GED, Schultze M (2014) A H<sup>+</sup>-ATPase That Energizes Nutrient Uptake during Mycorrhizal Symbioses in Rice and Medicago truncatula. *Plant Cell* 26:1818–1830. doi: 10.1105/tpc.113.120527
- Wang GL, Mackill DJ, Bonman JM, McCouch SR, Champoux MC, Nelson RJ (1994) RFLP mapping of genes conferring complete and partial resistance to blast in a durably resistant rice cultivar. *Genetics* 136:1421–34.
- Wang L, Wang Y, Wang Z, Marcel TC, Niks RE, Qi X (2010) The phenotypic expression of QTLs for partial resistance to barley leaf rust during plant development. *Theor Appl Genet* 121:857–864. doi: 10.1007/s00122-010-1355-0
- Wang W, Feng B, Zhou JM, Tang D (2020) Plant immune signaling: Advancing on two frontiers. *J Integr Plant Biol* 62:2–24. doi: 10.1111/jipb.12898
- Wang Y, Wang Y (2018) Trick or treat: Microbial pathogens evolved apoplastic effectors modulating plant susceptibility to infection. *Mol Plant-Microbe Interact* 31:6–12. doi: 10.1094/MPMI-07-17-0177-FI
- Wasternack C, Hause B (2013) Jasmonates: biosynthesis, perception, signal transduction and action in plant stress response, growth and development. An update to the 2007 review in *Annals of Botany*. *Ann Bot* 111:1021–1058. doi: 10.1093/aob/mct067
- Whisson SC, Boevink PC, Moleleki L, Avrova AO, Morales JG, Gilroy EM, Armstrong MR, Grouffaud S, van West P, Chapman S, Hein I, Toth IK, Pritchard L, Birch PRJ (2007) A translocation signal for delivery of oomycete effector proteins into host plant cells. *Nature* 450:115–118. doi: 10.1038/nature06203
- Wiethölter N, Graebner B, Mierau M, Mort AJ, Moerschbacher BM (2003) Differences in the Methyl Ester Distribution of Homogalacturonans from Near-Isogenic Wheat Lines Resistant and Susceptible to the Wheat Stem Rust Fungus. *Mol Plant-Microbe Interact* 16:945–952. doi: 10.1094/MPMI.2003.16.10.945
- Wu C-H, Krasileva K V., Banfield MJ, Terauchi R, Kamoun S (2015) The “sensor domains” of plant NLR proteins: more than decoys? *Front Plant Sci*. doi: 10.3389/fpls.2015.00134
- Xiang T, Zong N, Zou Y, Wu Y, Zhang J, Xing W, Li Y, Tang X, Zhu L, Chai J, Zhou J-M (2008) *Pseudomonas syringae* Effector AvrPto Blocks Innate Immunity by Targeting Receptor Kinases. *Curr Biol* 18:74–80. doi: 10.1016/j.cub.2007.12.020
- Xiao W, Zhao J, Fan S, Li L, Dai J, Xu M (2007) Mapping of genome-wide resistance gene analogs (RGAs) in maize (*Zea mays* L.). *Theor Appl Genet* 115:501–508. doi: 10.1007/s00122-007-0583-4

## 5. Bibliography

---

- Yang Q, He Y, Kabahuma M, Chaya T, Kelly A, Borrego E, Bian Y, El Kasmi F, Yang L, Teixeira P, Kolkman J, Nelson R, Kolomiets M, Dangl JL, Wisser R, Caplan J, Li X, Lauter N, Balint-Kurti P (2017) A gene encoding maize caffeoyl-CoA O-methyltransferase confers quantitative resistance to multiple pathogens. *Nat Genet* 49:1364–1372. doi: 10.1038/ng.3919
- Ye J, Zhong T, Zhang D, Ma C, Wang L, Yao L, Zhang Q, Zhu M, Xu M (2019) The Auxin-Regulated Protein ZmAuxRP1 Coordinates the Balance between Root Growth and Stalk Rot Disease Resistance in Maize. *Mol Plant* 12:360–373. doi: 10.1016/j.molp.2018.10.005
- Yu J, Holland JB, McMullen MD, Buckler ES (2008) Genetic design and statistical power of nested association mapping in maize. *Genetics* 178:539–551. doi: 10.1534/genetics.107.074245
- Yu X, Feng B, He P, Shan L (2017) From Chaos to Harmony: Responses and Signaling upon Microbial Pattern Recognition. *Annu Rev Phytopathol* 55:109–137. doi: 10.1146/annurev-phyto-080516-035649
- Zhang B, Horvath S (2005) A General Framework for Weighted Gene Co-Expression Network Analysis. *Stat Appl Genet Mol Biol*. doi: 10.2202/1544-6115.1128
- Zhang Z, Henderson C, Gurr S (2004) *Blumeria graminis* secretes an extracellular catalase during infection of barley: potential role in suppression of host defence. *Mol Plant Pathol* 5:537–547. doi: 10.1111/j.1364-3703.2004.00251.x
- Zheng Z, Qamar SA, Chen Z, Mengiste T (2006) Arabidopsis WRKY33 transcription factor is required for resistance to necrotrophic fungal pathogens. *Plant J* 48:592–605. doi: 10.1111/j.1365-3113.2006.02901.x
- Zipfel C (2008) Pattern-recognition receptors in plant innate immunity. *Curr Opin Immunol* 20:10–16. doi: 10.1016/j.coi.2007.11.003
- Zipfel C, Robatzek S, Navarro L, Oakeley EJ, Jones JDGG, Felix G, Boller T (2004) Bacterial disease resistance in Arabidopsis through flagellin perception. *Nature* 428:764–767. doi: 10.1038/nature02485
- Zuccaro A, Lahrmann U, Langen G (2014) Broad compatibility in fungal root symbioses. *Curr Opin Plant Biol* 20:135–145. doi: 10.1016/j.pbi.2014.05.013
- Zuo W, Chao Q, Zhang N, Ye J, Tan G, Li B, Xing Y, Zhang B, Liu H, Fengler KA, Zhao J, Zhao X, Chen Y, Lai J, Yan J, Xu M (2015) A maize wall-associated kinase confers quantitative resistance to head smut. *Nat Genet* 47:151–157. doi: 10.1038/ng.3170
- Zuo W, Depotter JR, Doehlemann G (2020a) Cas9HF1 enhanced specificity in *Ustilago maydis*. *Fungal Biol* 124:228–234. doi: 10.1016/j.funbio.2020.02.006
- Zuo W, Gupta DK, Depotter JR, Thines M, Doehlemann G (2020b) Cross-species analysis between the maize smut fungi *Ustilago maydis* and *Sporisorium reilianum* highlights the role of transcriptional plasticity of effector orthologs for virulence and disease. *bioRxiv* 2020.11.03.366443.
- Zuo W, Oekmen B, Depotter JRL, Ebert MK, Redkar A, Misas Villamil J, Doehlemann G (2019) Molecular Interactions between Smut Fungi and Their Host Plants. *Annu Rev Phytopathol* 57:411–430. doi: 10.1146/annurev-phyto-082718-100139

## 6 Appendix

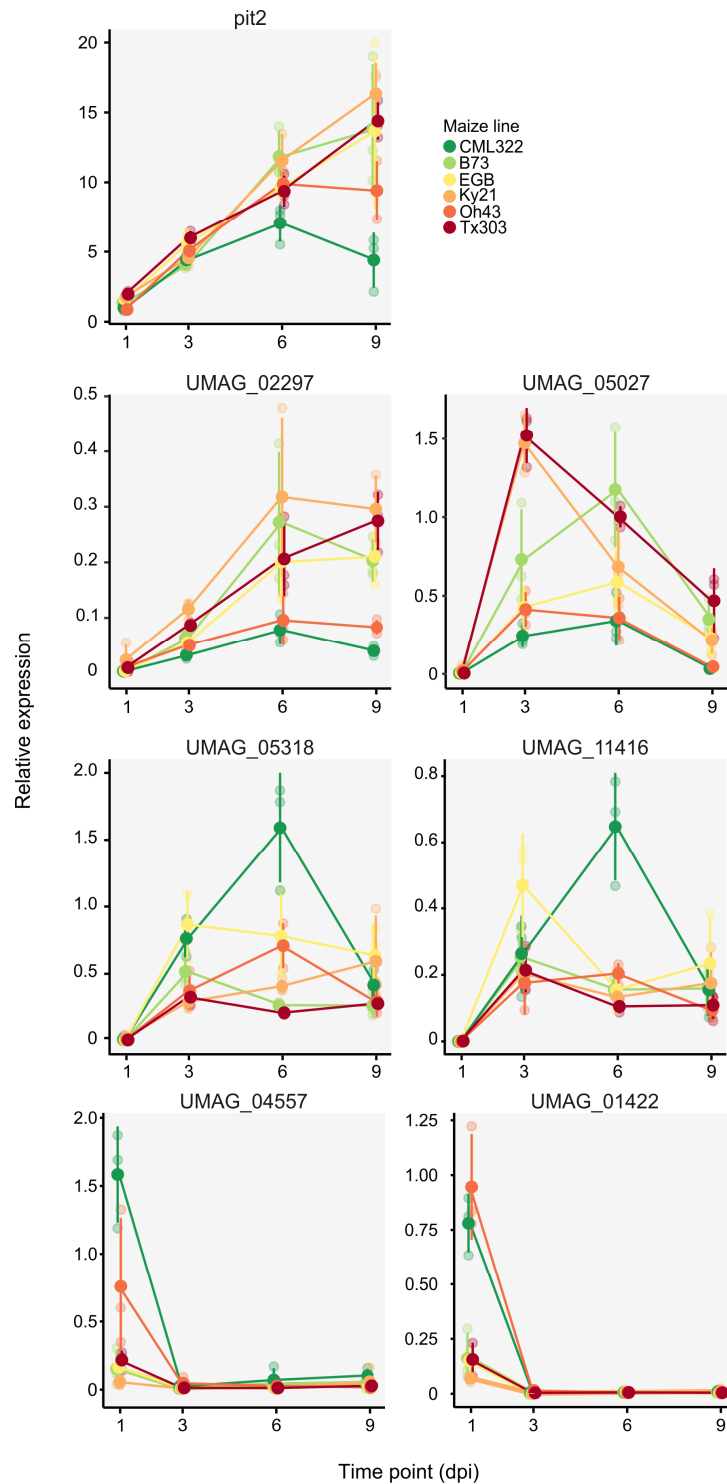


**Figure 6.1. Expression profile of candidate maize line-specific effectors.** Relative expression was quantified via qRT-PCR during infection progression at 1, 3, 6, and 9 days post infection (dpi). Solid points indicate mean ratios of the candidate effector gene to ppi ( $2^{-\Delta Ct}$ ) of three biological replicates, transparent points indicate individual values, and error bars denote the standard deviation. Respective gene names are shown at the top of each plot. pit2 (UMAG\_01375) was used as maize line-unspecific control.

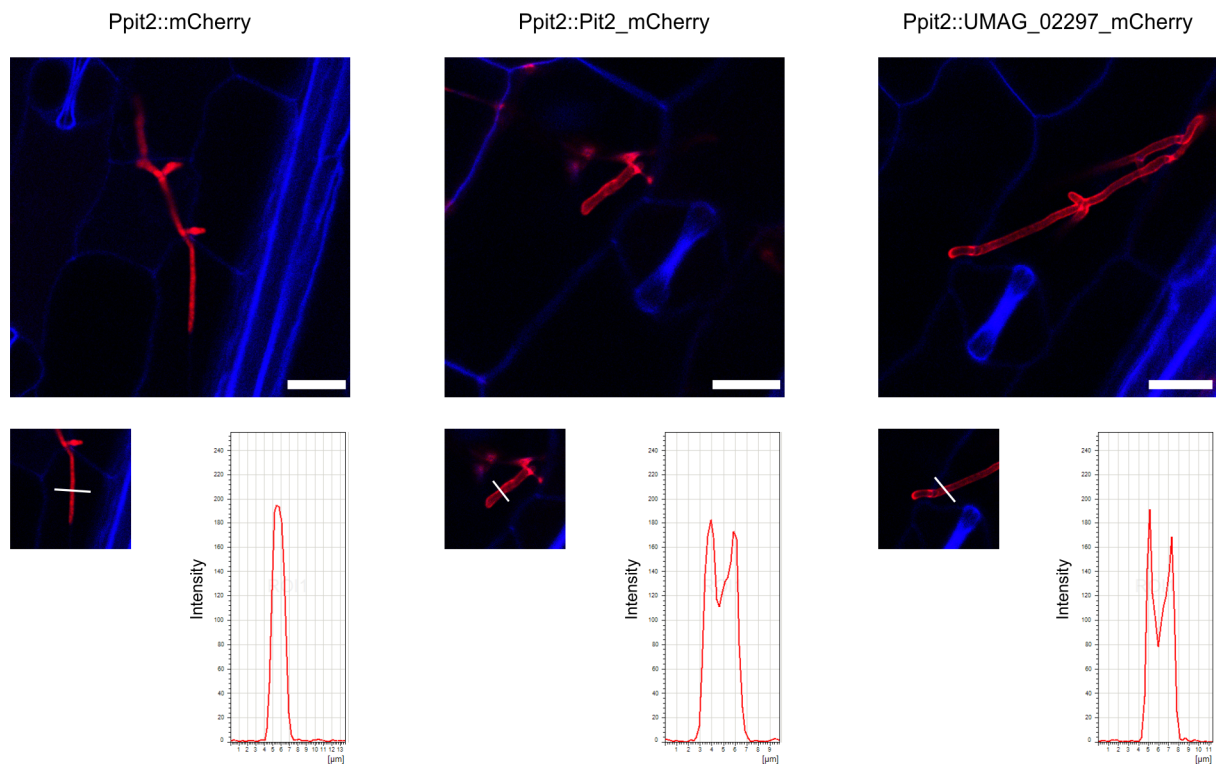


**Figure 6.2. Secretion of UMAG\_02297 during *U. maydis* infection.** Maize seedlings were infected with SG200\_mCherry (negative control), SG200\_Pit2-mCherry (positive control) and SG200\_UMAG\_02297-mCherry. mCherry fluorescence was observed 2 dpi. Scale bar: 25  $\mu\text{m}$ . Intensity profiles are shown at the bottom.

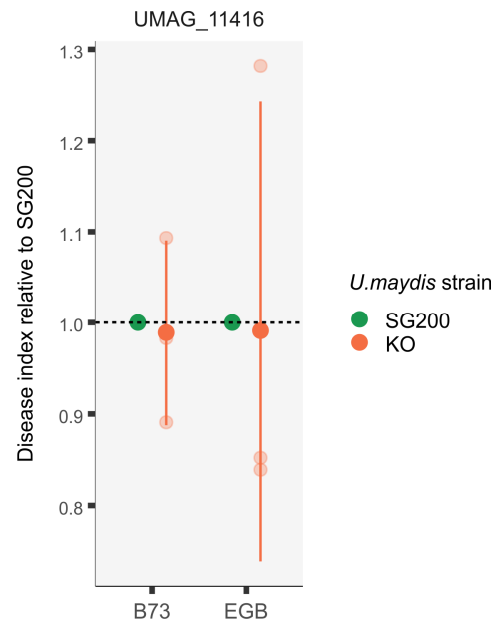


**Figure 6.3. Virulence function of UMG\_11416 in different maize lines.** The single knock-out (KO) strain of UMG\_11416 was injected into maize seedlings of the indicated line and symptoms were scored 12 days post infection (dpi). KO refers to the respective CRISPR/Cas9 KO strain. Disease indices reflect disease symptom severity and are shown in relation to SG200, which was set to unity. The experiment was performed in three biological replicates. Average number of infected plants per strain and maize line: 76.



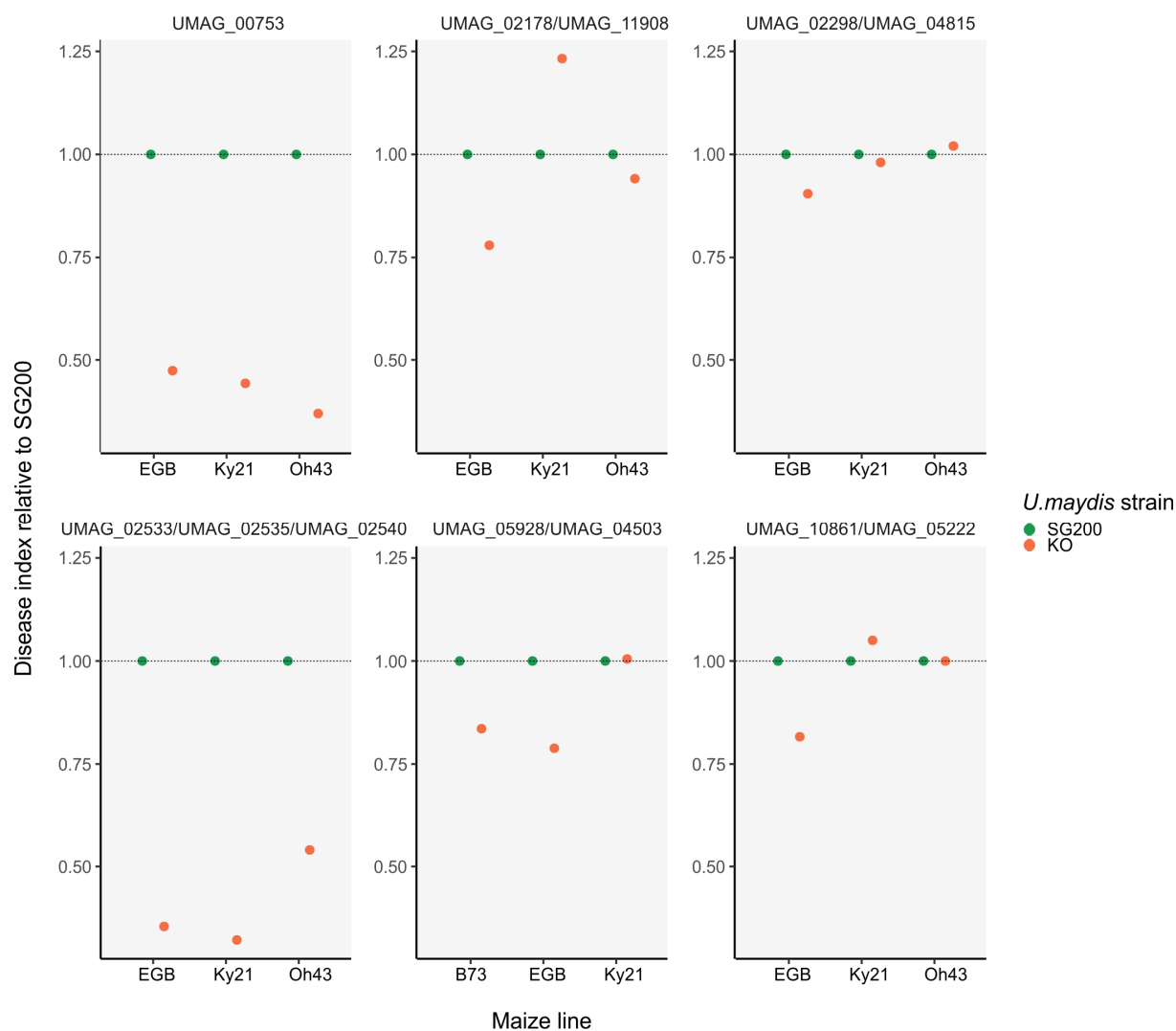


**Figure 6.4. Virulence functions of selected additional candidate maize line-specific effectors.** Single, double, or triple knock-out (KO) mutant strains of selected maize line-specific effectors were injected into maize seedlings of the indicated line and symptoms were scored 12 days post infection (dpi). Gene names are shown at the top. KO refers to the respective CRISPR/Cas9 knock-out (KO) strain. Gene names separated by slash indicate multiple KO of these genes. Disease indices reflect disease symptom severity and are shown in relation to SG200, which was set to unity. All experiments were performed in one biological replicate. Average number of infected plants per strain and maize line: 26.

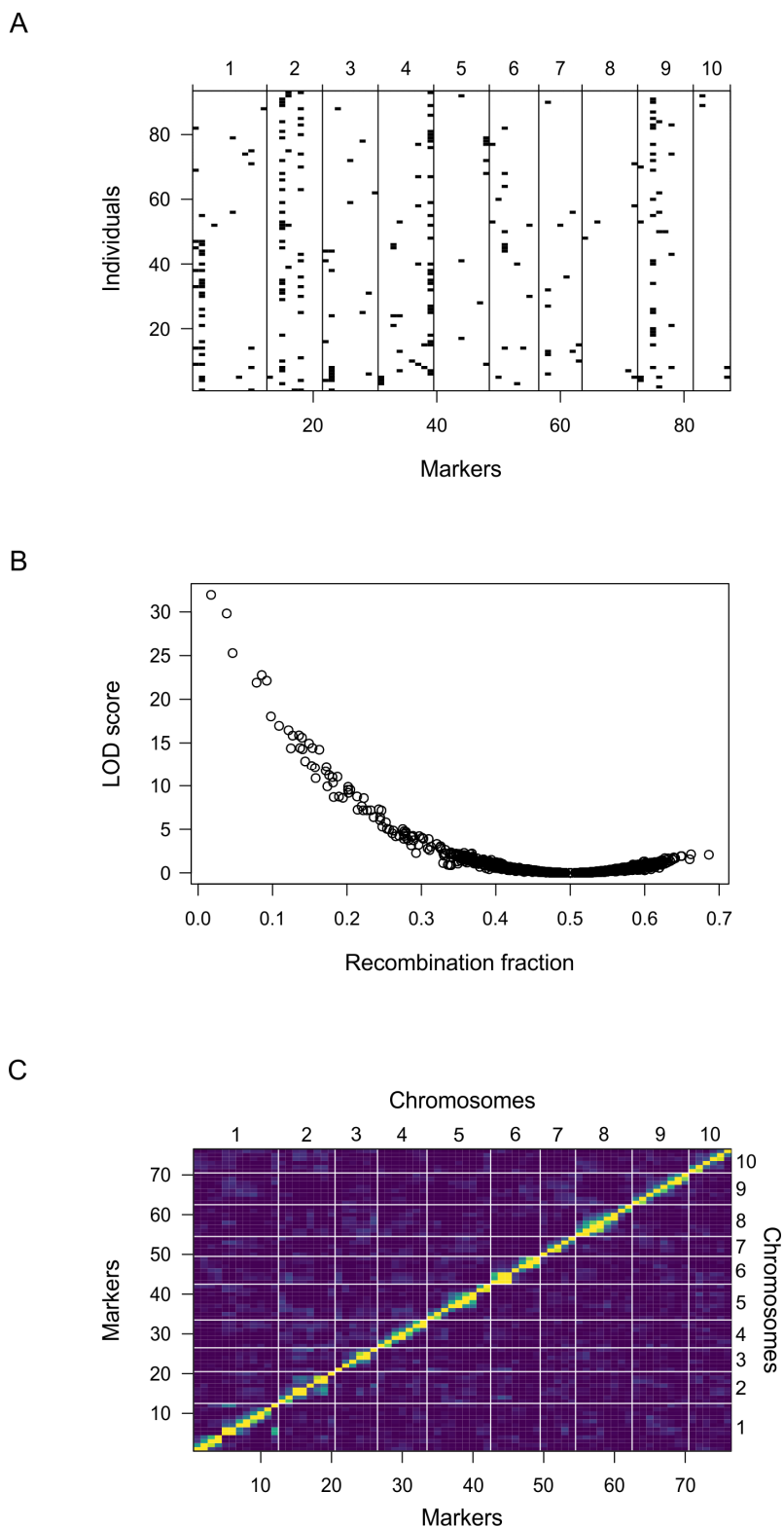


**Figure 6.5. Data quality assessment for genetic map construction. A) Missing genotype data for individuals and markers.** Black points represent missing data points after filtering. **B) LOD scores and recombination fraction of molecular markers.** **C) Recombination fractions and LOD scores for tests of linkage for all pairs of markers.** The LOD scores are for a test of  $r = 1/2$ . The recombination fractions are shown in the upper left triangle, the LOD scores are shown in the lower right triangle. Yellow corresponds to a large LOD score or a small recombination fraction (markers linked), purple corresponds to a small LOD score or a large recombination fraction (markers not linked).

## 6. Appendix

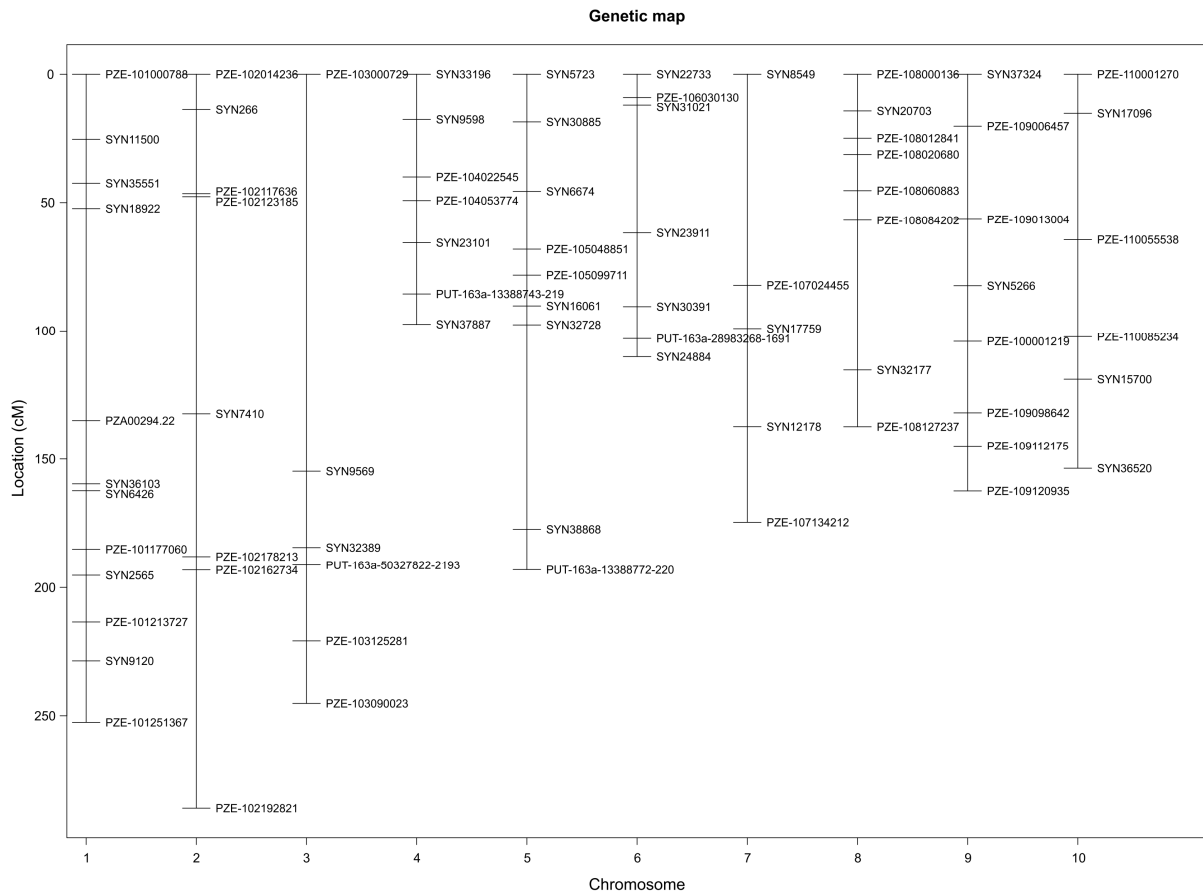


**Figure 6.6. Genetic map of molecular markers.** The genetic map was constructed with R/qtl v1.46-2 (Broman et al. 2003) using Haley-Knott regression in collaboration with Benjamin Stich.

## Eidesstattliche Erklärung

Hiermit versichere ich an Eides statt, dass ich die vorliegende Dissertation selbstständig und ohne die Benutzung anderer als der angegebenen Hilfsmittel und Literatur angefertigt habe. Alle Stellen, die wörtlich oder sinngemäß aus veröffentlichten und nicht veröffentlichten Werken dem Wortlaut oder dem Sinn nach entnommen wurden, sind als solche kenntlich gemacht. Ich versichere an Eides statt, dass diese Dissertation noch keiner anderen Fakultät oder Universität zur Prüfung vorgelegen hat; dass sie-abgesehen von unten angegebenen Teilpublikationen und eingebundenen Artikeln und Manuskripten-noch nicht veröffentlicht worden ist sowie, dass ich eine Veröffentlichung der Dissertation vor Abschluss der Promotion nicht ohne Genehmigung des Promotionsausschusses vornehmen werde. Die Bestimmungen dieser Ordnung sind mir bekannt. Darüber hinaus erkläre ich hiermit, dass ich die Ordnung zur Sicherung guter wissenschaftlicher Praxis und zum Umgang mit wissenschaftlichem Fehlverhalten der Universität zu Köln gelesen und sie bei der Durchführung der Dissertation zugrundeliegenden Arbeiten und der schriftlich verfassten Dissertation beachtet habe und verpflichte mich hiermit, die dort genannten Vorgaben bei allen wissenschaftlichen Tätigkeiten zu beachten und umzusetzen. Ich versichere, dass die eingereichte elektronische Fassung der eingereichten Druckfassung vollständig entspricht.

Teile dieser Arbeit wurden in folgenden Artikeln veröffentlicht oder zur Veröffentlichung eingereicht:

Schurack S, Depotter JRL, Gupta D, Thines M, Doehlemann G (2020) Transcriptome analysis in the maize-*Ustilago maydis* interaction identifies maize-line-specific activity of fungal effectors. bioRxiv 2020.10.30.361659.

Datum: 12.11.2020

Unterschrift: \_\_\_\_\_

## **Delimitation of own contribution**

The results presented in this study were acquired by me independently and without other assistance than that stated here. The experiments were conceived and the publication ‘Transcriptome analysis in the maize-*Ustilago maydis* interaction identifies maize-line-specific activity of fungal effectors‘ was written in collaboration with Prof. Dr. Gunther Döhlemann. The experimental contributions of other persons that participated in this study are listed in the following:

Dr. Jasper Depotter analysed the raw RNA-Seq data, generated the count files used for differential gene expression analyses, made the MDS plots, calculated the functional enrichments for the maize transcriptome data and analysed effector gene variation between *U. maydis* strains (Figures 2.3, 2.7-8, 2.10-11, 2.16-19).

Henriette Läßle generated the *U. maydis* strains KO\_UMAG\_05027/KO\_UMAG\_02297 and KO\_UMAG\_05027/KO\_UMAG\_02297/KO\_UMAG\_05319/KO\_UMAG\_03154 as part of her bachelor thesis (Figure 2.14).

The QTL mapping field experiment was conducted in collaboration with Prof. Dr. Benjamin Stich (Chapter 2.6). He generated the mapping population, calculated the adjusted entry means, and supervised genetic map construction and QTL detection.

Weiliang Zuo, Bilal Ökmen and Elaine Jaeger participated in the field inoculations for QTL mapping (Figure 2.21).

## Acknowledgements

My special thanks go to Prof. Dr. Gunther Döhlemann for giving me the opportunity to work on this exciting and multifaceted topic. I am very grateful for the freedom and helpful support throughout this project, and all the things I have learned thereby.

Thank you, Prof. Dr. Alga Zuccaro and Prof. Dr. Benjamin Stich for your advice and fruitful discussions in our TAC meetings. Also many thanks again to Prof. Dr. Benjamin Stich for collaborating on the QTL mapping experiment, and your accommodating help with the analysis.

I have appreciated being a member of the IMPRS so much. Stephan Wagner and Johanna Spandl, thanks for all your dedication and hard work to make PhD life better. I would also like to thank Isabell Witt from the GSfBS for organising such great and helpful workshops. Also, I am very thankful for all the greenhouse gardeners' help during my huge infection experiments.

I am enormously grateful to every member of the AG Döhlemann, past or present. Our coffee breaks, ice creams and beers on the wall have made lab life so much more enjoyable. ☺

Jasper, thank you so much for your help with the RNA-Seq. It was great having someone to talk about complicated analysis issues, even if we sometimes were more confused afterwards. Thank you Henni for being the best bachelor student! It was a pleasure working with you on this project, talking about cats and woolly things. Weiliang, thanks for all your helpful CRISPR- and maize pollination tips, to only state a few. Also a huge thank you to Elaine, Bilal, and again Weiliang for participating in the 'little' field trial adventure. I hope you do not suffer from persistent back problems. A big thanks to Ute and Rapha, who keep the lab running and organised, while just being the coolest TA's. A special thank you to Elaine, who always had great and helpful advice, nice music, and a sarcastic anecdote to share. Jan, thanks for all the cat memes, motivation for running and chocolate you have provided through the years.

A big thank you to Christina, the best proof-reader!

I am so grateful to my friends and family, especially Yannick, Zoë, and my parents, who kept me company, fed me, motivated, and supported me in so many aspects along the way.

Last and not least, I would like to acknowledge my couch that always had my back through the long hours of home office during these strange times...

# CV

Selma Schurack

Born 16<sup>th</sup> of May, 1990 in Berlin-Charlottenburg, Germany

## Education

---

10/2016 – 12/2020

### **PhD thesis**

CEPLAS/University of Cologne, Max-Planck-Institute for Plant Breeding Research  
Mechanisms of quantitative disease resistance in the maize - *Ustilago maydis* interaction (Prof. Dr. Gunther Döhlemann)

10/2013 – 09/2016

**MSc. Biosciences**, University of Münster  
Characterization of the *Claviceps purpurea* – rye interaction: The role of effectors (Prof. Dr. Paul Tudzynski)

10/2010 – 09/2013

**BSc. Biosciences**, University of Münster

2009

**University entrance diploma (Abitur)**  
Wolfgang-Ernst Gymnasium, Büdingen

## Fellowships and Awards

---

2016 – 2020

**International Max-Planck Research School (IMPRS)** Fellow at the Max-Planck-Institute for Plant Breeding Research

2015 and 2012

**ERASMUS+ and ERASMUS scholarships**

2008

Positioned 4<sup>th</sup> in the selection process of the **International Biology Olympiad** in Hessen

## International experience and internships

---

03/2015 – 06/2015

**Research Internship at the University of Copenhagen, Denmark**

09/2012 – 03/2013

**Semester abroad at the University of Alicante, Spain**

## Publications

---

- Schurack S, Depotter JRL, Gupta D, Thines M, Doehlemann G (2020) Transcriptome analysis in the maize-*Ustilago maydis* interaction identifies maize-line-specific activity of fungal effectors. bioRxiv 2020.10.30.361659.
- Eitzen K, Hüynck JS, Schurack S, Doehlemann G (2019) Krieg und Frieden: molekulares Ping-Pong zwischen Pilzen und Pflanzen. BioSpektrum 25:378–381. doi: 10.1007/s12268-019-1064-4
- Kind S, Schurack S, Hinsch J, Tudzynski P (2018) *Brachypodium distachyon* as alternative model host system for the ergot fungus *Claviceps purpurea*. Mol Plant Pathol 19:1005–1011. doi: 10.1111/mpp.12563
- Oeser B, Kind S, Schurack S, Schmutzer T, Tudzynski P, Hinsch J (2017) Cross-talk of the biotrophic pathogen *Claviceps purpurea* and its host *Secale cereale*. BMC Genomics 18:273. doi: 10.1186/s12864-017-3619-4